

Title	静電作用による脂質二分子膜小胞の秩序形成メカニズムの解明：2次元相分離構造と3次元膜孔形成のカップリング
Author(s)	姫野, 泰輝
Citation	
Issue Date	2015-03
Type	Thesis or Dissertation
Text version	ETD
URL	http://hdl.handle.net/10119/12773
Rights	
Description	Supervisor:高木 昌宏, マテリアルサイエンス研究科, 博士

Doctoral thesis

Investigation about effect of charged phospholipids
on structure of lipid bilayer vesicles
: coupling between
2D-phase separation and 3D-pore formation

Hiroki Himeno

Supervisor: Masahiro Takagi

School of Materials Science,
Japan Advanced Institute of Science and Technology

March 2015

Contents

Chapter 1 General Introduction

1-1 Phospholipid molecules · · · · ·	5
1-2 Biomembrane structure:	
2D dynamics (phase separation) and 3D dynamics (morphological change) · · ·	6
1-3 Model biomembrane: Cell size liposome · · · · ·	10
1-4 Reproductions of biomembrane 2D- and 3D- structure using GUVs · · · · ·	11
1-5 Charged lipid molecules and electrostatic interaction · · · · ·	14
1-6 Previous study about charged lipid membrane · · · · ·	16
1-7 Objects and outline · · · · ·	17
1-8 References · · · · ·	19

Chapter 2 The effect of charge on membrane 2D structure

2-1 Introduction · · · · ·	23
2-2 Materials and methods · · · · ·	26
2-3 Experimental results · · · · ·	31
2-3-1 Binary lipid mixtures (Unsaturated lipid/ Saturated lipid) · · · · ·	31
2-3-2 Ternary mixtures (Saturated lipid (Charge or neutral)/ Cholesterol) · · · ·	35
2-3-3 Four-component mixtures of lipid and cholesterol · · · · ·	40
2-4 Discussion · · · · ·	45
2-5 Conclusions · · · · ·	53
2-6 References · · · · ·	54

Chapter 3 Cholesterol localization in charged multi-component membranes

3-1 Introduction	59
3-2 Materials and methods	62
3-3 Experimental results	66
3-3-1 The localization of cholesterol in neutral DOPC/DPPC/Chol mixtures	66
3-3-2 The localization of cholesterol in charged DOPG ⁽⁻⁾ /DPPC/Chol mixtures	68
3-3-3 The localization of cholesterol in charged DOPC/DPPG ⁽⁻⁾ /Chol mixtures	71
3-3-4 The localization of cholesterol in charged DOPG ⁽⁻⁾ /DPPG ⁽⁻⁾ /Chol mixtures	74
3-4 Discussion	77
3-4-1 The localization of cholesterol in neutral DOPC/DPPC/Chol mixtures	77
3-4-2 The localization of cholesterol in DOPG ⁽⁻⁾ /DPPC/Chol mixtures	78
3-4-3 The localization of cholesterol in DOPC/DPPG ⁽⁻⁾ /Chol mixtures	80
3-4-3 The localization of cholesterol in DOPG ⁽⁻⁾ /DPPG ⁽⁻⁾ /Chol mixtures	82
3-5 Conclusion	83
3-6 References	84

Chapter 4 The effect of charge on membrane 3D structure

4-1 Introduction	87
4-2 Materials and methods	90
4-3 Experimental results	95
4-3-1 Binary lipid mixtures (Unsaturated lipid/ Saturated lipid)	95
4-3-2 Ternary lipid mixtures (Neutral and charged saturated lipids /Cholesterol)	100
4-4 Discussion	106
4-5 Conclusion	113
4-6 References	114

Chapter 5 General conclusion

5-1 General conclusion	119
------------------------	-----

Acknowledgements	121
-------------------------	-----

Chapter 1

General introduction

1-1 Phospholipid molecules

Phospholipid is main constituent of biomembrane. Phospholipid is composed of hydrophilic head group and two hydrocarbon tails, and is called amphiphilic molecule. Phospholipids are often named in the combination of the structure of the head group and acyl chain. For example, “phosphatidyl-choline (PC)”, “phosphatidyl-glycerol (PG⁽⁻⁾)”, “phosphatidyl-serine (PS⁽⁻⁾)” are major head group of phospholipids. PC head group has both positive and negative electric charge, and acts neutral lipid. PG⁽⁻⁾ and PS⁽⁻⁾ lipids have a negative electric charge. The chain length and unsaturated bond of hydrocarbon tails affect mainly phase transition temperature (T_m) of phospholipid. Transition temperature tends to increase with the number of methylene group (CH₂) which is corresponding to chain length. In the case of the number of carbons is 14, and 16, these structure are called “myristic acid”, and “palmitic acid”, respectively. On the other hand, the hydrocarbon tail which is called unsaturated chain includes at least one double bond between carbons. Unsaturated chain tends to decrease phase transition temperature significantly as compared with hydrocarbon tail that is same chain length composed of single bond. In the case of the number of carbons is 18 and hydrocarbon tail includes one double bond are called as “oleic acid”. Therefore, when the head group is phosphatidyl-choline, and both hydrocarbon chain are oleic acid, the lipid called “di-oleoyl-phosphatidyl-choline (DOPC)”. The phase transition temperature of DOPC is -20°C. And if the lipid is composed phosphatidyl-choline and two palmitic acid, this lipid called “di-palmitoyl- phosphatidyl-choline (DPPC)”. The phase transition temperature of DPPC shows 40°C (Fig.1-1). Phospholipid molecules tend to form bilayer structure spontaneously in aquatic solution.

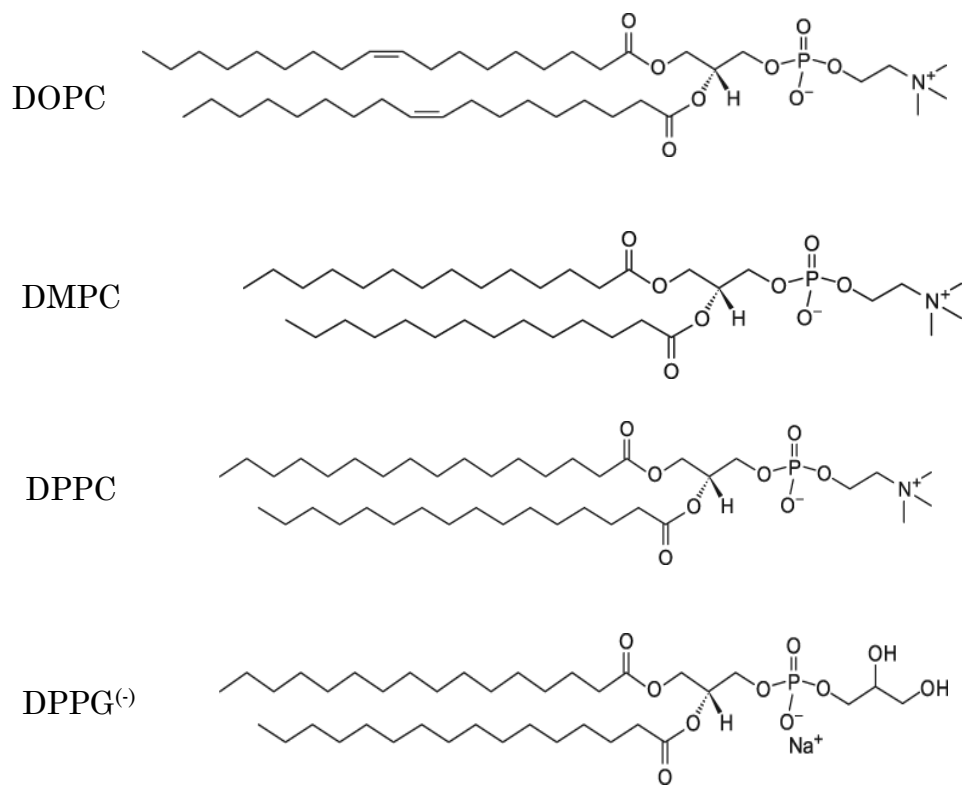


Fig.1-1 The chemical structure of various phospholipids

1-2 Biomembrane structure:

2D dynamics (phase separation) and 3D dynamics (morphological change)

The basic structure of biomembrane is lipid bilayer composed of various types of lipid molecules. Biomembranes not only distinguish between inner and outer environment of cell but also involve wide range of life phenomenon through the dynamic structural changes, such as two-dimensional (2D) phase separation, and three dimensional (3D) morphological changes. These structural changes are recognized as “membrane dynamics”. Membrane dynamics plays a very important role for expression of cell function.

The 2D-dynamics is represented by phase separation called “lipid raft”. Previously, the fluid mosaic model has been most considered as models of surface structure in biomembrane¹ (Fig.1-2A). In this model, various phospholipids and membrane proteins diffuse uniformly. However, phase separation structure called raft model has been suggested by recent researches²⁻⁴. Lipid rafts are micro domain structure which is enriched with saturated lipids, cholesterol(Fig.1-2B). In addition, various types of membrane protein such as receptor and membrane channels are localized in lipid rafts. Therefore, lipid rafts are expected to function as platforms on which proteins are attached during signal transduction and membrane trafficking^{5,6}.

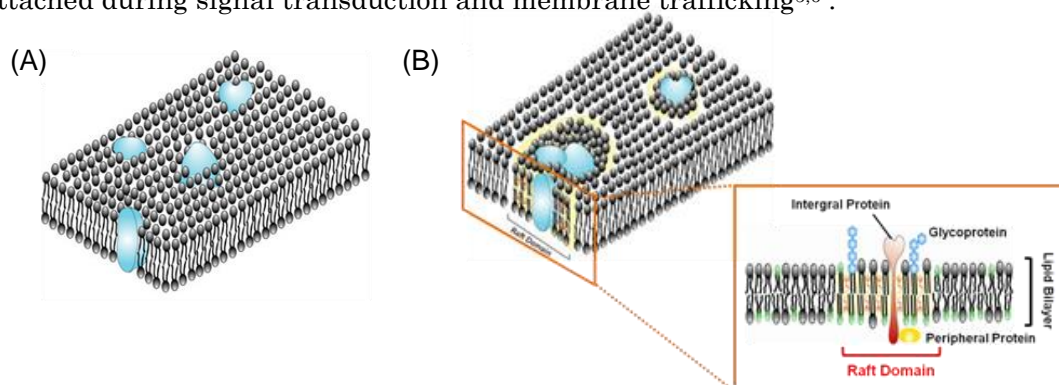


Fig.1 (A) fluid mosaic model and (B) raft model

The 3D-dynamics is morphological change⁴. Cellular organelles such as Golgi apparatus, mitochondria, and endoplasmic reticulum have complicated membrane morphology (Fig.1-3A). Regulation of the membrane morphological change is critical for many cellular processes. For example, curvature changes of membrane are observed in endocytosis, phagocytosis, and vesicular transport ⁷⁻⁹ (Fig.1-3B). In addition, the structural change of membrane from disk to sphere is observed in autophagy.

Moreover, coupling between membrane 2D and 3D dynamics is suggested in biomembrane^{10,11}. Lipids directly affect the physicochemical properties of lipid bilayer. For example, lipid rafts which are enriched saturated lipid and cholesterol have been shown to play a role of autophagy and endocytosis (Fig.1-4). Lipid shape or even more specifically, spontaneous curvature of lipid molecule contributes the regulation of this dynamics. Cone shape lipids prefer or induce positive curvature, whereas inverse cone shape lipids prefer or induce negative curvature. 2D dynamics induce 3D dynamics by controls specific localization of lipids which have spontaneous curvature.

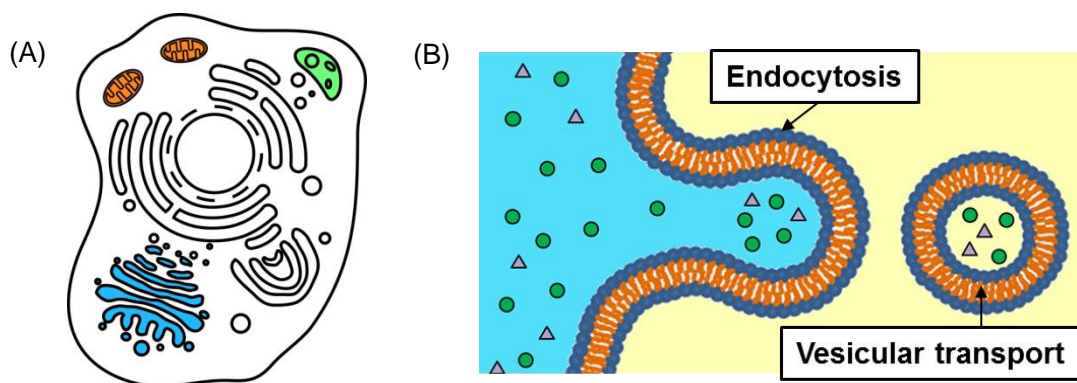


Fig.1-3 Schematic image of (A) cellular organelles and (B) endocytosis and vesicular transport

Therefore, membrane 2D and 3D dynamics are deeply committed various cellular functions and it is very important to explore the physicochemical properties of membrane to understanding the mechanisms of these functions. However, in living cell, biomembrane interacts complicatedly with various proteins, extracellular or intracellular fluid, nucleic acid, and each cell organelles. Thus, it is very difficult to detect only membrane property using living cell experiment.

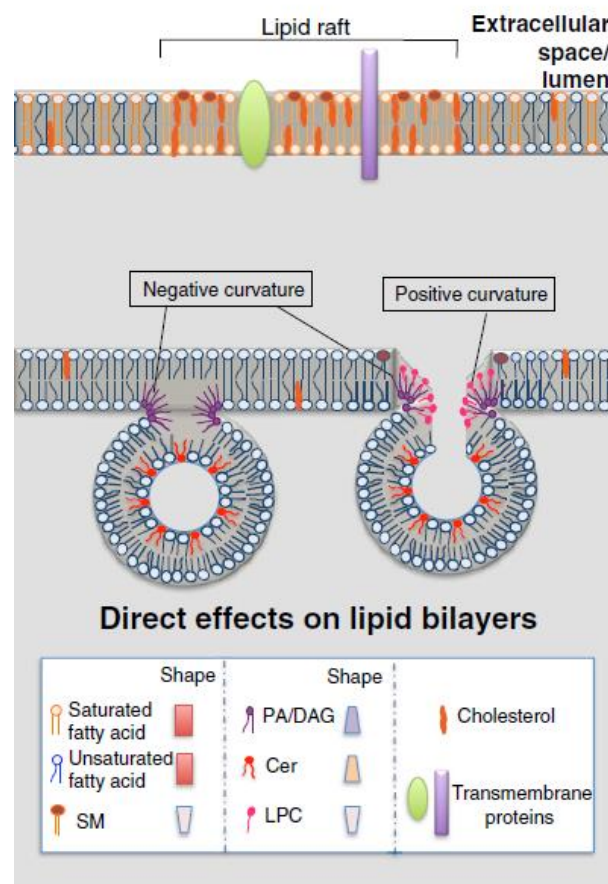


Fig.1-4 Model of coupling between 2D and 3D dynamics in biomembrane

1-3 Model biomembrane: Cell size liposome

Phospholipid molecule that is main component of biomembranes is consisting on hydrophilic part and hydrophobic part. In 1964, Bangham *et. al* found that the vesicular formation of lipid membrane when lipid molecules are suspended in an aqueous solution. This lipid vesicle is called as “liposome” (Fig.1-5)¹². The characteristics of the system of liposome, experiment processes such as preparation, observation, and analysis were easier than using living cell. In addition, liposome can prepare same size as living cell ($10\mu\text{m}\sim$), and it called “Giant unilamellar vesicles (GUVs)”. GUVs are large enough to be observed directly by microscopic methods^{13,14}. Therefore, to reveal the physicochemical properties of lipid membrane, liposome is commonly used as model for biomembranes.

Liposome also shows high affinity to biological object, and it has the potential to use in a wide range of biomedical application, such as carriers for drugs delivery system, micro actuator, cosmetics, and health foods.

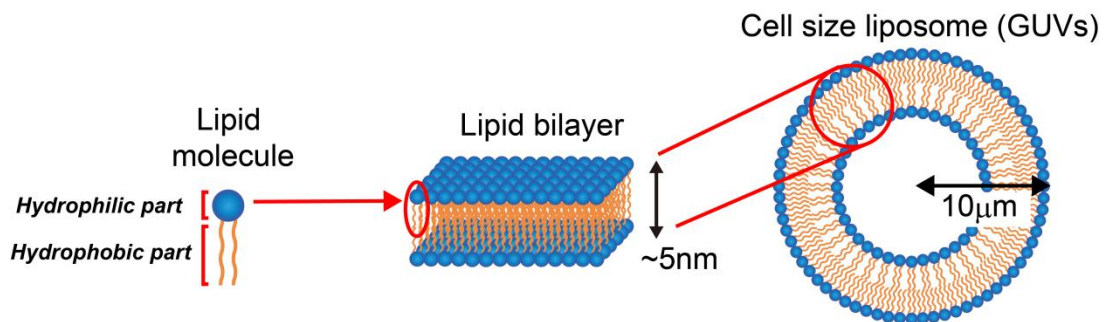


Fig.1-5 Schematic image of liposome

1-4 Reproductions of biomembrane 2D- and 3D- structure using GUVs

In recently studies, 2D- and 3D- structures of biomembrane were reproduced by using GUVs. In 2D-dynamics researches, phase separation structure was observed in mixtures composed of high melting temperature lipids (saturated lipid), low melting temperature lipids (unsaturated lipid), and cholesterol ^{15,16}. Fig.1-6 shows phase diagram and surface structures of GUVs in ternary mixtures of Unsaturated lipid dioleoyl-sn-glycero-3-phosphocholine (DOPC), Saturated lipid dipalmitoyl-sn-glycero-3-phosphocholine (DPPC), and Cholesterol (Chol). In high concentration of DOPC and Chol, GUVs shows one-phase structure. This phase structure is called liquid disorder (L_d) phase (Fig.1-6A). In middle concentration of Chol (15~40%), we can observe phase separation structure as shown in Fig.1-6B. The white region is L_d phase, whereas the circular black domains are liquid order (L_o) phase which is mainly composed of saturated lipid (DPPC) and Chol. Lipid raft of biomembrane is also composed of saturated lipid and cholesterol, L_d/L_o phase structure of GUVs is used as raft model. Moreover, in Chol concentration is low (~15%), anisotropic shape domain is observed (Fig.5C). This domain is enriched with DPPC, and called solid order (S_o) phase.

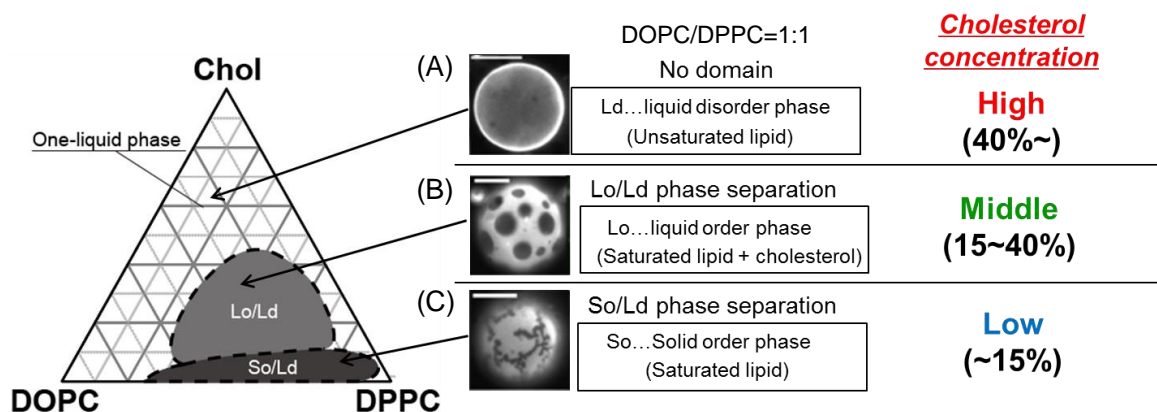


Fig.1-6 Phase diagram and microscopic image of GUVs

In 3D-dynamics researches, morphological changes were reproduced using GUVs by external stimuli. Hamada. *et. al* found the dynamic response by addition of osmotic pressure or surfactant¹⁷. Fig.1-7A shows the effect of osmotic stress by adding glucose on single phase GUVs of DOPC. Membrane morphology of GUV is changed from spherical shape to ellipsoid shape. This structural change is well known that the decrease in aqueous volume of inner GUVs due to osmotic pressure results in a various morphological change¹⁸. In addition, when GUVs are composed of DOPC/DPPC/Chol=40:40:20 exhibiting raft model structure, inner-budding like a endocytosis are observed by adding osmotic pressure (Fig.1-7B).

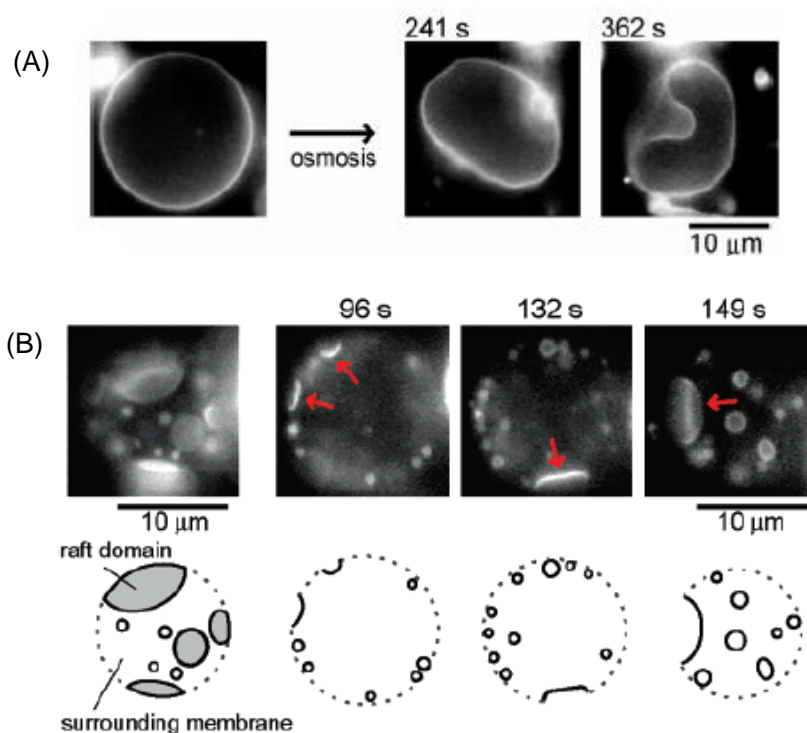


Fig.1-7 (A)Fluorescent images of the 3D-dynamics in homogeneous DOPC GUVs by osmotic pressure adding glucose (B) Fluorescent images of the 3D-dynamics in raft model GUVs by osmotic pressure adding glucose.

In this way, previous studies have succeeded in reproducing the membrane 2D and 3D dynamics such as phase separation and morphological change by using model biomembrane GUVs. However, it is poorly understood how biomembrane controls these 2D and 3D dynamics. The main reason for this belief is previous systems of model membrane were not considered the contribution of biomembrane environments.

1-5 Charged lipid molecules and electrostatic interaction

In the past, most of the studies have investigated the lipid membrane structure in uncharged model membranes^{19,20}. However, biomembranes also include negatively charged lipids. Table.1-1 shows the lipid composition in various biomembranes. In particular, phosphatidylglycerol (PG⁻) is found with high fractions in prokaryotic membranes. In this respect it is worth mentioning that in *Escherichia coli* membrane includes 15% of PG⁻²¹. Although the charged lipid fraction in eukaryotic plasma membranes is lower, its cellular organelles such as mitochondria and lysosome are enriched with several types of charged lipids²². For example, the inner membrane of mitochondria includes 20% of charged lipids such as cardiolipin (CL⁻), phosphatidylserine (PS⁻) and PG⁻²³.

Table.1-1 Lipid composition in biomembranes

source	PG	Cholesterol	PC	SM	PE	PI	PS	CL	PA	Glycolipids
Mitochondria (internal membrane)	2.0	3.0	45	2.5	24	6.0	1.0	18.0	0.7	—
(external membrane)	2.5	5.0	50	5.0	23	13.0	2.0	3.5	1.3	—
nucleic membrane	—	10.0	55	3.0	20	7.0	3.0	—	1.0	—
<i>E. coli</i>	15.0	0	0	—	80	—	—	5.0	—	—

Some important biomolecules such as nucleic acid and proteins have electric parts, it is considered that positively charged parts of biomolecule is attached to negatively charged membrane by electrostatic interaction. Lipid rafts include with negatively charged lipid PS⁽⁻⁾ and phosphatidic acid (PA⁽⁻⁾) , and may act specific landmarks for variety of biomolecules. Thus, it is very important to clarify the effect of charged lipid molecules on membrane 2D dynamics. Moreover, mitochondria shows complicate structure in internal membrane called Cristae, and CL⁽⁻⁾ contributes the stabilization of this structure(Fig.1-8) ²³. It is suggested that charged lipid molecules also affect membrane 3D dynamics. Therefore, it is indispensable to include the effects of electrostatic interactions on the 2D- and 3D- dynamics in biomembranes.

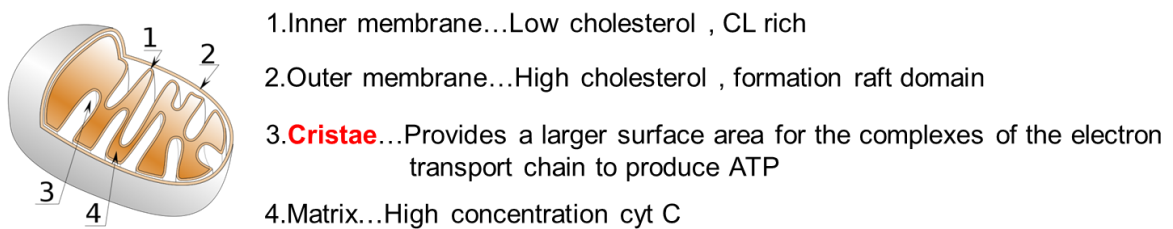


Fig.1-8 Schematic image of Mitochondria

1-6 Previous study about charged lipid membrane

In related studies, Shimokawa *et al*^{24,25} studied mixtures consisting of neutral saturated lipid (DPPC), negatively charged unsaturated lipid (DOPS⁽⁻⁾) and cholesterol(Fig.1-9). The main result is the suppression of the phase separation due to electrostatic interactions between the charged DOPS⁽⁻⁾ lipids. Other relevant studies are worth mentioning. Vequi-Suplicy *et al* reported the suppression of phase separation using other charged unsaturated lipids²⁶. Blosser *et al* investigated the phase diagram and miscibility temperature in mixtures containing charged lipids²⁷. Pataraia *et al*, have found to cytochrome c which is positive charged membrane protein existed in mitochondria induces micron-sized domains in ternary mixtures of charged unsaturated lipid(DOPG), egg sphingomyelin and cholesterol²⁸. However, the effects of electric charge on the phase structure in lipid/cholesterol mixtures have not been addressed so far systematically. In particular, the studies about phase behavior including charged saturated lipid mixtures, relationship between charged lipids and cholesterol localization, and the effect of charge on membrane morphology have not been performed nearly.

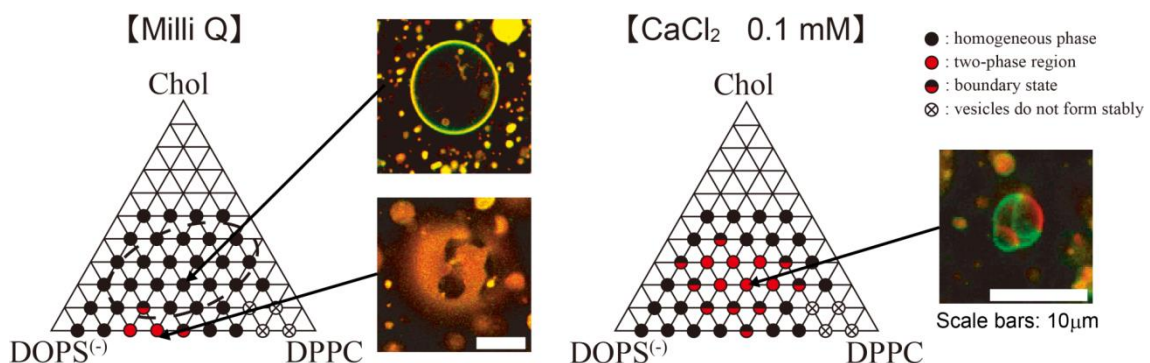


Fig.1-9 Ternary phase diagram of DOPS⁽⁻⁾/DPPC/Chol at room temperature. (A) Milli Q hydration. (B) hydrated with 0.1mM CaCl₂

1-7 Objects and outline

Previously, several 2D dynamics (phase separation) and 3D dynamic (morphological change) have been reproduced by change membrane composition in GUVs.

In the present study, we focus on the effects of electric charges of lipid molecules on membrane 2D and 3D dynamics. We investigate the physicochemical properties of model membranes containing various charged lipids, with the hope that the study will advance our understanding of biomembranes *in vivo*, which are much more complex. We clarify the electric charge effects on the 2D dynamics (phase behaviour) and 3D dynamics (membrane morphology) by direct observation using fluorescence microscopy and confocal laser scanning microscopy. In addition, the salt screening effect on charged membranes is also explored. We discuss the effects of charge on membrane 2D and 3D dynamics in below sections.

In chapter 2, we investigate the effects of charge on 2D dynamics in charged lipid GUVs. We observe phase behavior of charged lipid GUVs, and compare to non- charged lipid GUVs in simple binary mixtures (unsaturated lipid/ saturated lipid), ternary mixtures (neutral saturated lipid/charged saturated lipid/ cholesterol), and four-component mixtures (unsaturated lipid/ saturated lipid/cholesterol).

In chapter 3, we explore the effect of charge on localization of cholesterol in several mixtures including charged lipids. First, we observe the cholesterol localization in the typical neutral ternary system consisting of DOPC/DPPC/Chol. In the following, unsaturated lipid or saturated lipid is replaced with charged lipid. We also explored the salt screening effect, and compared the difference of electrostatic effect between monovalent cation (Sodium chloride: Na⁺) and bivalent cation (Magnesium chloride:

Mg²⁺).

In chapter 4, we investigated the effects of charge on 3D dynamics in binary mixtures (unsaturated lipid/ saturated lipid), ternary mixtures (neutral saturated lipid/charged saturated lipid/ cholesterol). We observed membrane morphology of charged lipid GUVs, and clarify the membrane properties by quantitatively measurement. Moreover, we discuss coupling between 2D and 3D dynamics of charged membranes by discussing qualitatively using a free energy modeling and numerical simulations.

1-8 References

1. Singer SJ, Nicolson GL. The fluid mosaic model of the structure of cell membranes. *Science (New York, N.Y.)* 1972;175(4023):720-31.
2. Simons K, Ikonen E. Functional rafts in cell membranes. *Nature* 1997;387(6633):569-572.
3. Simons K, Toomre D. Lipid rafts and signal transduction (vol 1, pg 31, 2000). *Nature Reviews Molecular Cell Biology* 2001;2(3):216-216.
4. Simons K, Sampaio JL. Membrane Organization and Lipid Rafts. *Cold Spring Harbor Perspectives in Biology* 2011;3(10).
5. Parton RG, Simons K. The multiple faces of caveolae. *Nature Reviews Molecular Cell Biology* 2007;8(3):185-194.
6. Simons K, Toomre D. Lipid rafts and signal transduction. *Nature Reviews Molecular Cell Biology* 2000;1(1):31-39.
7. Ishimoto H, Yanagihara K, Araki N, Mukae H, Sakamoto N, Izumikawa K, Seki M, Miyazaki Y, Hirakata Y, Mizuta Y and others. Single-cell observation of phagocytosis by human blood dendritic cells. *Japanese Journal of Infectious Diseases* 2008;61(4):294-297.
8. Rothman JE. Transport of the vesicular stomatitis glycoprotein to trans Golgi membranes in a cell-free system. *The Journal of biological chemistry* 1987;262(26):12502-10.
9. Beckers CJ, Block MR, Glick BS, Rothman JE, Balch WE. Vesicular transport between the endoplasmic reticulum and the Golgi stack requires the NEM-sensitive fusion protein. *Nature* 1989;339(6223):397-8.
10. Dall'Armi C, Devereaux KA, Di Paolo G. The Role of Lipids in the Control of Autophagy. *Current Biology* 2013;23(1):R33-R45.
11. Haucke V, Di Paolo G. Lipids and lipid modifications in the regulation of membrane. *Current Opinion in Cell Biology* 2007;19(4):426-435.
12. Bangham AD, Horne RW. NEGATIVE STAINING OF PHOSPHOLIPIDS AND THEIR STRUCTURAL MODIFICATION BY SURFACE-ACTIVE AGENTS AS OBSERVED IN THE ELECTRON MICROSCOPE. *Journal of molecular biology* 1964;8:660-8.
13. Cohen BE, Bangham AD. Diffusion of small non-electrolytes across liposome membranes. *Nature* 1972;236(5343):173-4.
14. Hamada T, Miura Y, Komatsu Y, Kishimoto Y, Vestergaard M, Takagi M.

- Construction of Asymmetric Cell-Sized Lipid Vesicles from Lipid-Coated Water-in-Oil Microdroplets. *Journal of Physical Chemistry B* 2008;112(47):14678-14681.
15. Veatch SL, Keller SL. Separation of liquid phases in giant vesicles of ternary mixtures of phospholipids and cholesterol. *Biophysical Journal* 2003;85(5):3074-3083.
 16. Saeki D, Hamada T, Yoshikawa K. Domain-growth kinetics in a cell-sized liposome. *Journal of the Physical Society of Japan* 2006;75(1):3.
 17. Hamada T, Miura Y, Ishii KI, Araki S, Yoshikawa K, Vestergaard M, Takagi M. Dynamic processes in endocytic transformation of a raft-exhibiting giant liposome. *Journal of Physical Chemistry B* 2007;111(37):10853-10857.
 18. Hotani H. Transformation pathways of liposomes. *Journal of molecular biology* 1984;178(1):113-20.
 19. Veatch SL, Keller SL. Organization in lipid membranes containing cholesterol. *Physical Review Letters* 2002;89(26):4.
 20. Baumgart T, Hess ST, Webb WW. Imaging coexisting fluid domains in biomembrane models coupling curvature and line tension. *Nature* 2003;425(6960):821-824.
 21. Dowhan W. Molecular basis for membrane phospholipid diversity: Why are there so many lipids? *Annual Review of Biochemistry* 1997;66:199-232.
 22. Schlame M. Thematic review series: Glycerolipids - Cardiolipin synthesis for the assembly of bacterial and mitochondrial membranes. *Journal of Lipid Research* 2008;49(8):1607-1620.
 23. Ardail D, Privat JP, Egretcharlier M, Levrat C, Lerme F, Louisot P. MITOCHONDRIAL CONTACT SITES - LIPID-COMPOSITION AND DYNAMICS. *Journal of Biological Chemistry* 1990;265(31):18797-18802.
 24. Shimokawa N, Hishida M, Seto H, Yoshikawa K. Phase separation of a mixture of charged and neutral lipids on a giant vesicle induced by small cations. *Chemical Physics Letters* 2010;496(1-3):59-63.
 25. Shimokawa N, Komura S, Andelman D. Charged bilayer membranes in asymmetric ionic solutions: Phase diagrams and critical behavior. *Physical Review E* 2011;84(3):10.
 26. Vequi-Suplicy CC, Riske KA, Knorr RL, Dimova R. Vesicles with charged domains. *Biochimica Et Biophysica Acta-Biomembranes* 2010;1798(7):1338-1347.
 27. Blosser MC, Starr JB, Turtle CW, Ashcraft J, Keller SL. Minimal Effect of Lipid Charge on Membrane Miscibility Phase Behavior in Three Ternary Systems. *Biophysical journal* 2013;104(12):2629-38.

28. Patarraia S, Liu Y, Lipowsky R, Dimova R. Effect of cytochrome c on the phase behavior of charged multicomponent lipid membranes. *Biochimica Et Biophysica Acta-Biomembranes* 2014;1838(8):2036-2045.

Chapter 2

The effect of charge on membrane 2D structure

2-1 Introduction

One of the major components of cell membranes is their lipid bilayer composed of a mixture of several phospholipids, all having a hydrophilic head group and two hydrophobic tails. Recently, a number of studies have investigated heterogeneities in lipid membranes in relation with the lipid raft hypothesis^{1,2}. Lipid rafts are believed to function as a platform on which proteins are attached during signal transduction and membrane trafficking³. It is commonly believed (but still debatable) that the raft domains are associated with phase separation that takes place in multi-component lipid membranes⁴.

In order to reveal the mechanism of phase separation in lipid membranes, giant unilamellar vesicles (GUV) consisting of mixtures of lipids and cholesterol have been used as model biomembranes⁵⁻⁷. In particular, studies of phase separation and membrane dynamics have been performed on such GUV consisting of saturated lipids, unsaturated lipids and cholesterol⁸. Multi-component membranes phase separate into domains rich in saturated lipids and cholesterol, whereas the surrounded fluid phase is composed largely of unsaturated lipids. The essential origin of this lateral phase separation was argued to be the hydrophobic interactions between acyl chains of lipid molecules.

In the past, most of the studies have investigated the phase separation in uncharged model membranes⁹⁻¹¹. However, biomembranes also include charged lipids, and, in particular, phosphatidylglycerol (PG⁽⁻⁾) is found with high fractions in prokaryotic membranes. In this respect it is worth mentioning that in *Staphylococcus aureus* the PG⁽⁻⁾ membranal fraction is as high as 80%, whereas the *Escherichia coli* membrane includes 15% of PG⁽⁻⁾¹². Although the charged lipid

fraction in eukaryotic plasma membranes is lower, its sub-cellular organelles such as mitochondria and lysosome are enriched with several types of charged lipids¹³. For example, mitochondria inner membrane includes 20% of charged lipids such as cardiolipin (CL⁽⁻⁾), phosphatidylserine (PS⁽⁻⁾) and PG⁽⁻⁾^{14,15}. It is indispensable to include the effect of electrostatic interactions on the phase behavior in biomembranes. To emphasize even further the key role played by the charges, we note that membranes composed of a binary mixture of charged lipids was reported to undergo a phase separation induced by addition of salt, even when the two lipids have same hydrocarbon tail¹⁶⁻¹⁸. For this charged lipid mixture, the segregation is mediated only by the electrostatic interaction between the lipids and the electrolyte.

In related studies, Shimokawa *et al*^{19,20} studied mixtures consisting of neutral saturated lipid (DPPC), negatively charged unsaturated lipid (DOPS⁽⁻⁾) and cholesterol. The main result is the suppression of the phase separation due to electrostatic interactions between the charged DOPS⁽⁻⁾ lipids. Two other relevant studies are worth mentioning. Veqi-Suplicy *et al*²¹, reported the suppression of phase separation using other charged unsaturated lipids, and more recently Blosser *et al*²² investigated the phase diagram and miscibility temperature in mixtures containing charged lipids. However, the effect of electric charge on the phase behaviour in lipid/cholesterol mixtures have not been addressed so far systematically.

In this chapter, we investigate the physicochemical properties of *model* membranes containing various mixtures of charged lipids, with the hope that the study will enhance our understanding of biomembranes *in-vivo*, which are much more complex. We examine the electric charge effect on the phase behaviour using fluorescent microscopy

and confocal laser scanning microscopy. In addition, the salt screening effect on charged membranes is explored. We discuss these effects in three stages starting from the simpler one. First, the phase diagram in charged *binary* mixtures of unsaturated and saturated lipids is presented. Second, we investigate the phase behaviour in *ternary* mixtures consisting of saturated lipids (charged and neutral) and cholesterol. And third, we include the change of phase behaviour when a charged saturated lipid is added as a *fourth* component to a ternary mixture of neutral saturated and unsaturated lipids and cholesterol. We conclude by discussing qualitatively the phase behaviour of charged membranes using a free energy modeling. The counterion concentration adjacent to the charged membrane is calculated in order to explore the relation between the electric charge and the ordering of hydrocarbon tail.

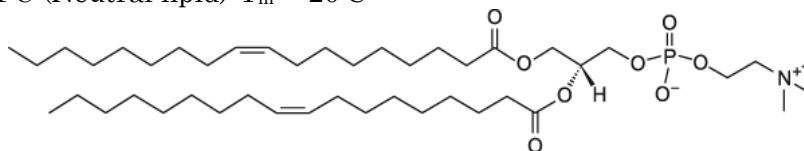
2-2 Materials and methods

Materials

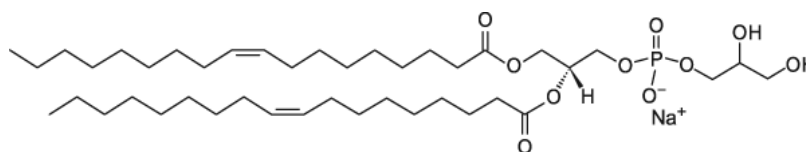
Materials are used in this chapter are shown in Fig.2-1. Neutral unsaturated lipid dioleoyl-sn-glycero-3-phosphocholine (DOPC, with chain melting temperature, $T_m = -20^\circ\text{C}$), neutral saturated lipid dipalmitoyl-sn-glycero-3-phosphocholine (DPPC, $T_m = 41^\circ\text{C}$), negatively charged unsaturated lipid 1,2-dioleoyl-sn-glycero-3-phospho-(1'-rac-glycerol) (sodium salt) (DOPG⁻, $T_m = -18^\circ\text{C}$), negatively charged saturated lipid 1,2-dipalmitoyl-sn-glycero-3-phospho-(1'-rac-glycerol) (sodium salt) (DPPG⁻, $T_m = 41^\circ\text{C}$), and cholesterol, were obtained from Avanti Polar Lipids (Alabaster, AL). BODIPY labelled cholesterol (BODIPY-Chol) and Rhodamine B 1,2-dihexadecanoyl-sn-glycero-3-phosphoethanolamine (Rhodamine-DHPE) were purchased from Invitrogen (Carlsbad, CA). Deionized water was obtained from a Millipore Milli-Q purification system. We chose phosphatidylcholine (PC) as the neutral lipid head and phosphatidylglycerol (PG⁻) as the negatively charged lipid head because the chain melting temperature of PC and PG⁻ lipids having the same acyl tails, is almost identical. In cellular membranes, PC is the most common lipid component, and PG is highly representative among charged lipids.

Unsaturated lipids

- DOPC (Neutral lipid) $T_m = -20^\circ\text{C}$

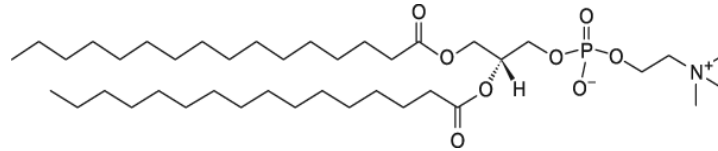


- DOPG⁻ (Negatively charged lipid) $T_m = -18^\circ\text{C}$

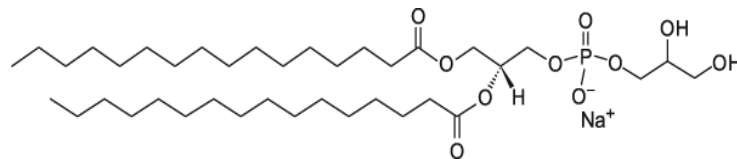


Saturated lipids

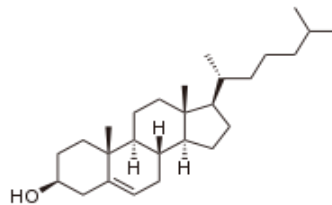
- DPPC (Neutral lipid) $T_m = 41^\circ\text{C}$



- DPPG⁽⁻⁾ (Negatively charged lipid) $T_m = 41^\circ\text{C}$

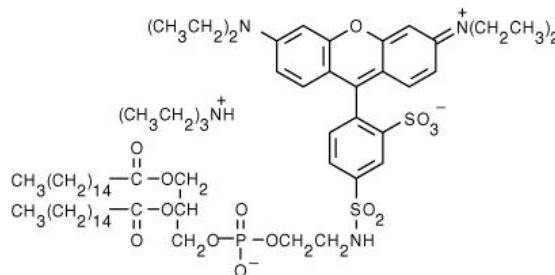


Cholesterol



Fluorescent dyes

- Rhodamine-DHPE (labels liquid phase)



- BODIPY-Cholesterol (labels cholesterol-rich phase)

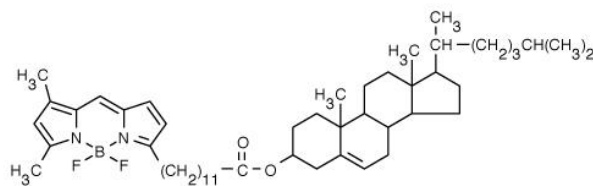


Fig.2-1 molecular structure of lipids and fluorescent dyes

Preparation of giant unilamellar vesicles

Giant unilamellar vesicles (GUVs) were prepared by gentle hydration method(Fig.2-2). Lipids and fluorescent dyes were dissolved in 2:1(vol/vol) chloroform/methanol solution. The organic solvent was evaporated under a flow of nitrogen gas, and the lipids were further dried under vacuum for 3h. The films were hydrated with 5 μL deionized water at 55 $^{\circ}\text{C}$ for 5 min (pre-hydration), and then with 200 μL deionized water or NaCl solution for 1-2 h at 37 $^{\circ}\text{C}$. The final lipid concentration was 0.2 mM. The fluorescent dyes NBD-PE, Rhodamine-DHPE and BODIPY-Chol concentrations were 0.1 μM , 0.1 μM and 0.2 μM , respectively (0.5% or 1% of lipid concentration).

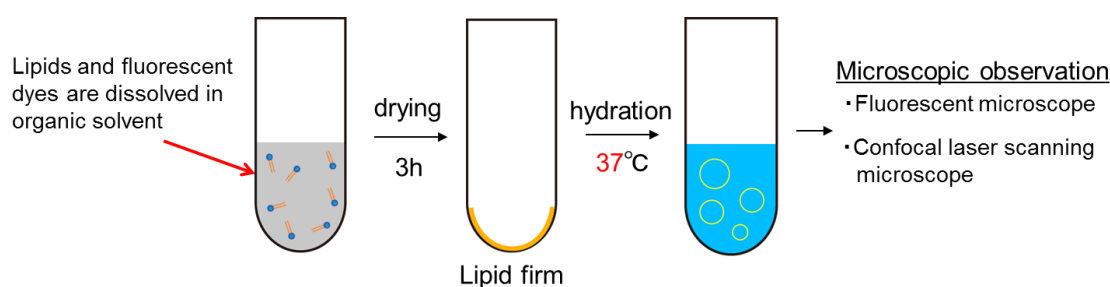


Fig.2-2 Preparation process of GUVs

Microscopic observation

The GUV solution was placed on a glass coverslip, which was covered with another smaller coverslip at a spacing of ca. 0.1 mm (Fig.2-3). We observed the membrane structures with a fluorescent microscope (IX71, Olympus, Japan) and a confocal laser scanning microscope (FV-1000, Olympus, Japan). In this chapter, Rhodamine-DHPE and BODIPY-Chol were used as fluorescent dyes. Rhodamine-DHPE labels the lipid liquid phase, whereas BODIPY-Chol labels the cholesterol-rich one. A standard filter set U-MWIG with excitation wavelength, $\lambda_{\text{ex}}=530\text{--}550\text{nm}$, and emission wavelength, $\lambda_{\text{em}}=575\text{ nm}$, was used to monitor the fluorescence of Rhodamine-DHPE, and another

filter, U-MNIBA with $\lambda_{\text{ex}}=470\text{--}495\text{ nm}$ and $\lambda_{\text{em}}=510\text{--}550\text{ nm}$, was used for the BODIPY-Chol dye. The sample temperature was controlled with a microscope stage (type 10021, Japan Hitec).

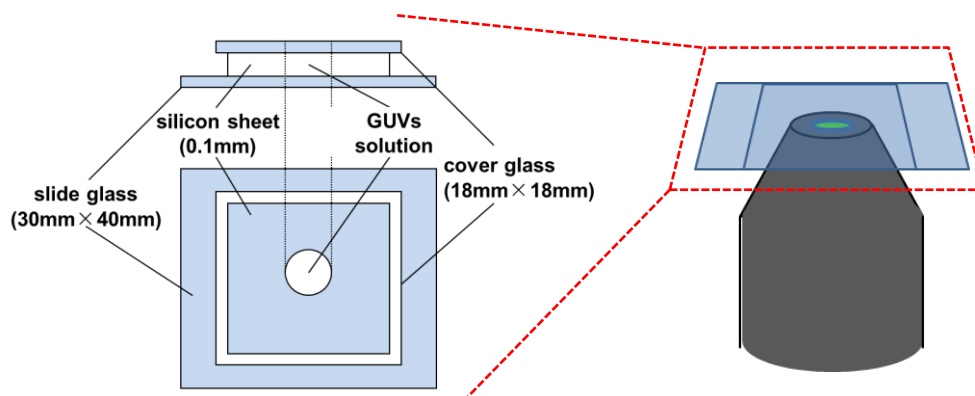


Fig.2-3 Schematic of sample chamber and observation method

Experimental condition

In this study, we controlled surface charging by change lipid composition and preparing with electrolyte for all studied systems. First, we changed the percentage of negatively charged lipids (Fig.2-4A). Second, we screened the head group charge of $\text{PG}^{(-)}$ by hydration with NaCl solution(Fig.2-4B). We observed surface structure of membrane for each condition. By comparison between these conditions, we can discuss the contribution of electric charge on membrane surface structure more deeply.

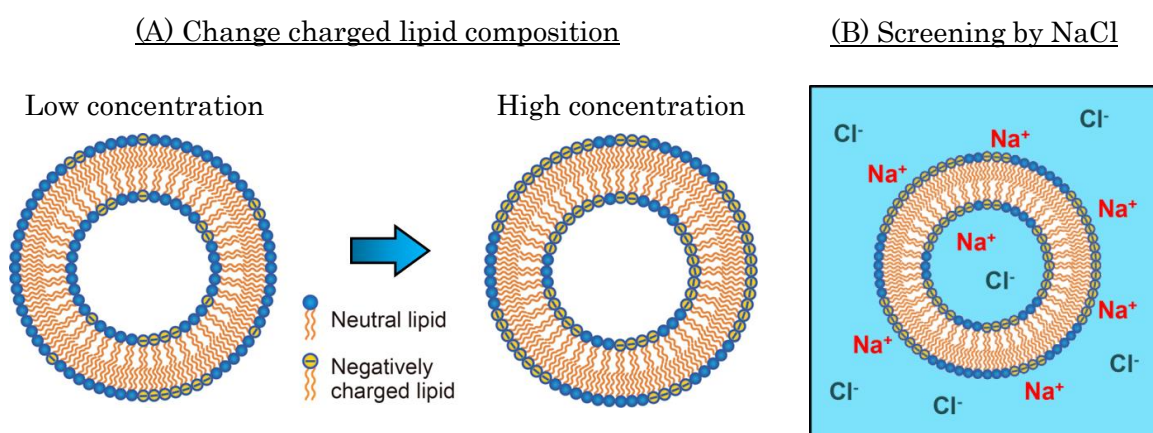


Fig.2-4 Schematic of experimental condition

Measurement of miscibility temperature

The miscibility temperature corresponds to the boundary between one- and two-phase regions. It is defined as the phase separation point at which more than 50% of the phase-separated domains have disappeared upon heating. The temperature was increased from room temperature to the desired temperature by 10 °C/min, and a further delay of 5 min was used in order to approach the equilibrium state. We then measured the percentage of vesicles that were in the two-phase coexisting region. If the percentage of such two-phase vesicles was over 50%, the temperature was further increased by 2 °C. We continued this procedure until the percentage of two-phase vesicles decreased below 50%.

Measurement of area percentage of domain

To clarify physiological property of charged membrane, we performed quantitative analysis of membrane surface structure. We measured the area percentage of phase separated domain from microscope image of GUV for each studied system. We used Image J or Fiji which are free software of image analysis. We binarized microscopic image of membrane surface, and measured domain area (black region). Percentage of domain is calculated by division process between membrane surface area and domain area (Fig.2-5).

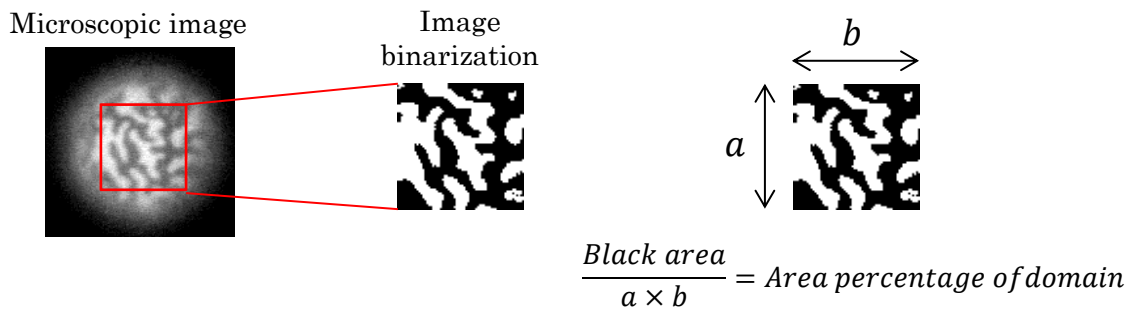


Fig.2-5 Measurement method of phase separated domain area

2-3 Experimental results

2-3-1 Binary lipid mixtures (Unsaturated lipid/ Saturated lipid)

First, we focused on the effect of charge on the phase separation of binary unsaturated lipid/ saturated lipid mixtures. In this section, we used neutral unsaturated lipid DOPC, neutral saturated DPPC, negatively unsaturated lipid DOPG⁽⁻⁾, and negatively saturated lipid DPPG⁽⁻⁾. The fluorescent dye Rho-DHPE was used for label liquid disorder (L_d) phase that is unsaturated lipid-rich phase. We observed the phase separation and measured the miscibility temperatures in four different binary mixtures: DOPC/DPPC (neutral system), DOPC/DPPG⁽⁻⁾, DOPG⁽⁻⁾/DPPC, and DOPG⁽⁻⁾/DPPG⁽⁻⁾. We also investigated phase behavior and miscibility temperatures in presence of salt (by hydration with NaCl), and compared experiment results each of binary mixtures. Fig.2-6 shows the phase behavior in three binary mixtures (DOPC/DPPC, DOPC/DPPG⁽⁻⁾, and DOPG⁽⁻⁾/DPPC) taken for three temperatures: $T = 22^\circ\text{C}$, 30°C , and 40°C . Each of images was taken by superimposing several pictures at slightly different focus position of the confocal laser scanning microscope. At room temperature (22°C), all three mixtures exhibit a phase separation (images 7,8, and 9). The red regions indicate the L_d phase that includes a large amount of the unsaturated lipid, while the dark regions represent the solid-ordered (S_o) phase that is enriched with saturated lipid. When the temperature raised to 30°C , the phase separation of DOPG⁽⁻⁾/DPPC mixture disappeared (image 6). On the other hand, the two other mixtures (DOPC/DPPC and DOPC/DPPG⁽⁻⁾) still retained the phase separated structure (image 4 and 5). As the temperature was further increased to 40°C , the DOPC/DPPC mixture also become homogeneous (image 1), whereas DOPC/DPPG⁽⁻⁾ mixture still retained its phase separated structure (image2). As a results, DOPC/DPPG⁽⁻⁾ mixture

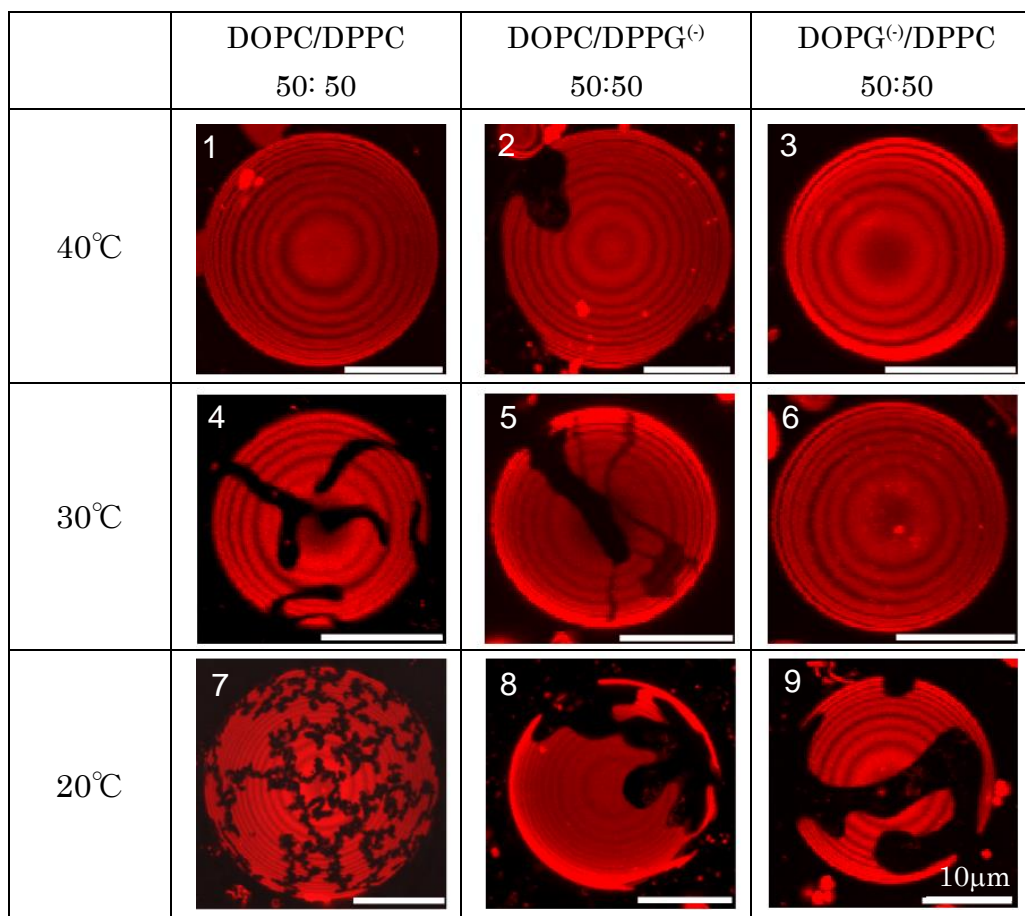


Fig.2-6 Microscopic image of the phase separation in binary lipid mixtures (DOPC/DPPC, DOPC/DPPG⁽⁻⁾, DOPG⁽⁻⁾/DPPC). Red region labeled by Rho-DHPE shows unsaturated-rich (L_a) phase. Black region indicates saturated-rich (S₀) phase.

shows highest miscibility temperature of all studied systems. Note that a similar phase-separated structure was reported in binary mixtures of egg sphingomyelin (eSM)/DOPG⁽⁻⁾^{21,23}.

Miscibility temperatures of binary mixtures are summarized in Fig.2-7. The filled circles denote the neutral lipid mixture, DOPC/DPPC. We also examined charged binary mixtures of two negatively charged lipids, DOPG⁽⁻⁾/DPPG⁽⁻⁾. The miscibility temperatures that are shown by open diamond in Fig.2-7 were quite similar to those of neutral DOPC/DPPC mixtures. When the neutral unsaturated lipid (DOPC) was replaced with the charged unsaturated lipid (DOPG⁽⁻⁾), the miscibility temperatures in

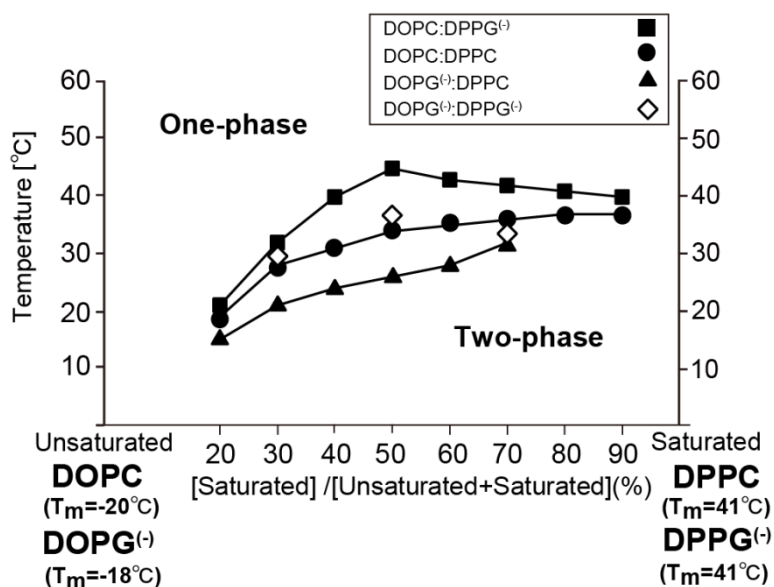


Fig.2-7 Phase boundary (miscibility temperature) between one-phase and two-phase regions (filled squares: DOPC/DPPG⁽⁻⁾, filled circles: DOPC/DPPC, filled triangles: DOPG⁽⁻⁾/DPPC, and open diamonds: DOPG⁽⁻⁾/DPPG⁽⁻⁾)

the DOPG⁽⁻⁾/DPPC that are by filled triangles in Fig.2-7 became lower as compared with a neutral lipid mixture, DOPC/DPPC. In other words, the phase separation is suppressed when a negatively charged unsaturated lipid is included. This result is consistent with previous studies performed on lipid mixtures containing negatively charged unsaturated lipids^{19,21-23}. At higher concentrations of DPPC, phase separated domains could not be observed for mixtures of DOPG⁽⁻⁾/DPPC = 20:80 and 10:90, because stable vesicle formation was prevented by the larger amount of DPPC.

We also replaced the neutral saturated lipid, DPPC, with the negatively charged saturated lipid, DPPG⁽⁻⁾. In the DOPC/DPPG⁽⁻⁾ mixture, the miscibility temperature (denoted by filled squares in Fig2-7) increases significantly as compared with the neutral system. In particular, we can see that a maximum in the miscibility temperature appears in the phase diagram around 50% relative concentration of the saturated lipid. Interestingly, at DOPC/DPPG⁽⁻⁾ = 50:50, the miscibility temperature of

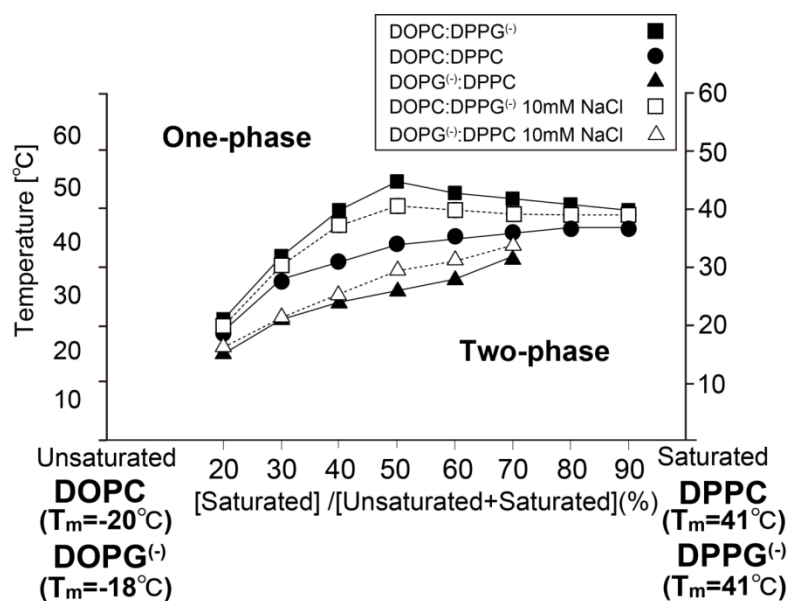


Fig.2-8 Comparison of miscibility temperatures between with or without salt in binary mixtures. (filled squares: DOPC/DPPG⁽⁻⁾, filled circles: DOPC/DPPC, filled triangles: DOPG⁽⁻⁾/DPPC, open squares: DOPC/DPPG⁽⁻⁾ with 10mM NaCl, and open triangles: DOPG⁽⁻⁾/DPPC)

about 44°C was higher than 41°C of the DPPG⁽⁻⁾ chain melting temperature. Thus, the phase separation is enhanced in mixtures containing the negatively charged saturated lipid (DPPG⁽⁻⁾). This result should be contrasted with the phase behaviour of the DOPG⁽⁻⁾/DPPC charged/ neutral mixture.

The phase behaviour of charged membranes is also investigated in the presence of salt (10 mM NaCl solution) for various charged/neutral mixtures. The miscibility temperatures of DOPG⁽⁻⁾/DPPC and DOPC/DPPG⁽⁻⁾ with NaCl solutions are indicated by open triangles and squares, respectively, in Fig. 2-8. The phase separation was enhanced by the addition of salt for DOPG⁽⁻⁾/DPPC, which is in agreement with the previous findings^{19,21}. On the other hand, the phase separation of DOPC/DPPG⁽⁻⁾ with NaCl was suppressed. It seems that the phase behaviour in charged membranes with salt approaches that of the neutral mixture, DOPC/DPPC. This is consistent with the fact that salt screens the electrostatic interactions of the charged DOPG⁽⁻⁾ and DPPG⁽⁻⁾.

2-3-2 Ternary mixtures (Saturated lipid (Charge or neutral)/ Cholesterol)

In general, cholesterol prefers to be localized in the saturated lipid-rich phase rather than in the unsaturated lipid-rich one. However, the localization of cholesterol also depends strongly on the structure of the lipid head group²⁴. In this ternary mixture, We used neutral saturated DPPC, negatively saturated lipid DPPG⁽⁻⁾, and cholesterol. The fluorescent dye Rho-DHPE and BODIPY-Chol was used for label liquid phase and cholesterol-rich phase, respectively. We investigated the localization of cholesterol and the resulting phase behaviour in ternary mixtures composed of a neutral saturated lipid, negatively charged saturated lipid and cholesterol, such as DPPC/DPPG⁽⁻⁾/Chol. The effect of the hydrocarbon tail was excluded by using lipids with the same acyl chain.

Microscopic images of saturated lipid/cholesterol mixtures are shown in Fig.10. For membranes consisting only of neutral lipids (DPPC/Chol = 80:20), the phase separation was not observed at room temperature, as shown in Fig. 2-9A. Both of Rho-DHPE and BODIPY-Chol were dispersed uniformly in this mixture. This result shows that observed phase was liquid order (L_o) phase rich in DPPC and Chol. In DPPC/Chol binary mixture, however, it was reported that the nanoscopic domains are formed even though they cannot be detected by optical microscopes²⁵. On the other hand, when we replaced a fraction of the DPPC with negatively charged lipid DPPG⁽⁻⁾, DPPC/DPPG⁽⁻⁾/Chol = 40:40:20, stripe-shaped domain was observed as shown in Fig. 2-9B. Since the stripe-shaped domain has an anisotropic shape, this is a strong indication that the domain is in the S_o phase. Localization of Rho-DHPE and BODIPY-Chol were conformed in this mixture, implies that striped S_o phase is surrounded by L_o phase.

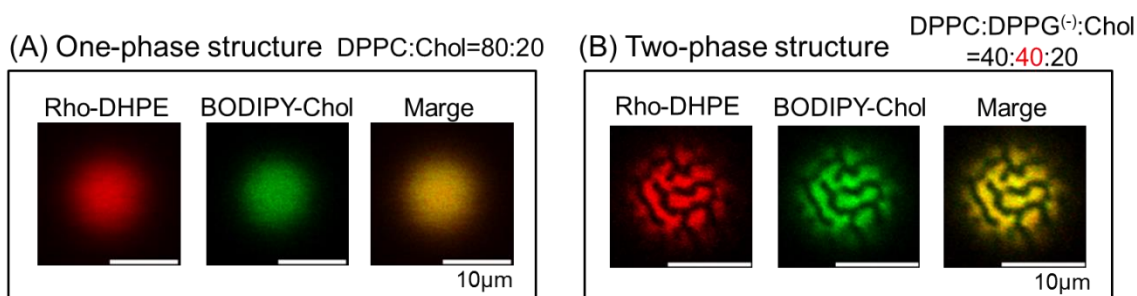


Fig.2-9 Microscopic images of phase separation in saturated lipid/cholesterol mixtures. Microscopic images of GUVs are taken at composition of DPPC/Chol = 80/20 (A) and DPPC/DPPG⁽⁻⁾/Chol=40:40:20 (B) in Milli Q water at 22°C

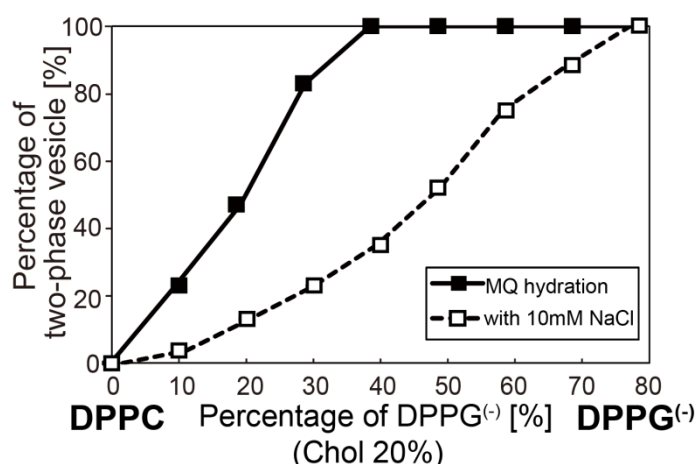


Fig.2-10 Percentage of two-phase vesicles at 22°C (Filled square: MQ hydration, Open square: with 10mM NaCl).

Next, we measured the percentage of two-phase vesicles and the area percentage of the S_0 phase for a fixed amount of Chol =20%. Fig.2-10 shows the percentage of two-phase vesicles. Percentage of two-phase vesicles increased continuously with DPPG⁽⁻⁾ concentration. However, in presence of salt (with 10mM NaCl hydration), the percentage of domain formation was decreased significantly. Fig.2-11 shows microscopic images of domain (Fig.2-11A) and area percentage of domain each of compositions (Fig.2-11B) for fixed Chol=20%. The area percentages of domain were increased with DPPG⁽⁻⁾ concentration, and were decreased in presence of salt.

The phase behavior of DPPC/DPPG⁽⁻⁾/Chol mixtures for Milli Q water and NaCl aqueous solutions is summarized in Fig. 2-12. Although the cholesterol solubility limit

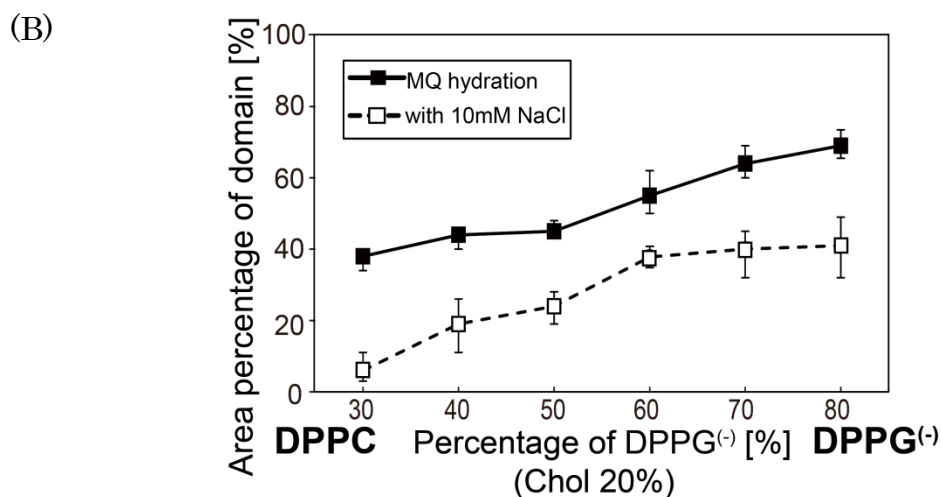
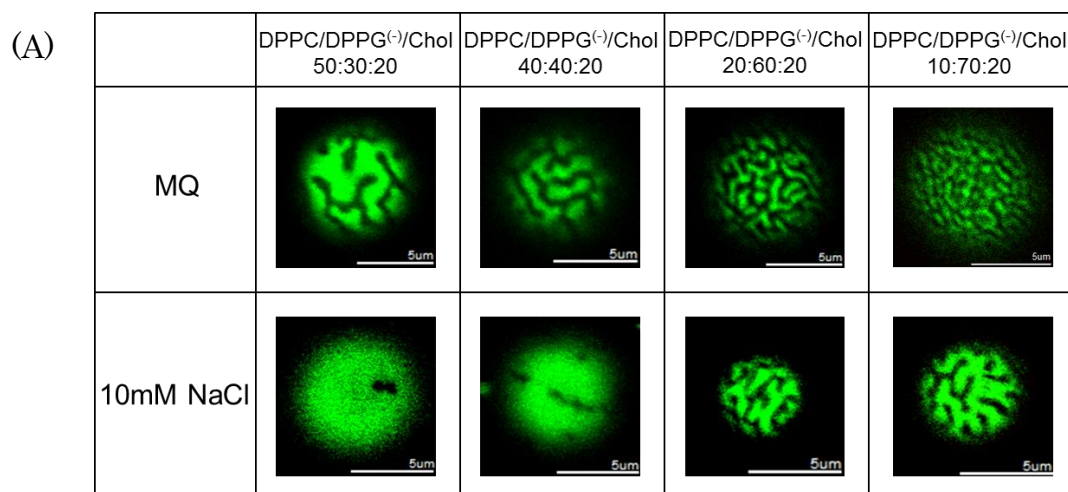


Fig.2-11 (A) Microscopic image of phase separation in DPPC/DPPG⁽⁻⁾/Chol mixtures for each component at 22°C. (B) Area percentage of the domain at 22°C as a function of DPPG⁽⁻⁾/DPPC ratio for fixed Chol = 20%. Filled and open squares indicate Milli Q and 10mM solution, respectively.

in phospholipid membranes is about 60%, we show the results for Chol > 60% to emphasize the phase boundary, especially in the case of Milli Q water. The phase behavior of DPPC/DPPG⁽⁻⁾/Chol mixtures in Milli Q water is summarized in the left diagram of Fig. 2-12. For higher concentrations of DPPC or cholesterol, two phase vesicles were not observed or rarely observed (open circles). On the other hand, their percentage clearly increases with the DPPG⁽⁻⁾ concentration (filled circles). In addition, the phase-separated regions with 1 mM and 10 mM of NaCl are indicated the center

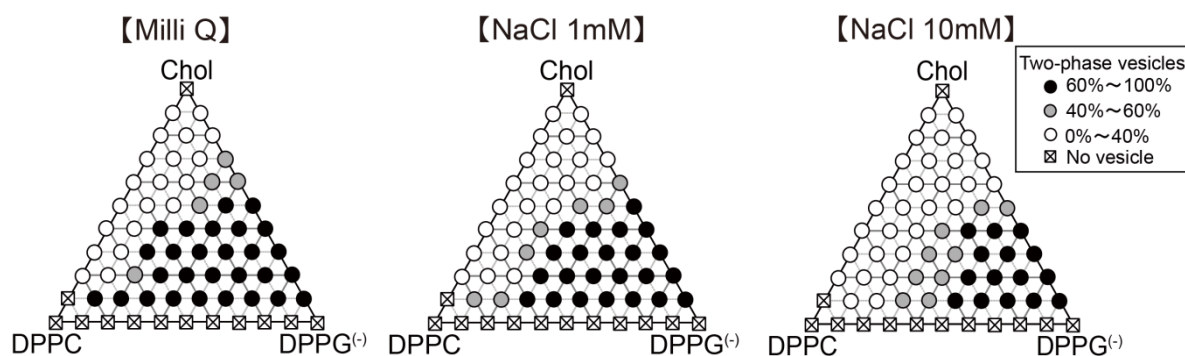


Fig.2-12 Phase diagrams of DPPC/DPPG⁽⁻⁾/Chol mixtures in Milli Q and NaCl solutions (left: Milli Q, centre: NaCl 1 mM, right: NaCl 10 mM) at room temperature (~22 °C). Filled, grey, and open circles correspond to systems where 60–100%, 40–60%, and 0–40% of the vesicles, respectively, exhibit two-phase regions.

and right of diagram in Fig.2-12. As the salt concentration is increased, the phase separation tends to be suppressed. This can be understood because DPPG⁽⁻⁾ is screened in the presence of salt and approaches the behaviour of the neutral DPPC. This observation is qualitatively consistent with the result of DOPC/DPPG⁽⁻⁾ mixtures shown in Fig. 2-7.

Three experimental findings led us to conclude that fluorescent (Red and green) and dark regions in the fluorescence images represent, respectively, DPPC/Chol-rich and DPPG⁽⁻⁾-rich phases. (i) The domain area (dark region) became larger as the percentage of DPPG⁽⁻⁾ was increased, as shown in Fig. 2-11. (ii) While the homogeneous phase is stable for DPPC/Chol mixtures, DPPG⁽⁻⁾/Chol mixtures show a phase separation. Therefore, cholesterol molecules mix easily with DPPC but not with DPPG⁽⁻⁾. (iii) We used BODIPY-Chol as a fluorescent probe that usually favors the cholesterol-rich phase. The BODIPY-Chol was localized in the red regions stained by Rhodamine-DHPE as shown in Fig.2-9. Although the bulky BODIPY-Chol may not behave completely like cholesterol, BODIPY-Chol is partitioned into the Chol-rich phase in all our experiments²⁶. In addition, we also observed the phase behaviors without BODIPY-

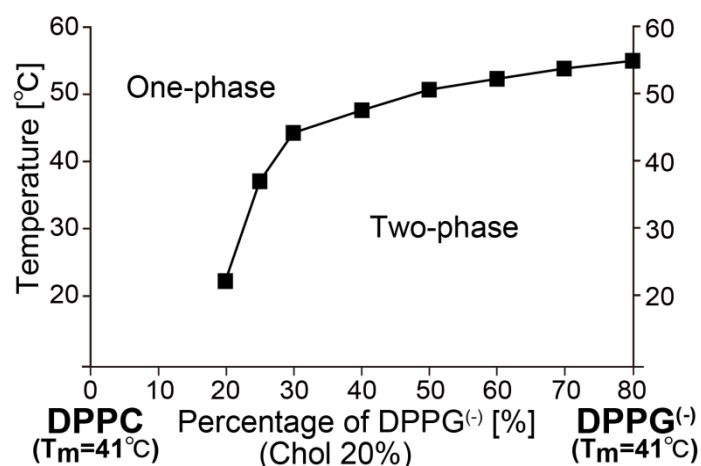


Fig.2-13 Phase boundary (miscibility temperature) between one-phase and two-phase regions in DPPC/DPPG⁻/Chol mixtures for fixed Chol=20%.

Chol, and the observed results did not change in any significant way. Thus, we think that bulky BODIPY–Chol plays a rather minor role in our study.

Since most of the cholesterol is included in the DPPC/Chol-rich region, the DPPC/Chol-rich region is identified as a liquid-ordered (L_o) phase. In contrast, the DPPG⁻-rich domain is in an S^o phase, because its domain shape is not circular but rather stripe-like. We also note that without cholesterol, a membrane composed of pure DPPG⁻ will be in an S_o phase at room temperature (lower than its chain melting temperature, $T_m = 41$ °C). Our results indicate that DPPG⁻ tends to repel DPPC and cholesterol. In other words, the interaction between the head groups of the lipids affects the localization of cholesterol. Furthermore, as the fraction of DPPG⁻ of DPPC/DPPG⁻/cholesterol membranes increases, the corresponding miscibility temperature also increases continuously (Fig. 2-13). For systems with the DPPG⁻ percentage of over 30%, a two-phase coexistence was observed even above the chain melting temperature of DPPG⁻. It implies that the head group interaction of DPPG⁻ makes a large contribution to the stabilization of the phase structure. We will further discuss this point in the Discussion section.

2-3-3 Four-component mixtures of lipid and cholesterol

From the results of ternary mixtures, we conclude that cholesterol prefers to be localized in the neutral DPPC-rich domains rather than in the DPPG⁽⁻⁾-rich ones.

Next, we investigated four-component mixtures of DOPC/DPPC/DPPG⁽⁻⁾/Chol. Previously, a number of studies have used the mixtures of DOPC/DPPC/Chol as a biomimetic system related to modelling of rafts⁸. In these mixtures, unsaturated lipids (DOPC) form an L_d-phase, whereas domains rich in saturated lipids (DPPC) and cholesterol form an L_o-phase. Aiming to reveal the effect of charge on the L_d /L_o phase separation, we replace a fraction of the DPPC component in the DOPC/DPPC/Chol mixture with negatively charged saturated lipid, DPPG⁽⁻⁾. We also screen head group charge by adding salt, and examined how the charged lipid, 4th component, affects phase organization of the ternary mixture.

In high concentration of DOPC for fixed at 60%, one-phase structure was observed in all components (Fig.2-14A and B). In this mixture, DOPC concentration was very high, so that it is possible that phase behavior showed L_d phase structure without forming phase separation.

Next, we fixed DOPC concentration at 40%. Fig.2-14C and D shows microscopic images and phase diagram in DOPC/DPPC/DPPG⁽⁻⁾/Chol mixtures for a fixed DOPC=40% and Chol=20%. For ternary mixtures with DOPC/DPPC/Chol = 40:40:20 (without the charged lipid), a phase separation is observed as shown in Fig.2-14(C1). The circular green domains labeled by BODIPY-Chol are rich in DPPC and cholesterol, inferring an L_o phase, while the red region labeled by Rhodamine-DHPE is a DOPC-rich (L_d) phase. When half of DPPC was replaced by the charged DPPG⁽⁻⁾, a distinct phase separation (three-phase coexistence) was

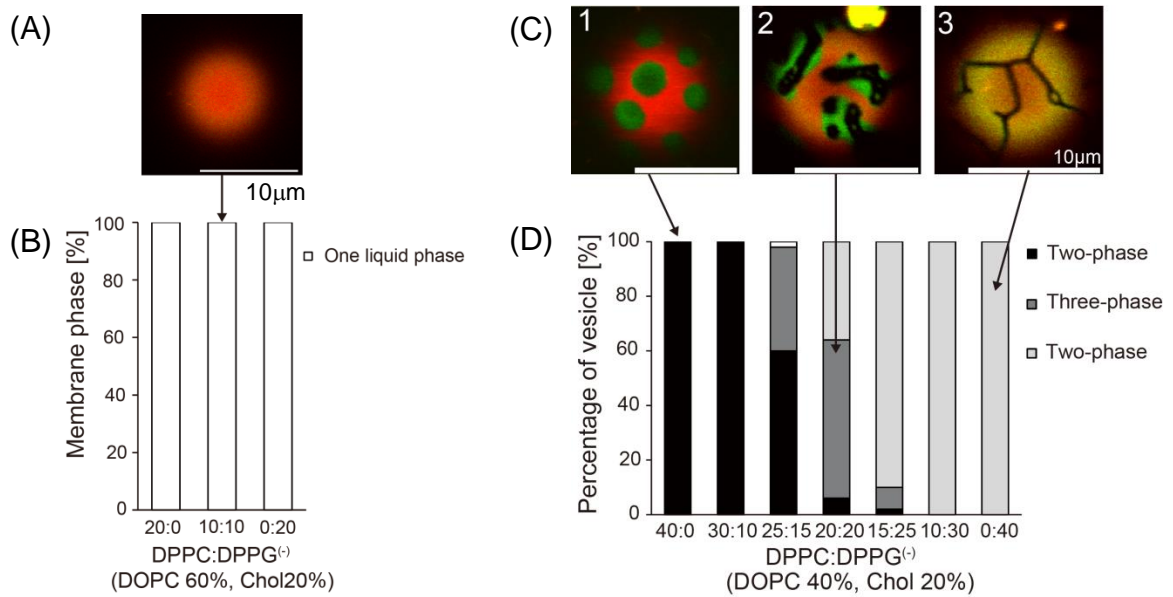


Fig.2-14 (A) Microscopic images of GUVs at compositions of DOPC/DPPC/DPPG⁽⁻⁾/Chol = 60/10/10/20. (B) The phase diagram of four-component mixtures fixed for DOPC=60%, and Chol=20% respectively. (C) Microscopic images of GUVs at compositions of DOPC/DPPC/Chol = 40/40/20 (image 1), DOPC/DPPC/DPPG⁽⁻⁾/Chol = 40/20/20/20 (image 2), and DOPC/DPPG⁽⁻⁾/Chol=40/40/20 (image 3) at 22 °C. Red, green, and dark regions indicate DOPC rich (L_d), DPPC/Chol rich (L_o), and DPPG⁽⁻⁾ rich (S_o) phases, respectively. The yellow region in image 3, which includes a large amount of DOPC and Chol indicates an L_d phase. (D) The phase diagram of four-component mixtures fixed for DOPC=40%, and Chol=20% respectively..

observed in the four-component mixture, DOPC/DPPC/DPPG⁽⁻⁾/Chol = 40:20:20:20, as shown in Fig. 2-14(C2). The black regions that appear inside the green domains, contain a large amount of DPPG⁽⁻⁾ as is the case of ternary mixtures. Because this black region excludes any fluorescent dyes, the DPPG⁽⁻⁾-rich region is inferred as the S_o phase. Moreover, for ternary mixtures of DOPC/DPPG⁽⁻⁾/Chol = 40:40:20 without DPPC, a coexistence between S_o and L_d phases is observed as shown in Fig. 2-14(C3). The phase diagram in four-component mixtures for fixed DOPC=40% and Chol20% is summarized in Fig.2-14D.

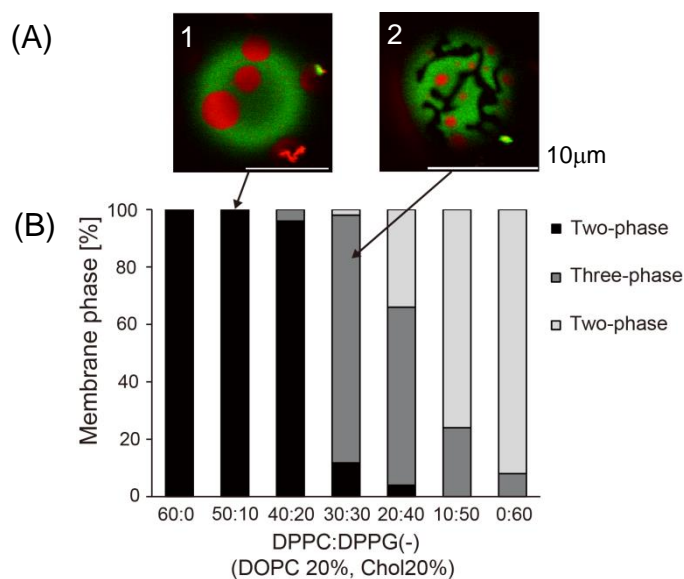


Fig.2-15 (A) Microscopic images of GUVs at compositions of DOPC/DPPC/Chol=20/60/20 (image 1), DOPC/DPPC/DPPG⁽⁻⁾/Chol = 20/30/30/20 (image 2). (B) The phase diagram of four-component mixtures fixed for DOPC=20%, and Chol=20% respectively.

Next, we fixed at low concentrations the DOPC=20%. In neutral mixture of DOPC/DPPC/Chol=20/60/20, L_d domain (red region) was formed in L_o phase (green region) (Fig.2-15(A1)). This phase structure is called as reverse domain structure⁸. When half of DPPC was replaced by the charged DPPG⁽⁻⁾, three-phase coexistence was observed in DOPC/DPPC/DPPG⁽⁻⁾/Chol = 20:30:30:20, as shown in Fig. 2-15(A2). In this three-phase structure, L_d domain and S_o domain (dark region) was appeared in L_o phase. Because this composition is accounted for 50% of DPPC and Chol which compose the L_o phase.

The phase diagram of DOPC/DPPC/DPPG⁽⁻⁾ for fixed Chol = 20% presented in Fig.2-16 shows that the phase-separation strongly depends on the DPPG⁽⁻⁾ concentration. The boundary between the L_o/S_o and L_d/S_o coexistence is not marked on the phase diagram, because from optical microscopy it was not possible to distinguish between the L_o and L_d phases. But the region where S_o

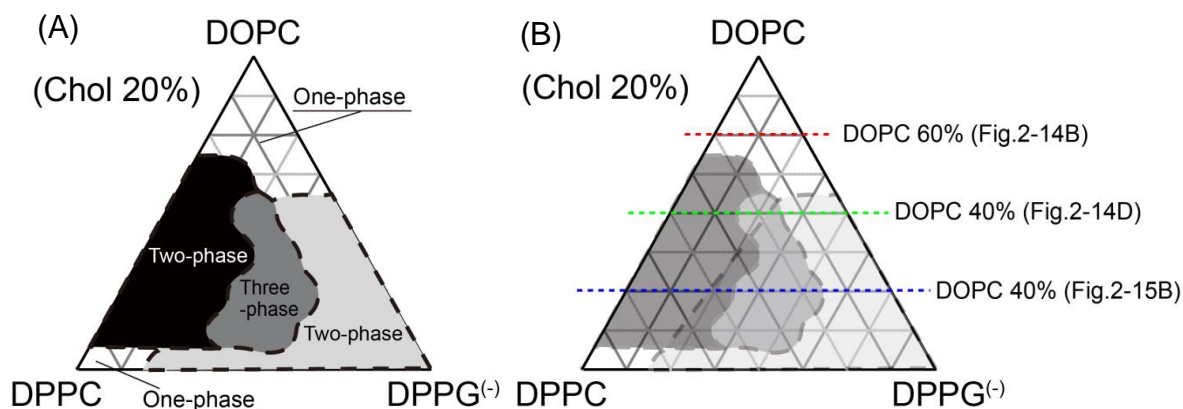


Fig.2-16 (A)Phase diagram of four-component mixtures of DOPC/DPPC/DPPG⁽⁻⁾/Chol for fixed Chol=20% at 22 °C. Black, grey, and light grey regions denote, respectively, L_o/L_d two-phase coexistence, L_o/L_d/S_o three-phase coexistence, and L_d/S_o or L_o/S_o two-phase coexistence.(B) Red dash line: DOPC 60%, Green dash line: DOPC 40%, Blue dash line: DOPC 20%, respectively.

coexists with either L_o or L_d is indicated as light grey region in the phase diagram.

Furthermore, we investigated the screening effects in four-component mixtures hydration with 10mM NaCl. Interestingly, at DPPC/DPPG⁽⁻⁾= 15:25, a transition between two-phase and three-phase coexistence was driven by adding salt, as is shown in the images of Fig. 2-17A. In Fig. 2-17B, the percentage of phase-separated vesicle hydrated with 10mM NaCl solution is presented for fixed fraction of DOPC=40% and Chol=20%. As shown in Fig. 2-17B, the phase separation changes with DPPG⁽⁻⁾ concentration. Without salt, the phase boundary between L_o/L_d two-phase coexistence, and L_o/L_d/S_o three-phase coexistence, is positioned at DPPC/DPPG⁽⁻⁾= 25:15 (Fig.2-14D). On the other hand, in 10mM NaCl solution, the phase boundary is DPPC/DPPG⁽⁻⁾= 20:20 (Fig.2-17B). The phase boundary between the L_o/L_d/S_o three-phase coexistence and L_d/S_o or L_o/S_o two-phase coexistence, also depends on the salt condition: the boundaries are

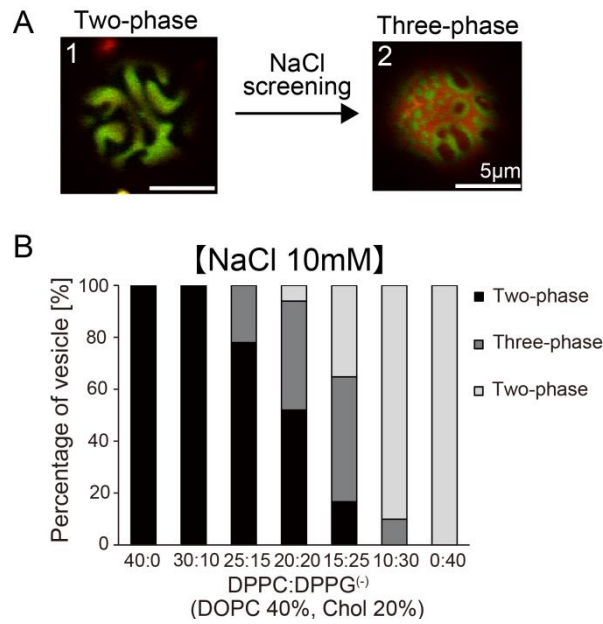


Fig.2-17 (A) Fluorescence microscopy images of phase separation in DOPC/DPPC/DPPG⁻/Chol=40:15:25:20 hydrated by Milli Q water (image 1) and 10mM NaCl solution (image 2) at 22 °C. (B) The phase diagram of four-component mixtures hydrated by 10mM NaCl solution. Temperature was fixed at 22 °C.

DPPC/DPPG⁻= 20:20 (without salt) and 15:25 (10mM NaCl). These results suggest that the addition of salt affects phase structure of DOPC/DPPC/DPPG⁻/Chol mixtures.

2-4 Discussion

One of our important results is that when neutral lipids are replaced by charged ones, the phase separation was suppressed for the DOPG⁽⁻⁾/DPPC mixtures, whereas it was enhanced for mixtures of DOPC/DPPG⁽⁻⁾. Furthermore, by adding salt, these two mixtures approached the behaviour of the non-charged DOPC/DPPC mixture. As mentioned above, it was reported in the past experiments^{19,21-23} that phase separation of other mixtures containing negatively charged unsaturated lipids was suppressed similarly to our DOPG⁽⁻⁾/DPPC result. However, the enhanced phase separation for DOPC/DPPG⁽⁻⁾ is novel and unaccounted for.

We discuss now several theoretical ideas that are related to these empirical observations based on a phenomenological free energy model^{19,20,27,28}.

The first step is to take into account only the electrostatic contribution to the free energy, f_{el} , using the Poisson-Boltzmann (PB) theory. For symmetric monovalent salts (e.g., NaCl), the electric potential $\Psi(z)$ at distance z from a charged membrane satisfies the PB equation:

$$\frac{d^2\Psi}{dz^2} = \frac{2en_b}{\epsilon_w} \sinh \frac{e\Psi}{k_B T}, \quad (1)$$

where e is the electronic charge, n_b the bulk salt concentration, and ϵ_w the dielectric constant of the aqueous solution, k_B the Boltzmann constant, and T the temperature. For a charged membrane with area fraction ϕ of negatively charged lipids, the surface charge density is written as $\sigma = -e\phi/\Sigma$. The cross-sectional area Σ of the two lipids is assumed, for simplicity, to be the same.

The PB equation (1) can be solved analytically by imposing σ as the electrostatic boundary condition, and the resulting electrostatic free energy is obtained as²⁹

$$f_{\text{el}}(\phi) = \frac{2k_{\text{B}}T}{\Sigma} \phi \left[\frac{1 - \sqrt{1 + (p_0\phi)^2}}{p_0\phi} + \ln(p_0\phi + \sqrt{1 + (p_0\phi)^2}) \right], \quad (2)$$

where $p_0 = 2\pi_B l_{\text{D}} / \Sigma$ is a dimensionless parameter proportional to the Debye screening length $l_{\text{D}} = \sqrt{\epsilon_{\text{w}} k_{\text{B}} T / 2e^2 n_{\text{b}}}$, and to $1/\Sigma$, while $l_{\text{B}} = e^2 / (4\pi\epsilon_{\text{w}} k_{\text{B}} T) \approx 7\text{\AA}$ is the Bjerrum length.

One essential outcome of the PB model is that for any p_0 , the electrostatic free energy f_{el} increases monotonically as a function of ϕ , and a large fraction of negatively charged lipid will increase the free energy substantially. This implies that any charged domain formed due to lipid/lipid lateral phase separation would cost an electrostatic energy. Hence, within the PB approach, the phase separation in charged/neutral mixtures of lipids should be suppressed (rather than enhanced) as compared with neutral ones. Indeed, phase diagrams calculated by using a similar PB approach clearly showed the suppression of the phase separation^{19,20,30,31}

The above argument does not explain all our experimental findings. Mixtures containing negatively charged saturated lipids are found to enhance the phase separation, and indicate that there should be an additional attractive mechanism between charged saturated lipids to overcome the electrostatic repulsion. Indeed, the demixing temperature in the DOPC/DPPG⁽⁻⁾ mixture (Fig. 2-6) was found to

be even higher than the chain melting temperature of pure DPPG⁽⁻⁾ ($T_m=41^\circ\text{C}$). Furthermore, the charged DPPG⁽⁻⁾/Chol binary mixtures exhibited the phase separation, whereas the neutral DPPC/Chol mixtures (see Fig. 11) did not.

The next step is to include entropic and enthalpic terms in the free energy for a membrane consisting of a mixture of negatively charged and neutral lipids,

$$f_{\text{tot}} = \frac{k_B T}{\Sigma} [\phi \ln \phi + (1 - \phi) \ln(1 - \phi) + \chi \phi(1 - \phi)] + f_{\text{el}} , \quad (3)$$

where the first and second terms in the square brackets account for the entropy and enthalpy of mixing between the charged and neutral lipids, respectively, while the last term, f_{el} , is the electrostatic free energy as in Eq. (2). As before, ϕ is the area fraction of the negatively charged lipid, $1 - \phi$ is that of neutral lipid, and χ is a dimensionless interaction parameter between the two lipids (of non-electrostatic origin). Note that we took for simplicity the cross-sectional area Σ of the two lipids to be the same, meaning that ϕ can be thought of as the charged lipid mole fraction. We note that the free energy formulation as in Eq. (3) was used in other studies, such as surfactant adsorption at fluid-fluid interface³² or lamellar-lamellar phase transition³³. In the case of a neutral lipid mixture membrane ($f_{\text{el}} = 0$), this model leads to a lipid/lipid demixing curve with a critical point located at $\phi_c = 0.5$, $\chi_c = 2$.

The phase behaviour difference between mixtures of DOPC/DPPG⁽⁻⁾ and DOPG⁽⁻⁾/DPPC also suggests a specific attractive interaction between DPPG⁽⁻⁾ molecules. This is not accounted for by the PB theory of Eq. (2), but the enhanced phase separation can effectively be explained in terms of an increased χ -value

in Eq. (3) for mixtures containing DPPG⁽⁻⁾. We plan to explore the origins of such non-electrostatic attractive contributions in a future theoretical study, and in particular, to explore the relationship between the electrostatic surface pressure and the phase separation^{34,35}.

Although DOPG⁽⁻⁾/DPPC and DOPC/DPPG⁽⁻⁾ mixtures look very similar from the electrostatic point of view, it is worthwhile to point out some additional difference between these mixtures (beside the value of the χ parameter). In particular, the phase behavior of DOPC/DPPG⁽⁻⁾ approaches that of neutral DOPC/DPPC system by adding salt. Since the attractive force between DPPG⁽⁻⁾ molecules vanishes by the addition of salt, we consider that this attractive force may be related to the charge effect. Because DOPG⁽⁻⁾ has an unsaturated bulky hydrocarbon tail, its cross-sectional area Σ is larger than that of DPPG⁽⁻⁾ that has a saturated hydrocarbon tail. In the literature, the cross-sectional areas of DOPG⁽⁻⁾ and DPPG⁽⁻⁾ are reported to be 68.6Å² (at $T=303\text{K}$) and 48Å² (at $T=293\text{K}$), respectively³⁶. This area difference affects the surface charge density $\sigma = -e\phi/\Sigma$. As a result, the counterion concentration near the charged membrane are different for DOPG⁽⁻⁾/DPPC as compared with DOPC/DPPG⁽⁻⁾. Based on the PB theory, Eq. (1), one can obtain the counterion concentration $n_0 = n^+(z \rightarrow 0)$, adjacent to the membrane

$$n_0 = n_b \left(p_0 \phi + \sqrt{(p_0 \phi)^2 + 1} \right)^2 . \quad (4)$$

This relation is known as the Grahame equation^{37,38}, and is used in Fig. 2-18 to plot n_0 for $n_b=10\text{mM}$. As shown in Fig. 2-18(A), n_0 sharply increases when the

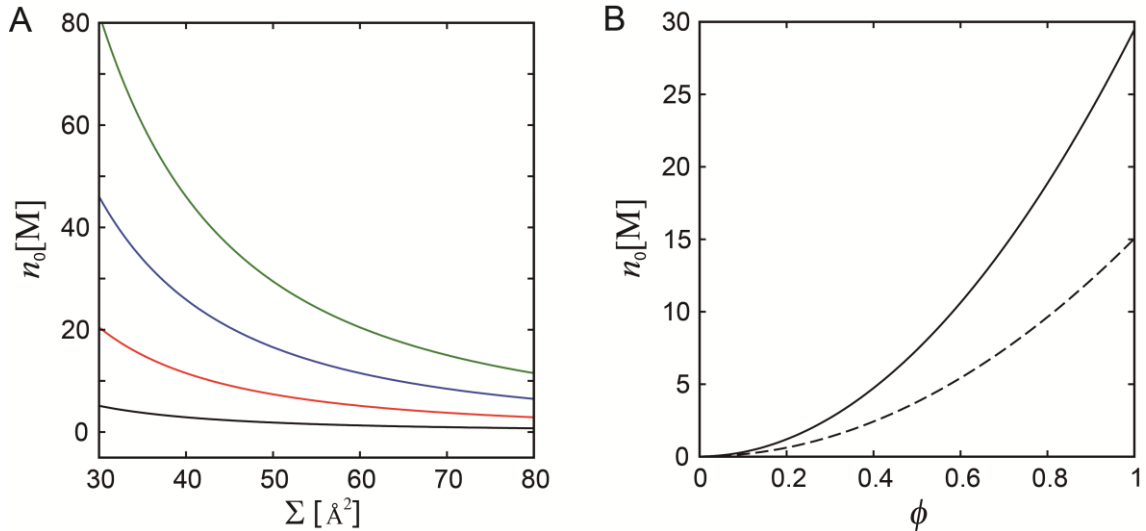


Fig.2-18 (A) The counterion concentration, $n_0 = n^+(z \rightarrow 0)$, extrapolated to the membrane vicinity as a function of cross-sectional area per lipid ϕ for the bulk salt concentration, $n_b = 10\text{mM}$. The different line colours represent $\phi = 0.25$ (black), 0.5 (red), 0.75 (blue), and 1.0 (green). (B) The counterion concentration at the membrane as a function of the charged lipid concentration, for bulk salt concentration, $n_b = 10\text{mM}$. The solid and dashed lines denote $a = 50 \text{ \AA}^2$ and 70 \AA^2 , respectively.

cross-sectional area Σ decreases. This tendency is significantly enhanced at higher area fraction ϕ of the charged lipid. In Fig. 2-18(B), n_0 is plotted for $\Sigma = 50 \text{ \AA}^2$ (solid line) and 70 \AA^2 (dashed line), which to a good approximation correspond to the values of DPPG⁽⁻⁾ and DOPG⁽⁻⁾, respectively. The larger value of n_0 for DPPG⁽⁻⁾ may influence the relative domain stability that cannot be described by the simple continuum PB theory. We also speculate that the hydrogen bonds between charged head groups and water molecules can be affected by the presence of a large number of counterions. Although this counter-ion condensation is one of the possible explanations for the strong attraction between DPPG⁽⁻⁾ molecules, it is not enough in order to describe the underlying mechanism completely. In addition, it is important to understand whether this attractive force is also observed in systems including other types of

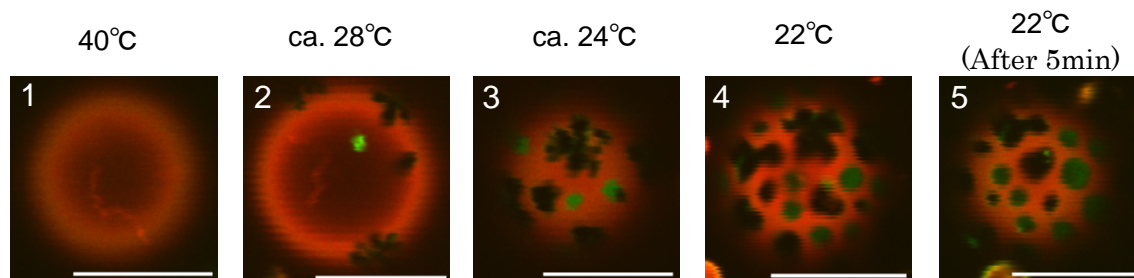


Fig.2-19 Phase behavior of cooling process in DOPC/DPPC/DPPG⁽⁻⁾/Chol = 40/20/20/20. The three-phase coexistence reappears at the room temperature when the system is heated and cooled again.

charged lipids (e.g. phosphatidylserine (PS⁽⁻⁾)). Such questions remain for future explorations.

In addition, we found that ternary mixtures of DPPC/DPPG⁽⁻⁾/Chol exhibit phase separation between DPPC/cholesterol-rich and DPPG⁽⁻⁾-rich phases. This is because the strong attraction between DPPG⁽⁻⁾ molecules excludes cholesterol from DPPG⁽⁻⁾-rich domains. In addition, the difference of the molecular tilt between different lipids may also affect this phase separation. The localization of cholesterol strongly depends on the molecular shape of membrane phospholipids. It was reported that polar lipids, such as DPPC, which contain both positively and negatively charges in their head group, tend to tilt due to electrostatic interaction between the neighboring polar lipids^{39,40}. The tilting produces an intermolecular space that cholesterol can occupy. However, since the molecular orientation of DPPG⁽⁻⁾ is almost perpendicular to the membrane surface, it will be unfavorable for cholesterol to occupy such a narrow space between neighboring DPPG⁽⁻⁾ molecules.

Moreover, we observed three phase coexistence in four-component mixtures DOPC/DPPC/DPPG⁽⁻⁾/Chol=40:20:20:20. We confirmed that this observed three-phase coexistence was equilibrium state. We raised temperature of sample

solution at 40°C, and observed process of domain growth with cooling process shown in Fig.2-19. After starting the cooling process, S_o phase (dark region) first appeared (image2). Continuing with the cooling, L_o phase (green region) appeared around the S_o phase. Finally, in room temperature at 22°C, the three-phase coexistence reappears at the same temperature. The three phase coexistence in four-component mixtures of DOPC/DPPC/DPPG⁽⁻⁾/Chol=40:20:20:20 could be caused by the same mechanism of ternary mixtures of DPPC/DPPG⁽⁻⁾/Chol. Unsaturated DOPC forms L_d phase, whereas cholesterol, which is localized in DPPC domains, form L_o phase. Thus, the DPPG⁽⁻⁾-rich region results in an S_o phase. Since the hydrocarbon tails of DPPG⁽⁻⁾ in the S_o phase are highly ordered, whereas the DOPC hydrocarbon tails in the L_d phase are disordered, the S_o/L_d line tension is larger than the line tension of the S_o/L_o interface. Therefore, S_o domains are surrounded by L_o domains in order to prevent a direct contact between S_o and L_d domains.

Although charged lipids in biomembranes are generally assumed to be in the fluid phase, the S_o phase with a large amount of charged lipids is observed in our experiments (on 4-component mixtures). Notably, the formation of the S_o phase has been reported in model membrane systems either by decreasing the cholesterol fraction or by increasing the membrane surface tension^{7,8}. Although the S_o phase has not been seen *in vivo*, we believe that our study on model membrane is meaningful and will help to reveal some important physicochemical mechanisms that underlie the phase behaviour and domain formation of lipid membranes *in vivo*. The L_o domains in artificial membranes can be regarded as models mimicking rafts in biomembranes. Because most of proteins have electric

charges, sections of the proteins that have positive charges can easily be attached to the negatively charged domains due to electrostatic interactions. Conversely, negatively charged sections of proteins are electrically excluded from such domains. Thus, such charged domains may play an important role in the selective adsorption of charged biomolecules.

Finally, we comment that, in all of our experiments, the salt concentration was 10mM. This concentration is lower than the concentration in physiological conditions of living cells, where the monovalent salt concentration is about ~140mM. From our results, we can see that screening by the salt is significant even for 10mM^{19,20,30,31}.

2-5 Conclusions

In this chapter, we investigated the phase separation induced by negatively charged lipids. As compared to the phase-coexistence region (in the phase diagram) of neutral DOPC/DPPC mixtures, the phase separation in the charged DOPG⁽⁻⁾/DPPC case is suppressed, whereas it is enhanced for the charged DOPC/DPPG⁽⁻⁾ system. The phase behaviours of both charged mixtures approach that of the neutral mixture when salt is added due to screening of electrostatic interactions. In DPPC/DPPG⁽⁻⁾/Chol ternary mixtures, the phase separation occurs when the fraction of charged DPPG⁽⁻⁾ is increased. This result implies that cholesterol localization is influenced by the head group structure as well as the hydrocarbon tail structure. Furthermore, we observed three-phase coexistence in four-component DOPC/DPPC/DPPG⁽⁻⁾/Chol mixtures, and that the phase-separation strongly depends on the amount of charged DPPG⁽⁻⁾.

Our findings shed some light on how biomembranes change their own structures, and may help to understand the mechanisms that play an essential role in the interactions of proteins with lipid mixtures during signal transduction.

2-6 References

1. Simons K, Sampaio JL. Membrane Organization and Lipid Rafts. Cold Spring Harbor Perspectives in Biology 2011;3(10).
2. Suzuki KGN, Kusumi A. Mechanism for signal transduction in the induced-raft domains as revealed by single-molecule tracking. Trends in Glycoscience and Glycotechnology 2008;20(116):341-351.
3. Vestergaard M, Hamada T, Takagi M. Using model membranes for the study of amyloid Beta : Lipid interactions and neurotoxicity. Biotechnology and Bioengineering 2008;99(4):753-763.
4. Lipowsky R, Dimova R. Domains in membranes and vesicles. Journal of Physics-Condensed Matter 2003;15(1):S31-S45.
5. Hamada T, Miura Y, Ishii KI, Araki S, Yoshikawa K, Vestergaard M, Takagi M. Dynamic processes in endocytic transformation of a raft-exhibiting giant liposome. Journal of Physical Chemistry B 2007;111(37):10853-10857.
6. Hamada T, Kishimoto Y, Nagasaki T, Takagi M. Lateral phase separation in tense membranes. Soft Matter 2011;7(19):9061-9068.
7. Hamada T, Yoshikawa K. Cell-Sized Liposomes and Droplets: Real-World Modeling of Living Cells. Materials 2012;5(11):2292-2305.
8. Veatch SL, Keller SL. Separation of liquid phases in giant vesicles of ternary mixtures of phospholipids and cholesterol. Biophysical Journal 2003;85(5):3074-3083.
9. Veatch SL, Keller SL. Organization in lipid membranes containing cholesterol. Physical Review Letters 2002;89(26):4.
10. Baumgart T, Hess ST, Webb WW. Imaging coexisting fluid domains in biomembrane models coupling curvature and line tension. Nature 2003;425(6960):821-824.
11. Bagatolli L, Kumar PBS. Phase behavior of multicomponent membranes: Experimental and computational techniques. Soft Matter 2009;5(17):3234-3248.
12. Dowhan W. Molecular basis for membrane phospholipid diversity: Why are there so many lipids? Annual Review of Biochemistry 1997;66:199-232.
13. Schlame M. Thematic review series: Glycerolipids - Cardiolipin synthesis for the assembly of bacterial and mitochondrial membranes. Journal of Lipid Research 2008;49(8):1607-1620.
14. William D, Mikhail B, Mileykovskaya. Functional roles of lipids in membranes. In: Vance DE, Vance JE, editors. Biochemistry of Lipids, Lipoproteins and Membranes.

- 5 ed. Elsevier Press 2008. p 1-37.
15. Ardail D, Privat JP, Egretcharlier M, Levrat C, Lerme F, Louisot P. MITOCHONDRIAL CONTACT SITES - LIPID-COMPOSITION AND DYNAMICS. *Journal of Biological Chemistry* 1990;265(31):18797-18802.
 16. Iot T, Ohnishi S, Ishinaga M, Kito M. Synthesis of a new phosphatidylserine spin-label and calcium-induced lateral phase separation in phosphatidylserine-phosphatidylcholine membranes. *Biochemistry* 1975;14(14):3064-9.
 17. Mittlerneher S, Knoll W. CA²⁺-INDUCED LATERAL PHASE-SEPARATION IN BLACK LIPID-MEMBRANES AND ITS COUPLING TO THE ION TRANSLOCATION BY GRAMICIDIN. *Biochimica Et Biophysica Acta* 1993;1152(2):259-269.
 18. Denisov G, Wanaski S, Luan P, Glaser M, McLaughlin S. Binding of basic peptides to membranes produces lateral domains enriched in the acidic lipids phosphatidylserine and phosphatidylinositol 4,5-bisphosphate: An electrostatic model and experimental results. *Biophysical Journal* 1998;74(2):731-744.
 19. Shimokawa N, Hishida M, Seto H, Yoshikawa K. Phase separation of a mixture of charged and neutral lipids on a giant vesicle induced by small cations. *Chemical Physics Letters* 2010;496(1-3):59-63.
 20. Shimokawa N, Komura S, Andelman D. Charged bilayer membranes in asymmetric ionic solutions: Phase diagrams and critical behavior. *Physical Review E* 2011;84(3):10.
 21. Veqi-Suplicy CC, Riske KA, Knorr RL, Dimova R. Vesicles with charged domains. *Biochimica Et Biophysica Acta-Biomembranes* 2010;1798(7):1338-1347.
 22. Blosser MC, Starr JB, Turtle CW, Ashcraft J, Keller SL. Minimal Effect of Lipid Charge on Membrane Miscibility Phase Behavior in Three Ternary Systems. *Biophysical journal* 2013;104(12):2629-38.
 23. Patarraia S, Liu Y, Lipowsky R, Dimova R. Effect of cytochrome c on the phase behavior of charged multicomponent lipid membranes. *Biochimica Et Biophysica Acta-Biomembranes* 2014;1838(8):2036-2045.
 24. Bibhu SR, Sanat K, V.A R. X-ray and Neutron Scattering Studies of Lipid-Sterol Model Membranes. Elsevier; 2010.
 25. Marsh D. Liquid-ordered phases induced by cholesterol: A compendium of binary phase diagrams. *Biochimica Et Biophysica Acta-Biomembranes* 2010;1798(3):688-699.
 26. Wustner D. Fluorescent sterols as tools in membrane biophysics and cell biology.

- Chemistry and Physics of Lipids 2007;146(1):1-25.
27. Guttman GD, Andelman D. ELECTROSTATIC INTERACTIONS IN 2-COMPONENT MEMBRANES. *Journal De Physique Ii* 1993;3(9):1411-1425.
 28. May S, Harries D, Ben-Shaul A. Macroion-induced compositional instability of binary fluid membranes. *Physical Review Letters* 2002;89(26).
 29. D EE, Hakan W. *The Colloidal Domain: Where Physics, Chemistry, Biology, and Technology Meet*. New York: WILEY-VCH; 1999.
 30. May S. Stability of macroion-decorated lipid membranes. *Journal of Physics-Condensed Matter* 2005;17(32):R833-R850.
 31. Mbamala EC, Ben-Shaul A, May S. Domain formation induced by the adsorption of charged proteins on mixed lipid membranes. *Biophysical Journal* 2005;88(3):1702-1714.
 32. Diamant H, Andelman D. Kinetics of surfactant adsorption at fluid-fluid interfaces. *Journal of Physical Chemistry* 1996;100(32):13732-13742.
 33. Harries D, Podgornik R, Parsegian VA, Mar-Or E, Andelman D. Ion induced lamellar-lamellar phase transition in charged surfactant systems. *Journal of Chemical Physics* 2006;124(22).
 34. Jahnig F. Electrostatic free energy and shift of the phase transition for charged lipid membranes. *Biophysical chemistry* 1976;4(4):309-18.
 35. Reinhard L, Erich S. *Structure and Dynamics of Membranes*. Amsterdam: Elsevier Science; 1995.
 36. Kim JH, Kim MW. Temperature effect on the transport dynamics of a small molecule through a liposome bilayer. *European Physical Journal E* 2007;23(3):313-317.
 37. Grahame DC. The electrical double layer and the theory of electrocapillarity. *Chemical reviews* 1947;41(3):441-501.
 38. Jacob IN. *Intermolecular and Surface Forces*. USA: Elsevier Inc; 2011.
 39. Juyang H, Feigenson GW. A microscopic interaction model of maximum solubility of cholesterol in lipid bilayers. *Biophysical Journal* 1999;76(4):2142-2157.
 40. Kurrle A, Rieber P, Sackmann E. RECONSTITUTION OF TRANSFERRIN RECEPTOR IN MIXED LIPID VESICLES - AN EXAMPLE OF THE ROLE OF ELASTIC AND ELECTROSTATIC FORCES FOR PROTEIN LIPID ASSEMBLY. *Biochemistry* 1990;29(36):8274-8282.

Chapter 3

Cholesterol localization in charged multi-component membranes

3-1 Introduction

Biomembrane is bilayer structure which is consisting on various types of lipid molecules. Below a certain temperature, lipid molecules are not distributed homogeneously, and form heterogeneous structures called as lipid rafts^{1,2}. Lipid rafts are micro domain structure which is enriched with saturated lipids and cholesterol. It is proposed that lipid rafts performed as a functional platforms in signal transduction and membrane trafficking^{3,4}. According to previous researches, raft regions isolated from animal cells (RBL-2H3) are found to be enriched with cholesterol⁵. Moreover, when cholesterol was depleted from cell membrane, signal transduction was disrupted^{6,7}. Thus, cholesterol is essential component in formation of lipid rafts, as well as plays an important role in structural regulation of lipid membrane.

To explore the mechanism of phase separation in lipid membranes, giant unilamellar vesicles (GUVs) have been used as model biomembranes^{8,9}. When the GUVs were prepared in ternary mixtures of unsaturated lipid/saturated lipid/cholesterol, phase separation structures are observed according to the lipid composition¹⁰. The phase structures are classified into three states: liquid-disorder phase (L_d) enriched with unsaturated lipid, liquid-order phase (L_o) enriched with saturated lipid and cholesterol, and solid-order phase (S_o) enriched with saturated lipid, respectively¹¹. In high concentration of cholesterol 45%~60%, phase-separated structure is not observed. On the other hand, in middle concentration of cholesterol 15%~45%, two-liquid coexistence that is L_o/L_d phase separation is observed. It is known that cholesterol prefers to localize in saturated lipid than unsaturated lipid, and results in L_o phase¹²⁻¹⁴. This phase structure is attracting significant attention as “raft model”¹⁵⁻¹⁷. Furthermore, when

cholesterol concentration is very low (~15%), solid-liquid coexistence S_o/L_d phase separation is observed. These results indicate that cholesterol affects phase behavior of lipid membrane. In biomembrane, it is possible that cholesterol-lipid interaction plays structural and regulatory role of lipid rafts in biomembranes.

Although biomembranes also include charged lipids^{18,19}, most of the studies investigated the phase separation in uncharged model membranes^{10,15}. In particular, investigation of the interaction between charged lipid and cholesterol is not nearly. In chapter 2, we investigated the effect of charge on phase behavior in various mixtures of charged lipids²⁰. We revealed that charged unsaturated lipid “di-oleoyl-phosphatidyl-glycerol (DOPG⁽⁻⁾)” suppress phase separation, while charged saturated lipid “di-palmitoyl-phosphatidyl-glycerol (DPPG⁽⁻⁾)” enhance phase separation. In addition, charged saturated lipid DPPG⁽⁻⁾ induces phase separation in saturated lipid/cholesterol mixtures. In neutral DPPC/Chol mixtures, phase separation is not observed. On the other hand, phase separation structure is observed in DPPG⁽⁻⁾/Chol mixture. It is possible that head group charge affects phase behavior because the structures of hydrocarbon chain of DPPC and DPPG⁽⁻⁾ are same. Thus, it is important to clarify the interaction between cholesterol and charged lipids. Moreover, it is considered that lipid rafts composed of saturated lipid and cholesterol. However, the result of chapter 2 indicates the localization of cholesterol may different between neutral saturated lipid and charged saturated lipid.

In this chapter, we investigated the localization of cholesterol and phase behavior in various mixtures containing charged lipid and cholesterol. First, we observe the cholesterol localization in the typical neutral ternary system consisting of DOPC/DPPC/Chol. In the following, unsaturated lipid or saturated lipid is replaced

with charged lipid, thus we investigate DOPG⁽⁻⁾/DPPC/Chol and DOPC/DPPG⁽⁻⁾/Chol ternary systems. We also explored the salt screening effect, and compared the difference of electrostatic effect between monovalent cation (Sodium chloride: Na⁺) and bivalent cation (Magnesium chloride: Mg²⁺) in both DOPG⁽⁻⁾/DPPC/Chol and DOPC/DPPG⁽⁻⁾/Chol systems.

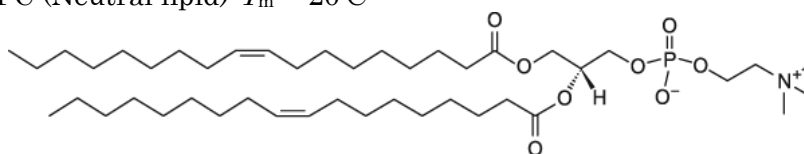
3-2 Materials and methods

Materials

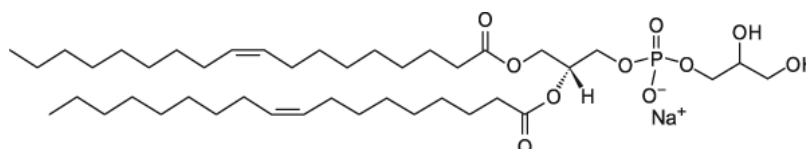
Materials are used in this chapter are shown in Fig.3-1. Neutral unsaturated lipid 1,2-dioleoyl-sn-glycero-3-phosphocholine (DOPC, with chain melting temperature, $T_m = -20^\circ\text{C}$), neutral saturated lipid 1,2-dipalmitoyl-sn-glycero-3-phosphocholine (DPPC, $T_m = 41^\circ\text{C}$), negatively charged unsaturated lipid 1,2-dioleoyl-sn-glycero-3-phospho-(1'-rac-glycerol) (sodium salt) (DOPG⁻, $T_m = -18^\circ\text{C}$), negatively charged saturated lipid 1,2-dipalmitoyl-sn-glycero-3-phospho-(1'-rac-glycerol) (sodium salt) (DPPG⁻, $T_m = 41^\circ\text{C}$), and cholesterol, were obtained from Avanti Polar Lipids (Alabaster, AL). BODIPY labelled cholesterol (BODIPY-Chol) and Rhodamine B 1,2-dihexadecanoyl-sn-glycero-3-phosphoethanolamine (Rhodamine-DHPE) were purchased from Invitrogen (Carlsbad, CA). Deionized water was obtained from a Millipore Milli-Q purification system. We chose phosphatidylcholine (PC) as the neutral lipid head and phosphatidylglycerol (PG⁻) as the negatively charged lipid head because the chain melting temperature of PC and PG⁻ lipids having the same acyl tails, is almost identical. In cellular membranes, PC is the most common lipid component, and PG is highly representative among charged lipids.

Unsaturated lipids

- DOPC (Neutral lipid) $T_m = -20^\circ\text{C}$

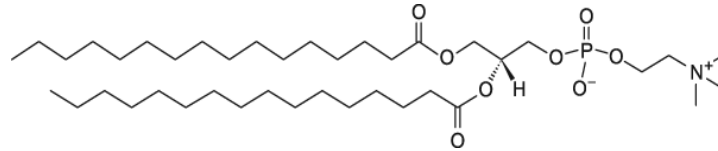


- DOPG⁻ (Negatively charged lipid) $T_m = -18^\circ\text{C}$

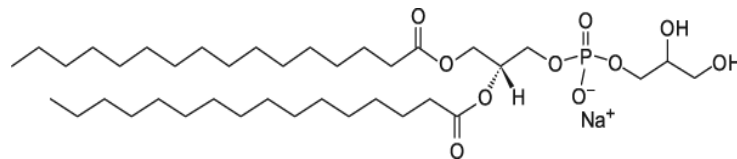


Saturated lipids

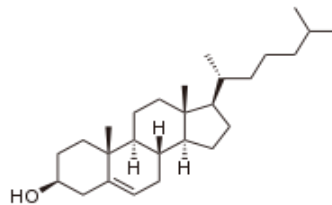
- DPPC (Neutral lipid) $T_m = 41^\circ\text{C}$



- DPPG⁽⁻⁾ (Negatively charged lipid) $T_m = 41^\circ\text{C}$

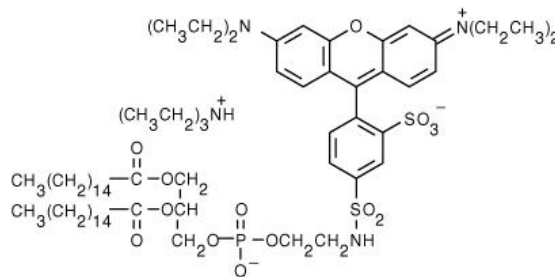


Cholesterol



Fluorescent dyes

- Rhodamine-DHPE (labels unsaturated lipid-rich phase)



- BODIPY-Cholesterol (labels cholesterol-rich phase)

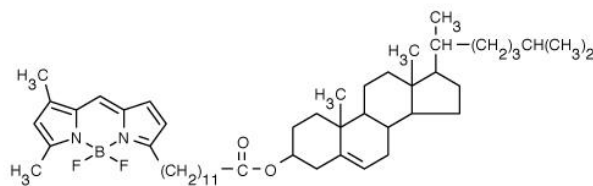


Fig.3-1 molecular structure of lipids and fluorescent dyes

Preparation of giant unilamellar vesicles

Giant unilamellar vesicles (GUVs) were prepared by gentle hydration method (Fig.3-2). Lipids and fluorescent dyes were dissolved in 2:1(vol/vol) chloroform/methanol solution. The organic solvent was evaporated under a flow of nitrogen gas, and the lipids were further dried under vacuum for 3h. The films were hydrated with 5 μL deionized water at 55 $^{\circ}\text{C}$ for 5 min (pre-hydration), and then with 200 μL deionized water, NaCl solution, or MgCl_2 solution for 1-2 h at 37 $^{\circ}\text{C}$. The final lipid concentration was 0.2 mM. The fluorescent dyes Rhodamine-DHPE and BODIPY-Chol concentrations were 0.1 μM , 0.1 μM and 0.2 μM , respectively (0.5% or 1% of lipid concentration).

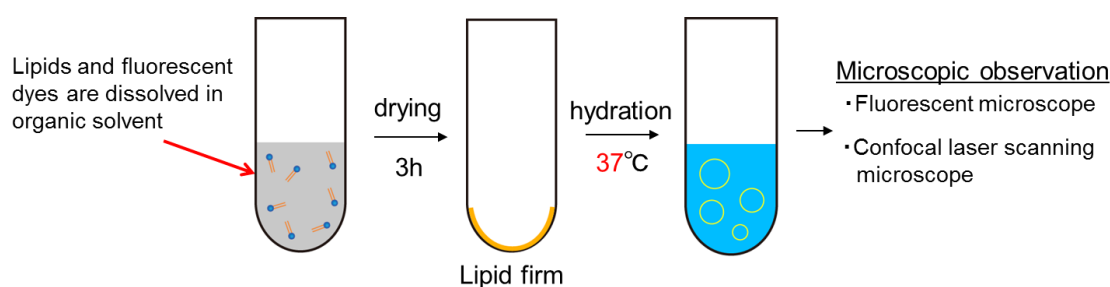


Fig.3-2 Preparation process of GUVs

Microscopic observation

The GUV solution was placed on a glass coverslip, which was covered with another smaller coverslip at a spacing of ca. 0.1 mm (Fig.3-3). We observed the membrane structures with a fluorescent microscope (IX71, Olympus, Japan) and a confocal laser scanning microscope (FV-1000, Olympus, Japan). In this chapter, Rhodamine-DHPE and BODIPY-Chol were used as fluorescent dyes. Rhodamine-DHPE labels the unsaturated lipid-rich phase, whereas BODIPY-Chol labels the cholesterol-rich one. A standard filter set U-MWIG with excitation wavelength, $\lambda_{\text{ex}}=530\text{--}550\text{nm}$, and emission wavelength, $\lambda_{\text{em}}=575\text{ nm}$, was used to monitor the fluorescence of Rhodamine-DHPE,

and another filter, U-MNIBA with $\lambda_{ex}=470-495$ nm and $\lambda_{em}=510-550$ nm, was used for the BODIPY-Chol dye. The sample temperature was controlled with a microscope stage (type 10021, Japan Hitec).

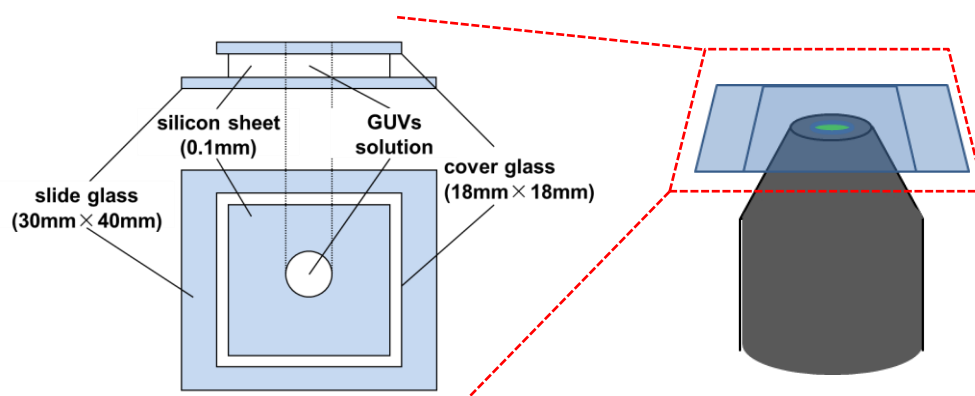


Fig.3-3 Schematic of sample chamber and observation method

3-3 Experimental results

3-3-1 The localization of cholesterol in neutral DOPC/DPPC/Chol mixtures

First, we observed the localization of cholesterol in neutral mixtures of DOPC/DPPC/Chol. Fig.3-4 shows the microscopic images and phase diagram of DOPC/DPPC/Chol mixtures for a fixed amount of Chol=20%. We found three types of phase separation; isotropic shape dark domain, dark circular domain, and bright circular domain. In general, the isotropic shape dark domain is appeared at lower cholesterol concentration region. This domain is mainly consisting of DPPC and is called “solid-order phase”. Since this domain is formed by the lipid which takes solid phase, the domain is stiff and takes isotropic shape. At Chol=20%, we cannot often observe this domain, because the cholesterol concentration is too high to form So domain. On the other hand, the dark circular domain which is represented in Fig.3-4(A)1, is called “liquid-order (L_o) domain” mainly consisting of DPPC and Chol.

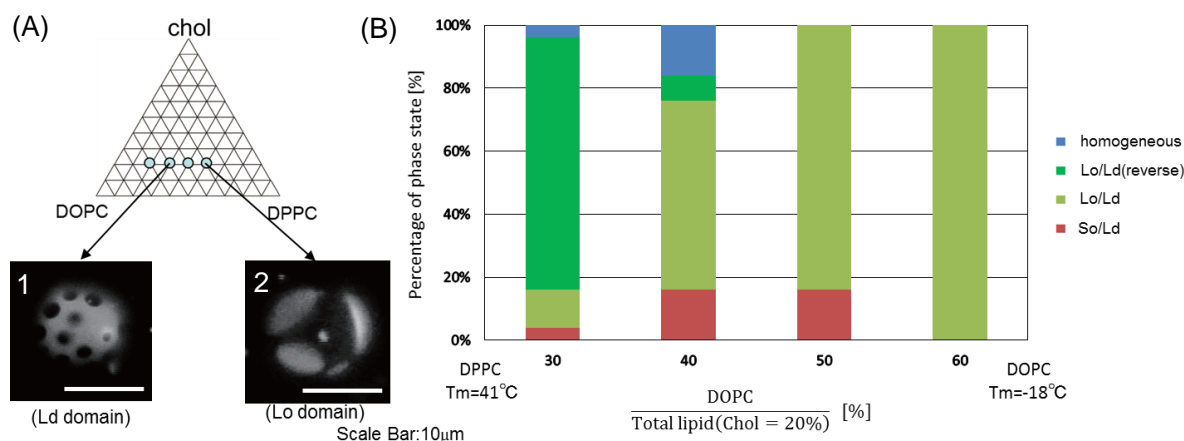


Fig.3-4 (A) Microscopic images of phase separation in DOPC/DPPC/Chol mixture. L_d domain was observed in low concentration of DOPC (image 1), whereas L_o domain was observed in high concentration of DOPC (image 2). (B)Phase diagram of DOPC/DPPC/Chol mixtures for a fixed amount of Chol=20%.

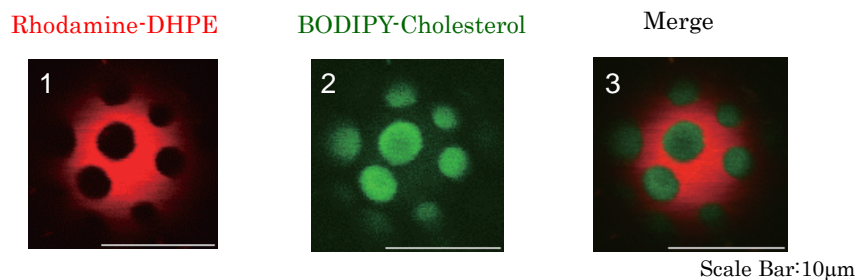


Fig.3-5 Microscopic images of phase separation in DOPC/DPPC/Chol=40:40:20 by confocal laser microscopy. Rhodamine-DHPE labels L_d phase (image 1). BODIPY-cholesterol labels cholesterol-rich phase (image 2). Both images are merged in image 3.

The region which surrounds L_o domains is “liquid-disorder (L_d) phase” which contains the large amount of DOPC. When the amount of DOPC is relatively decreased compared with sum of DPPC and Chol, L_d phase forms domain and such a phase structure is called reverse domain as shown in Fig.3-4(A)2. In Fig.3-4(B), we summarized the phase behavior of DOPC/DPPC/Chol mixture. L_o/L_d phase separation can be observed over entire range of composition. Therefore, the cholesterol molecules tend to be localized in DPPC-rich phase in DOPC/DPPC/Chol mixture. To confirm this cholesterol localization directly, Fig.3-5 shows the microscopic images obtained from confocal laser microscopy in DOPC/DPPC/Chol=40:40:20. Red region is L_d phase labeled by Rhodamine-DHPE dye (image 1), while Green region is cholesterol-rich phase labeled by BODIPY-Chol (image 2). In these mixtures, cholesterol localized in DPPC-rich region and resulted in L_o phase.

3-3-2 The localization of cholesterol in charged DOPG⁽⁻⁾/DPPC/Chol mixtures

We replaced neutral unsaturated lipid DOPC with the charged unsaturated lipid DOPG⁽⁻⁾, and observed the phase behavior and localization of cholesterol in charged mixtures of DOPG⁽⁻⁾/DPPC/Chol. Fig.3-6 shows the microscopic images and phase diagram of DOPG⁽⁻⁾/DPPC/Chol mixtures for a fixed amount of Chol=20%. In low concentration of DOPG⁽⁻⁾, L_o/L_d phase separation was mainly observed same as neutral mixture of DOPC/DPPC/Chol. However, solid-liquid coexistence of S_o/L_d phase separation was observed in DOPG⁽⁻⁾/DPPC/Chol=40:40:20 and 50:30:20. We investigated the localization of cholesterol in this composition by double staining using Rhodamine-DHPE and BODIPY-Cholesterol as shown in Fig.3-7. According to microscopic images, cholesterol was localized in the DOPG⁽⁻⁾-rich phase. It is surprising result because cholesterol commonly prefers to localize in saturated lipid-rich phase¹²⁻¹⁴. Moreover, when DOPG⁽⁻⁾ concentration is high, one-liquid structure of L_d phase was observed. This result is consistent with previous studies in that charged unsaturated lipids suppress phase separation^{20,21}.

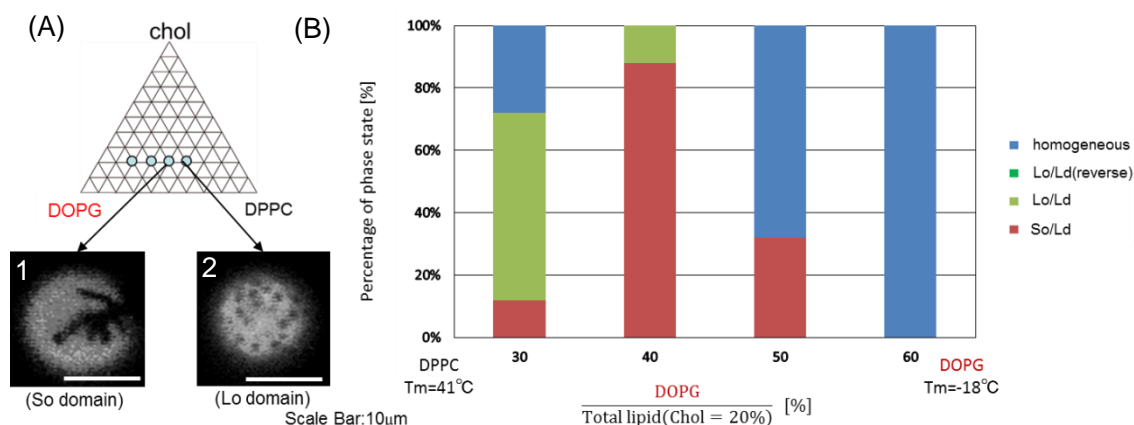


Fig.3-6 (A) Microscopic images of phase separation in DOPG⁻/DPPC/Chol mixture. So/L_d phase separation was mainly observed in DOPG⁻/DPPC/Chol =40:40:20 (image 1), whereas L_o/L_d domain was observed in DOPG⁻/DPPC/Chol =30:50:20 (image 2). (B)Phase diagram of DOPG⁻/DPPC/Chol mixtures for a fixed amount of Chol=20%.

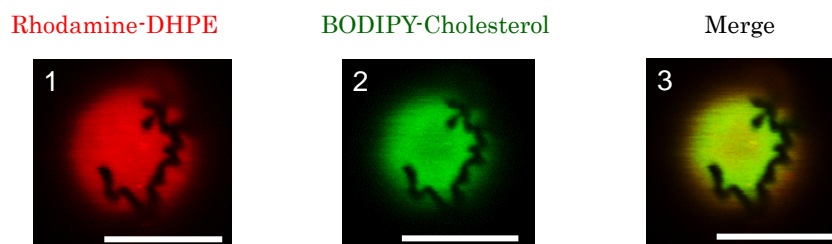


Fig.3-7 Microscopic images of phase separation in DOPG⁻/DPPC/Chol=40:40:20 by confocal laser microscopy. Rhodamine-DHPE labels L_d phase (image 1). BODIPY-cholesterol labels cholesterol-rich phase (image 2). Both images are merged in image 3.

We also explored the phase behavior in presence of salt in DOPG⁻/DPPC/Chol mixtures. First, we prepared GUVs in these mixtures with NaCl solution which monovalent ion of Na⁺ dissociates in water. Fig.3-8 shows the percentage of L_o/L_d phase separation and homogeneous structure in DOPG⁻/DPPC/Chol mixtures hydrated with NaCl solution. The percentage of L_o/L_d phase separation was increased with NaCl concentration (Fig.3-8 A). On the other hand, the percentage of homogeneous structure was not changed significantly by NaCl concentration (Fig.3-8 B). Second, we prepared GUVs in DOPG⁻/DPPC/Chol mixtures with MgCl₂ solution which bivalent ion of Mg²⁺

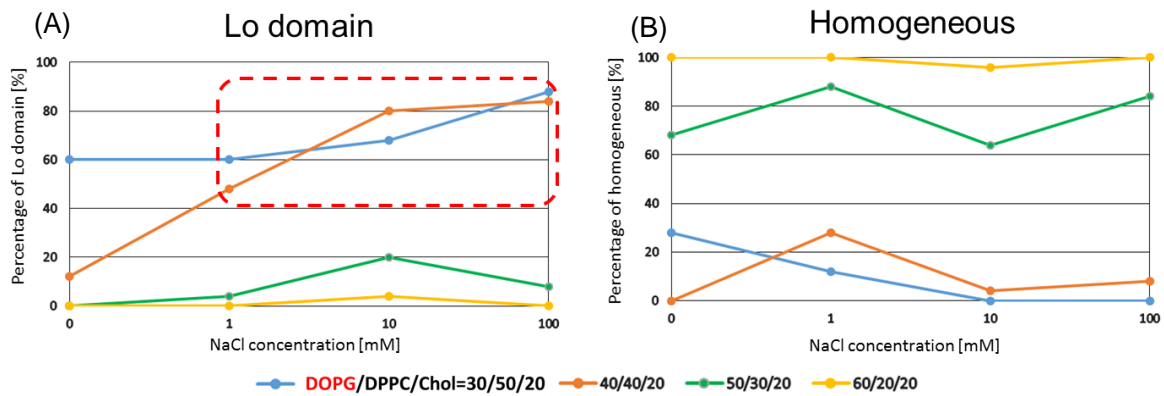


Fig.3-8 Phase diagram in DOPG⁽⁻⁾/DPPC/Chol mixture by hydration with NaCl. (A) Percentage of L₀/L_d domain formation. (B) Percentage of homogeneous structure.

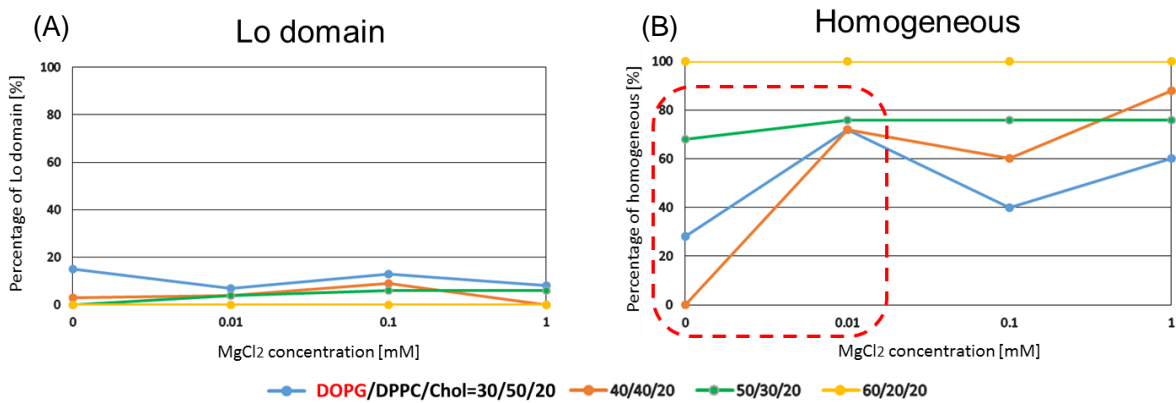


Fig.3-9 Phase diagram in DOPG⁽⁻⁾/DPPC/Chol mixture by hydration with MgCl₂²⁺. (A) Percentage of L₀/L_d domain formation. (B) Percentage of homogeneous structure.

dissociates in water. Fig.3-9 shows the percentage of L₀/L_d phase separation and homogeneous structure in DOPG⁽⁻⁾/DPPC/Chol mixtures hydrated with MgCl₂ solution. The percentage of L₀/L_d phase separation was not increased in contrast with NaCl hydration. However, the percentage of homogeneous structure was increased significantly hydration with 0.01mM MgCl₂. These results suggest that the screening effects between Na⁺ and Mg²⁺ are different.

3-3-3 The localization of cholesterol in charged DOPC/DPPG⁽⁻⁾/Chol mixtures

Next, we replaced neutral saturated lipid DPPC with the charged saturated lipid DPPG⁽⁻⁾, and observed the phase behavior and localization of cholesterol in charged mixtures of DOPC/DPPG⁽⁻⁾/Chol. Fig.3-10 shows the microscopic images and phase diagram of DOPC/DPPG⁽⁻⁾/Chol mixtures for a fixed amount of Chol=20%. In this mixtures, solid-liquid S_o/L_d coexistence was mainly observed as shown in Fig.3-10B. We investigated the localization of cholesterol in S_o/L_d phase separation by double staining using Rhodamine-DHPE and BODIPY-Cholesterol. According to the Fig.3-11, cholesterol was localized in DOPC-rich phase. From the results so far indicates that cholesterol tends to be localized in the order of DOPG⁽⁻⁾>DPPC>DOPC>DPPG⁽⁻⁾. Previously, the localization of cholesterol has been considered mainly the contribution of hydrocarbon chain of lipid tail groups. But our results suggest that head group charge of lipid molecules also affects cholesterol localization.

We also investigated the phase behavior in presence of salt in DOPC/DPPG⁽⁻⁾/Chol mixtures. First, we prepared GUVs in these mixtures with NaCl solution which monovalence ion of Na⁺ dissociates in water. Fig.3-12 shows the percentage of S_o/L_d phase separation and L_o/L_d phase separation in DOPC/DPPG⁽⁻⁾/Chol mixtures hydrated with NaCl solution. The percentage of S_o/L_d phase separation was decreased with NaCl concentration (Fig.3-12 A). In addition, the percentage of L_o/L_d phase separation was increased in hydration at high NaCl concentration (Fig.3-12 B). Second, we prepared GUVs in DOPC/DPPG⁽⁻⁾/Chol mixtures with MgCl₂ solution which divalent ion of Mg²⁺ dissociates in water. Fig.3-13 shows the percentage of S_o/L_d phase separation and L_o/L_d phase separation in DOPC/DPPG⁽⁻⁾/Chol mixtures hydrated with MgCl₂. The percentage

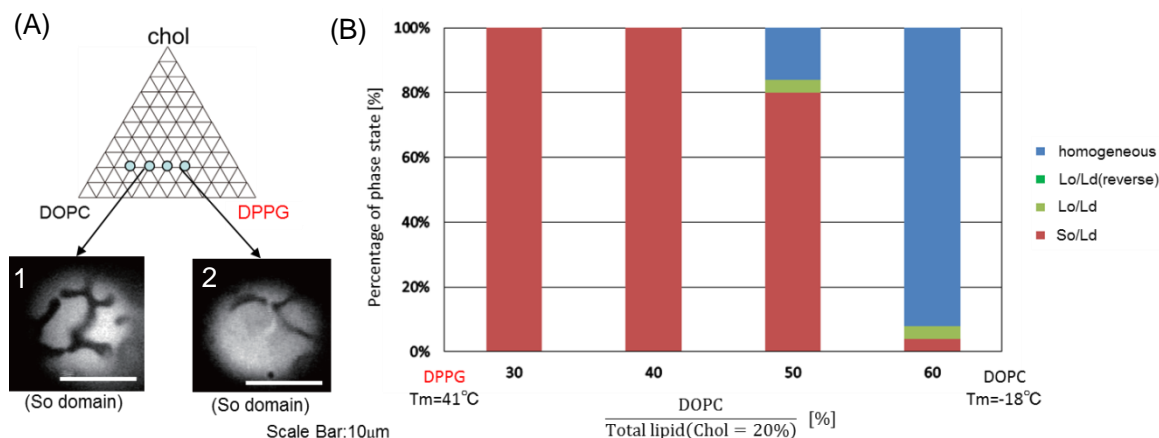


Fig.3-10 (A) Microscopic images of phase separation in DOPC/DPPG⁻/Chol mixture. S_o/L_d phase separation was observed in DOPC/DPPG⁻/Chol =50:30:20 (image 1) and 40:40:20 (image 2). (B)Phase diagram of DOPC/DPPG⁻/Chol mixtures for a fixed amount of Chol=20%.

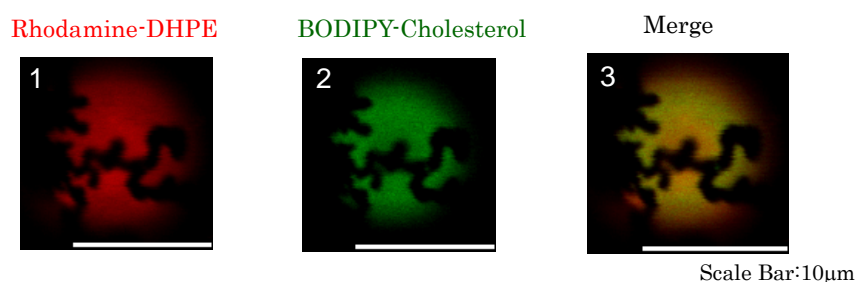


Fig.3-11 Microscopic images of phase separation in DOPC/DPPG⁻/Chol=40:40:20 by confocal laser microscopy. Rhodamine-DHPE labels L_d phase (image 1). BODIPY-cholesterol labels cholesterol-rich phase (image 2). Both images are merged in image 3.

of S_o/L_d phase separation was increased in DOPC/DPPG⁻/Chol =60:20:20 hydrated with 0.01mM MgCl₂ solution. However, in hydration with 0.1mM and 1mM MgCl₂ solutions, the percentage of S_o/L_d phase separation was decreased with MgCl₂ concentration in all compositions (Fig.3-13A). On the other hand, the percentage of L_o/L_d phase separation was increased with MgCl₂ concentration in all compositions (Fig.3-13B).

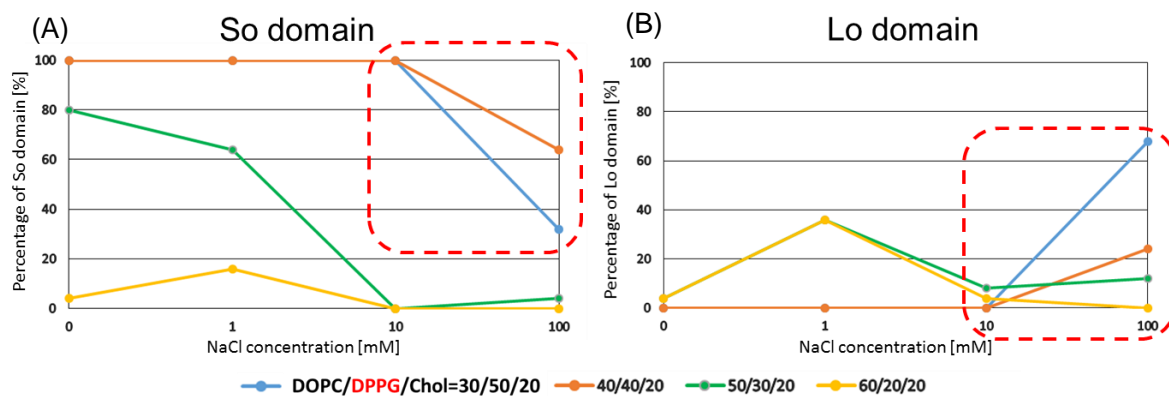


Fig.3-12 Phase diagram in DOPC/DPPG⁽⁻⁾/Chol mixture by hydration with NaCl. (A) Percentage of S_o/L_d domain formation. (B) Percentage of L_o/L_d domain formation.

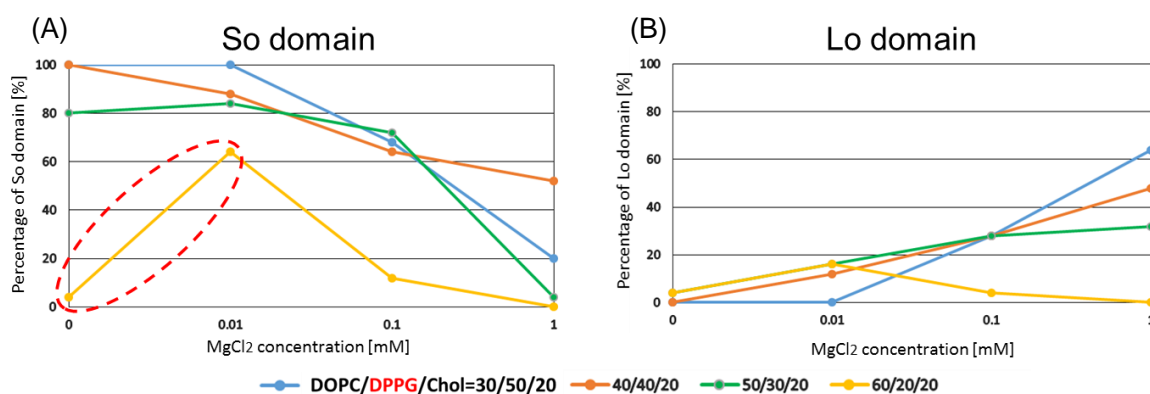


Fig.3-13 Phase diagram in DOPC/DPPG⁽⁻⁾/Chol mixture by hydration with MgCl₂. (A) Percentage of S_o/L_d domain formation. (B) Percentage of L_o/L_d domain formation.

3-3-4 The localization of cholesterol in charged DOPG⁽⁻⁾/DPPG⁽⁻⁾/Chol mixtures

Finally, we observed the phase behavior and localization of cholesterol in DOPG⁽⁻⁾/DPPG⁽⁻⁾/Chol mixtures including both charged unsaturated lipid and saturated lipid. Fig.3-14 shows the microscopic images and phase diagram of DOPG⁽⁻⁾/DPPG⁽⁻⁾/Chol mixtures for a fixed amount of Chol=20%. The S_o/L_d phase separation was observed in many components as shown in Fig.3-14B, and homogeneous structure was observed in DOPG⁽⁻⁾/DPPG⁽⁻⁾/Chol =60:20:20. We investigated the localization of cholesterol in S_o/L_d phase separation by double staining using Rhodamine-DHPE and BODIPY-Cholesterol (Fig.3-15). Cholesterol was localized in DOPG⁽⁻⁾-rich phase without localized in DPPG⁽⁻⁾-rich phase (image 2).

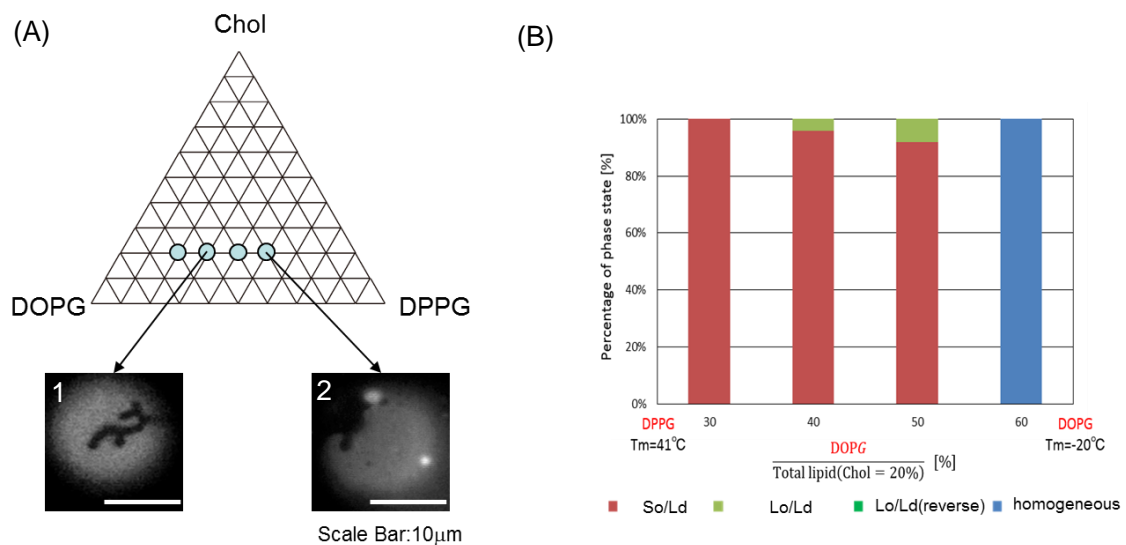


Fig.3-14 (A) Microscopic images of phase separation in DOPG⁽⁻⁾/DPPG⁽⁻⁾/Chol mixture. S_o/L_d phase separation was observed in DOPG⁽⁻⁾/DPPG⁽⁻⁾/Chol =50:30:20 (image 1), and 30:50:20 (image 2). (B)Phase diagram of DOPG⁽⁻⁾/DPPG⁽⁻⁾/Chol mixtures for a fixed amount of Chol=20%.

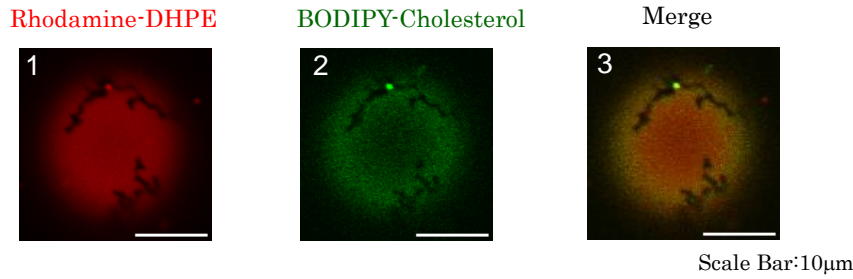


Fig.3-15 Microscopic images of phase separation in DOPG⁻/DPPG⁻/Chol=40:40:20 by confocal laser microscopy. Rhodamine-DHPE labels L_d phase (image 1). BODIPY-cholesterol labels cholesterol-rich phase (image 2). Both images are merged in image 3.

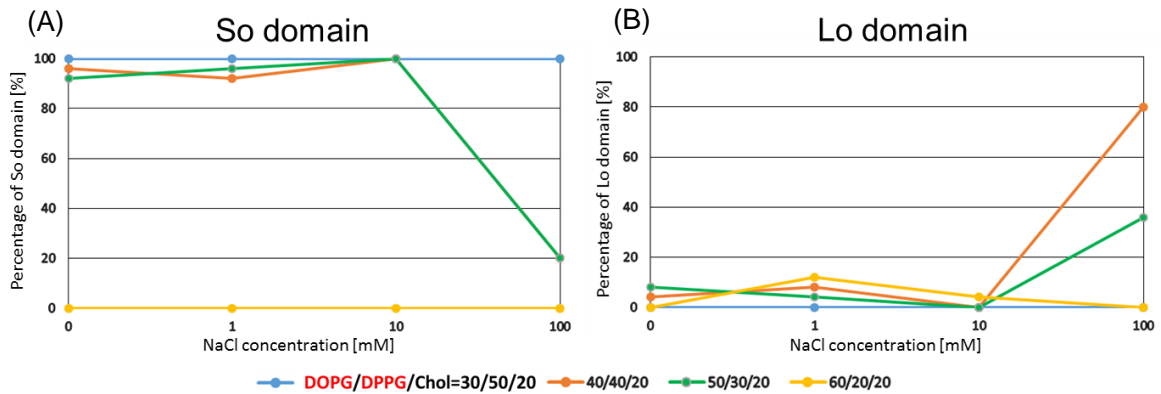


Fig.3-16 Phase diagram in DOPG⁻/DPPG⁻/Chol mixture by hydration with NaCl. (A) Percentage of S_o/L_d domain formation. (B) Percentage of L_o/L_d domain formation.

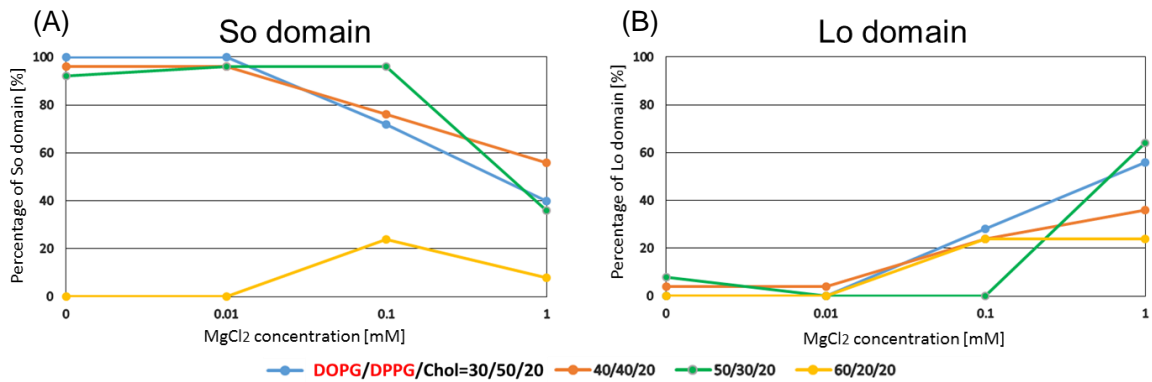


Fig.3-17 Phase diagram in DOPG⁻/DPPG⁻/Chol mixture by hydration with MgCl₂. (A) Percentage of S_o/L_d domain formation. (B) Percentage of L_o/L_d domain formation.

Next, we investigated the phase behavior in presence of salt in DOPG⁻/DPPG⁻/Chol mixtures. First, we prepared GUVs in these mixtures with NaCl solution which

monovalent ion of Na^+ dissociates in water. Fig.3-16 shows the percentage of S_o/L_d phase separation and L_o/L_d phase separation in $\text{DOPG}^{(-)}/\text{DPPG}^{(-)}/\text{Chol}$ mixtures hydrated with NaCl solution. The percentage of S_o/L_d phase separation was decreased at high concentration of NaCl (Fig.3-16 A). In addition, the percentage of L_o/L_d phase separation was increased at high concentration of NaCl (Fig.3-16 B). Second, we prepared GUVs in $\text{DOPG}^{(-)}/\text{DPPG}^{(-)}/\text{Chol}$ mixtures with MgCl_2 solution which divalent ion of Mg^{2+} dissociates in water. Fig.3-17 shows the percentage of S_o/L_d phase separation and L_o/L_d phase separation in $\text{DOPG}^{(-)}/\text{DPPG}^{(-)}/\text{Chol}$ mixtures hydrated with MgCl_2 solution. The percentage of S_o/L_d phase separation was decreased with MgCl_2 concentration (Fig.3-17A). On the other hand, the percentage of L_o/L_d phase separation was increased with MgCl_2 concentration (Fig.3-13B).

3-4 Discussion

3-4-1 The localization of cholesterol in neutral DOPC/DPPC/Chol mixtures

In present study, the localization of cholesterol is affected by charged lipid molecules and presence of salt. We discuss the mechanisms of phase behavior based on umbrella model²². In neutral lipid mixture of DOPC/DPPC/Chol, dipolar head group of saturated lipid DPPC tilts to neighboring DPPC due to electrostatic interaction (Fig.3-18). Cholesterol has small hydrophilic part, thereby induces energy loss when non-polar part of cholesterol expose to water. In presence of saturated lipid DPPC, cholesterol can be localized into the space between DPPC molecules. DPPC head group acts as a cover of cholesterol from exposure to water. Thus, cholesterol prefers to localize into DPPC-rich region and results in L_0 phase in neutral DOPC/DPPC/Chol mixture.

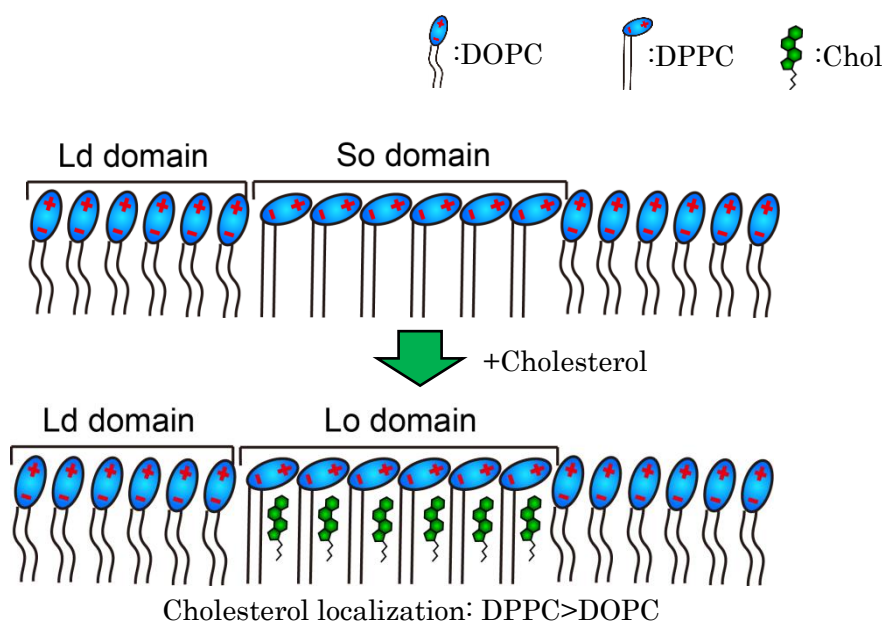


Fig.3-18 Schematic image of the cholesterol localization in DOPC/DPPC/Chol mixture.

3-4-2 The localization of cholesterol in DOPG⁽⁻⁾/DPPC/Chol mixtures

We observed the localization of cholesterol in charged mixtures of DOPG⁽⁻⁾/DPPC/Chol. According to the results, cholesterol is localized in DOPG⁽⁻⁾-rich phase rather than DPPC-rich phase (Fig.3-6). In chapter2, we discussed that the electrostatic repulsion is occurred between charged unsaturated lipid DOPG⁽⁻⁾. This repulsive force could expand molecular distance between DOPG⁽⁻⁾. Thus, it is possible that cholesterol is localized in DOPG⁽⁻⁾-rich phase due to less steric constraint than DPPC as shown in Fig.3-19. When DOPG⁽⁻⁾/DPPC/Chol mixtures were prepared with NaCl solution, L_o/L_d phase separation tends to be increased with NaCl concentration (Fig.3-8). In this case, electric repulsion between DOPG⁽⁻⁾ is suppressed by screening effect of Na⁺, and DOPG⁽⁻⁾ behaves like a neutral unsaturated lipid. As a result, cholesterol is localized in DPPC-rich phase. In addition, when DOPG⁽⁻⁾/DPPC/Chol mixtures were prepared with MgCl₂ solution, homogeneous phase tends to be increased with MgCl₂ concentration (Fig.3-9). It is

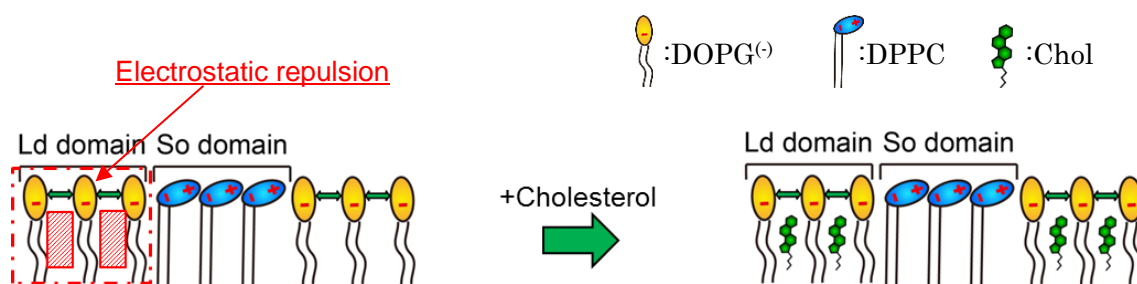


Fig.3-19 Schematic model of the cholesterol localization in DOPG⁽⁻⁾/DPPC/Chol mixture.

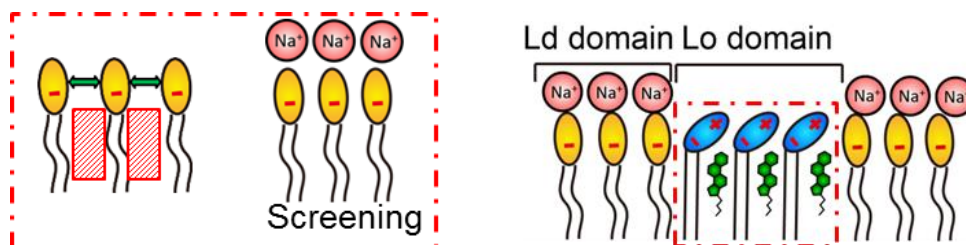


Fig.3-20 Schematic model of the effect of NaCl screening in DOPG⁽⁻⁾/DPPC/Chol

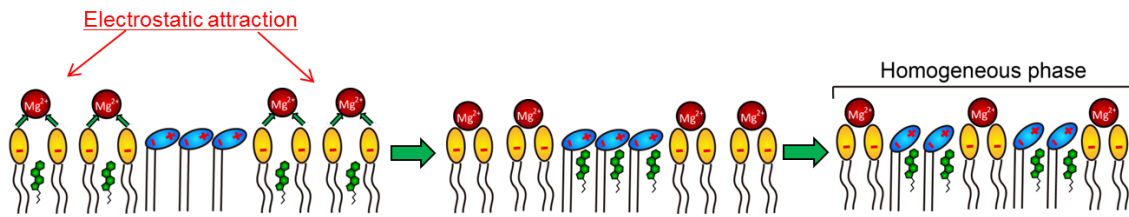


Fig.3-21 Schematic model of the effect of MgCl_2 screening in $\text{DOPG}^{(-)}/\text{DPPC}/\text{Chol}$

possible that electric attraction is occurred between $\text{DOPG}^{(-)}$ and divalent cation of Mg^{2+} . The membrane fluidity of $\text{DOPG}^{(-)}$ -rich phase is decreased by electrostatic attraction, and may come close to DPPC-rich phase. As a result, all lipids are mixed each other and membrane forms homogeneous phase.

3-4-3 The localization of cholesterol in DOPC/DPPG⁽⁻⁾/Chol mixtures

We also investigated the localization of cholesterol in DOPC/DPPG⁽⁻⁾/Chol mixtures. In this mixture, cholesterol is localized in DOPC-rich phase rather than DPPG⁽⁻⁾-rich phase (Fig.3-11). In chapter2, electrostatic attraction mediated by counter ion between DPPG⁽⁻⁾ molecules is dominant than electric repulsion between head group charge of DPPG⁽⁻⁾. This interaction causes the enhancement of phase separation and formation of DPPG⁽⁻⁾-rich phase. Therefore, cholesterol cannot be localized in DPPG⁽⁻⁾-rich phase as a result, S₀/L_d phase separation is appeared as shown in Fig.3-22. When DOPC/DPPG⁽⁻⁾/Chol mixtures were prepared with NaCl solution, S₀/L_d phase separation tends to be decreased while L₀/L_d tends to be increased with NaCl concentration (Fig.3-12). It is suggested that electric attraction mediated by counter ion is suppressed by adding NaCl. This behavior is same as DOPC/DPPG⁽⁻⁾ approaches DOPC/DPPC neutral system by adding salt as mentioned in chapter2. As a result, DPPG⁽⁻⁾ behave like a neutral saturated lipid which has dipolar head group, and cholesterol is localized in DPPC-rich phase (Fig.3-23). We also examined the screening effect using MgCl₂ solution (Fig.3-13). The phase behavior shows almost same as NaCl hydration. The S₀/L_d phase separation tends to be decrease while L₀/L_d tends to increase with MgCl₂ concentration. However, in the case of DOPC/DPPG/Chol=60/20/20, homogeneous

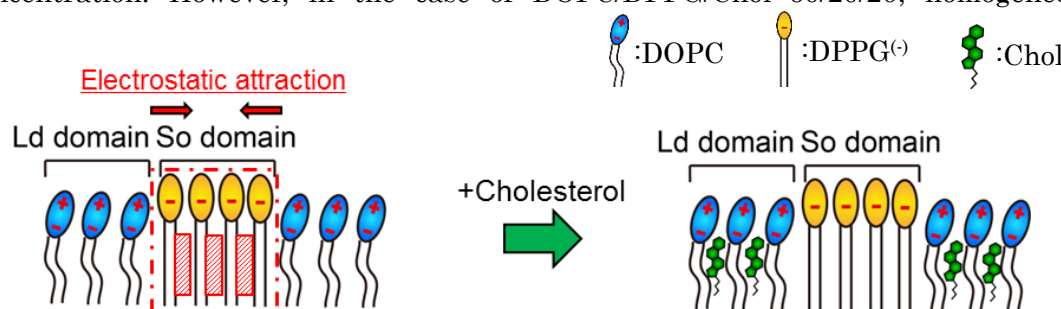


Fig.3-22 Schematic model of the cholesterol localization in DOPC/DPPG⁽⁻⁾/Chol mixture.

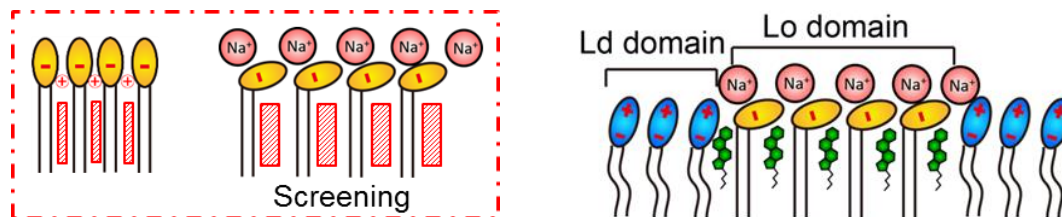


Fig.3-23 Schematic model of the effect of NaCl screening in DOPC/DPPG⁽⁻⁾/Chol mixture.

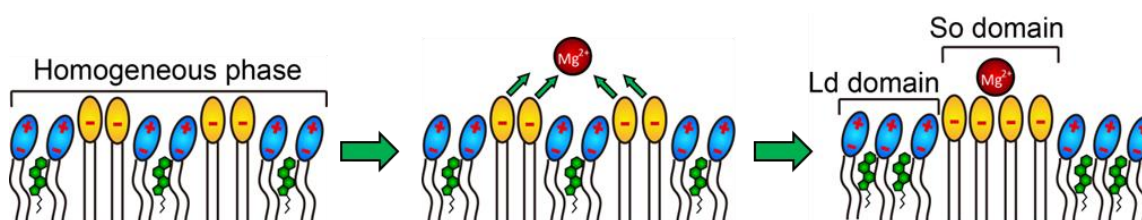


Fig.3-24 Schematic model of the effect of MgCl₂ screening in DOPC/DPPG⁽⁻⁾/Chol=60:20:20 mixture.

structure was observed in absence of MgCl₂, whereas S₀/L_d phase separation was observed in 0.01mM MgCl₂. It is possible that DPPG⁽⁻⁾ molecules distributed on lipid membrane are accumulated by electrostatic interaction of divalent cation Mg²⁺, and low concentration of Mg²⁺ induced electric attraction between DPPG⁽⁻⁾ head group and Mg²⁺.

3-4-3 The localization of cholesterol in DOPG⁽⁻⁾/DPPG⁽⁻⁾/Chol mixtures

Finally, we clarified the localization of cholesterol in DOPG⁽⁻⁾/DPPG⁽⁻⁾/Chol mixtures. Cholesterol is localized in DOPG⁽⁻⁾-rich phase rather than DPPG⁽⁻⁾-rich phase (Fig.3-14). Thus, S₀/L_d phase separation was mainly observed in this mixture. In DOPG⁽⁻⁾/DPPG⁽⁻⁾/Chol=60:20:20, homogeneous structure is formed in all vesicles. It suggests that the effect of electrostatic repulsion between DOPG⁽⁻⁾ molecules is dominant than electrostatic attraction of DPPG⁽⁻⁾ in this mixture. In presence of salt, S₀/L_d phase separation tends to be decreased while L_o/L_d tends to be increased with NaCl or MgCl₂ concentration. These results indicate that both charged unsaturated lipid DOPG⁽⁻⁾ and saturated lipid DPPG⁽⁻⁾ behave like neutral lipids by salt screening (Fig.3-25).

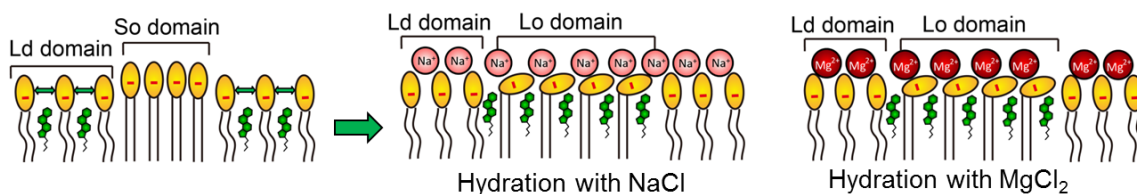


Fig.3-25 Schematic model of the effect of salt screening in DOPG⁽⁻⁾/DPPG⁽⁻⁾/Chol mixture.

3-5 Conclusion

In this chapter, we investigated the localization of cholesterol and phase behavior in various mixtures of charged lipid membranes. Cholesterol prefers to be localized in DOPG⁽⁻⁾-rich phase, while does not to be localized in DPPG⁽⁻⁾-rich phase. Our results showed that cholesterol tends to be localized in the order of DOPG⁽⁻⁾>DPPC>DOPC>DPPG⁽⁻⁾. In presence of salt, localization of cholesterol was changed significantly. In addition, the screening effects in phase behavior by presence of monovalent cation Na⁺ and divalent cation Mg²⁺ are also difference. These results suggest that the interaction between charged lipid and cholesterol plays an important role in structural regulation of phase separation in lipid membrane. Biomembrane may also use this interaction for control of distribution or accumulation of lipid rafts during the signal transduction.

3-6 References

1. Simons K, Ikonen E. Functional rafts in cell membranes. *Nature* 1997;387(6633):569-572.
2. Simons K, Sampaio JL. *Membrane Organization and Lipid Rafts*. Cold Spring Harbor Perspectives in Biology 2011;3(10).
3. Simons K, Toomre D. Lipid rafts and signal transduction (vol 1, pg 31, 2000). *Nature Reviews Molecular Cell Biology* 2001;2(3):216-216.
4. Sedwick CE, Altman A. Ordered just so: lipid rafts and lymphocyte function. *Science's STKE : signal transduction knowledge environment* 2002;2002(122):re2-re2.
5. Mingtao G, Field KA, Aneja R, Holowka D, Baird B, Freed JH. Electron spin resonance characterization of liquid ordered phase of detergent-resistant membranes from RBL-2H3 cells. *Biophysical Journal* 1999;77(2):925-33.
6. Kabouridis PS, Janzen J, Magee AL, Ley SC. Cholesterol depletion disrupts lipid rafts and modulates the activity of multiple signaling pathways in T lymphocytes. *European Journal of Immunology* 2000;30(3):954-963.
7. Parpal S, Karlsson M, Thorn H, Stralfors P. Cholesterol depletion disrupts caveolae and insulin receptor signaling for metabolic control via insulin receptor substrate-1, but not for mitogen-activated protein kinase control. *Journal of Biological Chemistry* 2001;276(13):9670-9678.
8. Bangham AD, Horne RW. NEGATIVE STAINING OF PHOSPHOLIPIDS AND THEIR STRUCTURAL MODIFICATION BY SURFACE-ACTIVE AGENTS AS OBSERVED IN THE ELECTRON MICROSCOPE. *Journal of molecular biology* 1964;8:660-8.
9. Cohen BE, Bangham AD. Diffusion of small non-electrolytes across liposome membranes. *Nature* 1972;236(5343):173-4.
10. Veatch SL, Keller SL. Organization in lipid membranes containing cholesterol. *Physical Review Letters* 2002;89(26):4.
11. van Meer G. Membrane lipids, where they are and how they behave: Sphingolipids on the move. *Faseb Journal* 2010;24.
12. Veatch SL, Polozov IV, Gawrisch K, Keller SL. Liquid domains in vesicles investigated by NMR and fluorescence microscopy. *Biophysical Journal* 2004;86(5):2910-2922.
13. Almeida RFM, Fedorov A, Prieto M. Sphingomyelin/phosphatidylcholine/cholesterol

- phase diagram: Boundaries and composition of lipid rafts. *Biophysical Journal* 2003;85(4):2406-2416.
14. Ariola FS, Li ZG, Cornejo C, Bittman R, Heikal AA. Membrane Fluidity and Lipid Order in Ternary Giant Unilamellar Vesicles Using a New Bodipy-Cholesterol Derivative. *Biophysical Journal* 2009;96(7):2696-2708.
 15. Baumgart T, Hess ST, Webb WW. Imaging coexisting fluid domains in biomembrane models coupling curvature and line tension. *Nature* 2003;425(6960):821-824.
 16. Saeki D, Hamada T, Yoshikawa K. Domain-growth kinetics in a cell-sized liposome. *Journal of the Physical Society of Japan* 2006;75(1):3.
 17. Vestergaard M, Hamada T, Takagi M. Using model membranes for the study of amyloid Beta : Lipid interactions and neurotoxicity. *Biotechnology and Bioengineering* 2008;99(4):753-763.
 18. Dowhan W. Molecular basis for membrane phospholipid diversity: Why are there so many lipids? *Annual Review of Biochemistry* 1997;66:199-232.
 19. William D, Mikhail B, Mileykovskaya. Functional roles of lipids in membranes. In: Vance DE, Vance JE, editors. *Biochemistry of Lipids, Lipoproteins and Membranes*. 5 ed. Elsevier Press 2008. p 1-37.
 20. Himeno H, Shimokawa N, Komura S, Andelman D, Hamada T, Takagi M. Charge-induced phase separation in lipid membranes. *Soft matter* 2014;10(40):7959-67.
 21. Shimokawa N, Hishida M, Seto H, Yoshikawa K. Phase separation of a mixture of charged and neutral lipids on a giant vesicle induced by small cations. *Chemical Physics Letters* 2010;496(1-3):59-63.
 22. Juyang H, Feigenson GW. A microscopic interaction model of maximum solubility of cholesterol in lipid bilayers. *Biophysical Journal* 1999;76(4):2142-2157.

Chapter 4

The effect of charge on membrane 3D structure

4-1 Introduction

Basic structure of biomembrane is lipid bilayer which is composed of various types of phospholipid. Biomembranes not only distinguish between inner and outer environment of living cell, but also involve wide range of life phenomena through the dynamic structural changes. Biomembranes exhibit various two-dimensional (2D) and three dimensional (3D) dynamics, and play a very important role in regulation of cellular function. The 2D dynamic is represented by phase separation called “lipid raft formation”^{1,2}. Lipid rafts which are enriched with saturated lipid, cholesterol, and various membrane proteins, are expected to function as platforms on which proteins are attached during signal transduction and membrane trafficking^{3,4}. The 3D membrane structures are morphological changes⁵. Regulation of the membrane morphology is critical for many cellular processes, such as budding of endo- and exocytosis⁶, fission-fusion sequence of vesicular transport⁷⁻⁹, and pore formation of autophagy^{10,11}. Moreover, coupling between membrane 2D and 3D dynamics is suggested in biomembrane. Lipid rafts have been shown to play a role of autophagy and endocytosis^{12,13}. In these membrane dynamics, physicochemical properties of lipid molecules should play a very important role as well as protein function.

In several studies, synthetic lipid vesicles consisting of some lipid molecules are used commonly as models for biomembranes to investigate the physicochemical properties of lipid membrane. Giant unilamellar lipid vesicles (GUVs) are made from phospholipids, and have the same size as a cell and are large enough to be observed directly by optical microscopies^{14,15}. Previously, using GUVs, several studies have succeeded in observation the 2D and 3D membrane dynamics such as phase separation (2D) and morphological

change (3D). In 2D dynamics, when GUVs simply composed of unsaturated and saturated lipids with cholesterol, lateral phase separation can be observed according to a membrane component¹⁶. In 3D dynamics, Hamada. *et. al* found the dynamic response by addition of osmotic pressure or surfactant¹⁷. They also succeed to control membrane shape to use photo responsive amphiphile (KAON12)¹⁸. However, it is not clear how biomembranes controls such structures. Because previous experimental systems of GUVs have not considered to the living cell environment.

In the past, most of the studies have investigated the primary physical property of lipid membrane in uncharged model systems ^{19,20}. However, biomembranes also include charged lipids. In particular, some organelles such as lysosome²¹ and mitochondria^{22,23} are enriched with charged lipids. As physicochemical properties of lipid membranes, charged lipids are one of the important factors to be considered. In addition, surface charge of membrane could be controlled by cellular ion such as sodium ion, and calcium ion.

In related studies focusing on charged lipids, several studies investigated the 2D dynamics of phase behavior. Shimokawa *et al* studied mixtures consisting of neutral saturated lipid (DPPC), negatively charged unsaturated lipid (DOPS⁻) and cholesterol^{24,25}. The main result is the suppression of the phase separation due to electrostatic interactions between the charged DOPS⁻ lipids²⁵. Other relevant studies are worth mentioning. Vequi-Suplicy *et al*, reported the suppression of phase separation using other charged unsaturated lipids²⁶. Blosser *et al* investigated the phase diagram and miscibility temperature in mixtures containing charged lipids²⁷. Patariaia *et al*, have found to cytochrome c which is positive charged membrane protein induces micron-sized domains in ternary mixtures of charged unsaturated lipid(DOPG), egg

sphingomyelin and cholesterol²⁸.

In chapter 2, we investigated the 2D dynamics of phase behavior induced by negatively charged lipids in binary mixtures of unsaturated and saturated lipids, ternary mixtures of saturated (neutral and charged) lipids and cholesterol, and four-component mixtures of unsaturated lipid, saturated (neutral and charged) lipids, and cholesterol, respectively. In binary mixture, as compared to neutral lipid mixture, the phase separation is suppressed by charged unsaturated lipid, whereas it is enhanced for the charged saturated lipid. In ternary mixtures, the phase separation occurs when the fraction of charged saturated lipid is increased. Furthermore, we observed three-phase coexistence in four-component mixtures, and that the phase separation strongly depends on the amount of charged saturated lipid. The phase behaviors of all charged mixtures approach that of the neutral mixture due to screening of electrostatic interactions by adding the salt. In this way, the effect of electric charge on 2D structure of phase behavior has been explored. However, the effects of charge on 3D structure of membrane morphology have not been explored.

In this chapter, we clarify the effect charge on 3D structure in various mixtures of charged lipids. We observe morphology of GUVs by using fluorescence microscopy and confocal laser scanning microscopy, and compare membrane morphology to neutral lipid mixture. We also control the temperature of the sample of charged lipid mixtures GUVs, and investigated membrane dynamics. In addition, the salt screening effect on charged membranes is explored. These effects are examined in binary mixtures of unsaturated lipid and saturated lipid, and ternary mixtures of saturated lipids (charged and neutral) and cholesterol, respectively. Furthermore, we discuss coupling between membrane 2D and 3D dynamics by comparison between the study of chapter 2 and this chapter.

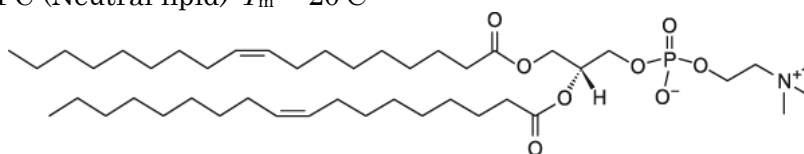
4-2 Materials and methods

Materials

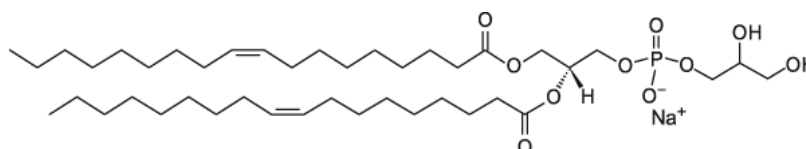
Materials are used in this chapter are shown in Fig.4-1. Neutral unsaturated lipid 1,2-dioleoyl-sn-glycero-3-phosphocholine (DOPC, with chain melting temperature, $T_m = -20^\circ\text{C}$), neutral saturated lipid 1,2-dipalmitoyl-sn-glycero-3-phosphocholine (DPPC, $T_m = 41^\circ\text{C}$), negatively charged unsaturated lipid 1,2-dioleoyl-sn-glycero-3-phospho-(1'-rac-glycerol) (sodium salt) (DOPG⁻, $T_m = -18^\circ\text{C}$), negatively charged saturated lipid 1,2-dipalmitoyl-sn-glycero-3-phospho-(1'-rac-glycerol) (sodium salt) (DPPG⁻, $T_m = 41^\circ\text{C}$), and cholesterol, were obtained from Avanti Polar Lipids (Alabaster, AL). BODIPY labelled cholesterol (BODIPY-Chol) and Rhodamine B 1,2-dihexadecanoyl-sn-glycero-3-phosphoethanolamine (Rhodamine-DHPE) were purchased from Invitrogen (Carlsbad, CA). Deionized water was obtained from a Millipore Milli-Q purification system. We chose phosphatidylcholine (PC) as the neutral lipid head and phosphatidylglycerol (PG⁻) as the negatively charged lipid head because the chain melting temperature of PC and PG⁻ lipids having the same acyl tails, is almost identical. In cellular membranes, PC is the most common lipid component, and PG is highly representative among charged lipids.

Unsaturated lipids

- DOPC (Neutral lipid) $T_m = -20^\circ\text{C}$

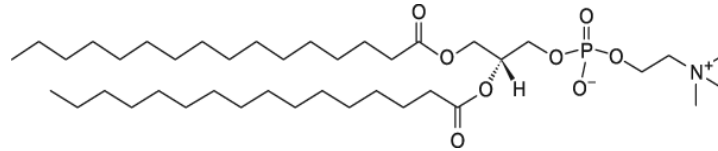


- DOPG⁻ (Negatively charged lipid) $T_m = -18^\circ\text{C}$

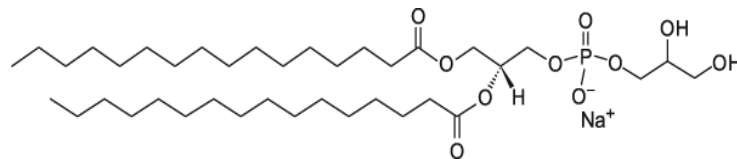


Saturated lipids

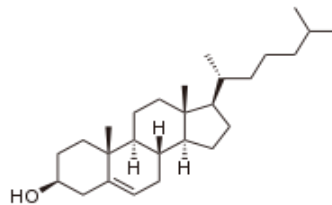
- DPPC (Neutral lipid) $T_m = 41^\circ\text{C}$



- DPPG⁽⁻⁾ (Negatively charged lipid) $T_m = 41^\circ\text{C}$

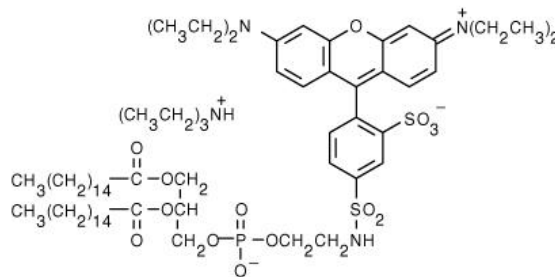


Cholesterol



Fluorescent dyes

- Rhodamine-DHPE (labels unsaturated-rich phase)



- BODIPY-Cholesterol (labels cholesterol-rich phase)

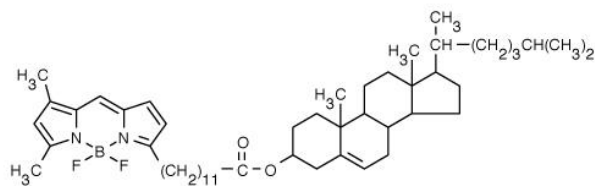


Fig.4-1 molecular structures of lipids and fluorescent dyes

Preparation of giant unilamellar vesicles

Giant unilamellar vesicles (GUVs) were prepared by gentle hydration method (Fig.4-2). Lipids and fluorescent dyes were dissolved in 2:1(vol/vol) chloroform/methanol solution. The organic solvent was evaporated under a flow of nitrogen gas, and the lipids were further dried under vacuum for 3h. The films were hydrated with 5 μL deionized water at 55 $^{\circ}\text{C}$ for 5 min (pre-hydration), and then with 200 μL deionized water or NaCl solution for 1-2 h at 37 $^{\circ}\text{C}$. The final lipid concentration was 0.2 mM. The fluorescent dyes Rhodamine-DHPE and BODIPY-Chol concentrations were 0.1 μM , 0.1 μM and 0.2 μM , respectively (0.5% or 1% of lipid concentration).

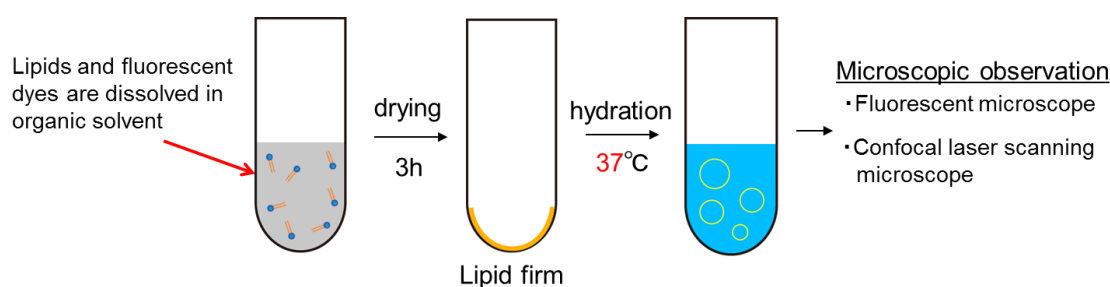


Fig.4-2 Preparation process of GUVs

Microscopic observation

The GUV solution was placed on a glass coverslip, which was covered with another smaller coverslip at a spacing of ca. 0.1 mm (Fig.4-3). We observed the membrane structures with a fluorescent microscope (IX71, Olympus, Japan) and a confocal laser scanning microscope (FV-1000, Olympus, Japan). In this chapter, Rhodamine-DHPE and BODIPY-Chol were used as fluorescent dyes. Rhodamine-DHPE labels the unsaturated lipid-rich phase, whereas BODIPY-Chol labels the cholesterol-rich one. A standard filter set U-MWIG with excitation wavelength, $\lambda_{\text{ex}}=530\text{--}550\text{nm}$, and emission wavelength, $\lambda_{\text{em}}=575\text{ nm}$, was used to monitor the fluorescence of Rhodamine-DHPE,

and another filter, U-MNIBA with $\lambda_{ex}=470-495$ nm and $\lambda_{em}=510-550$ nm, was used for the BODIPY-Chol dye. The sample temperature was controlled with a microscope stage (type 10021, Japan Hitec).

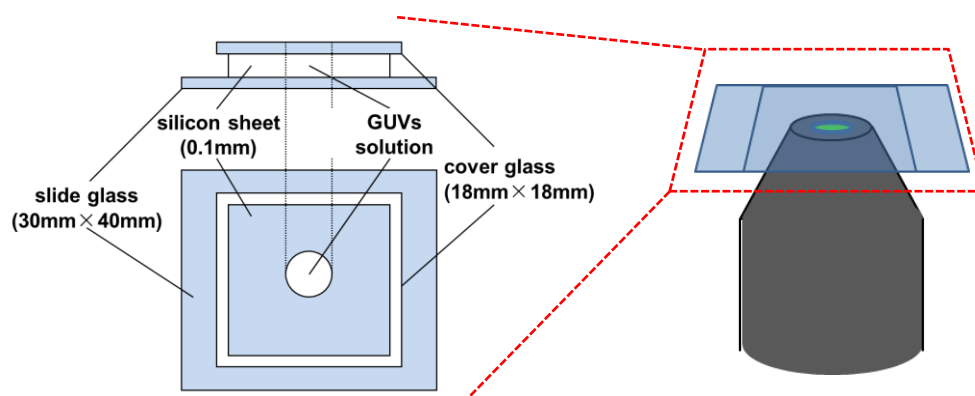


Fig.4-3 Schematic of sample chamber and observation method

Experimental condition

In this chapter, we controlled surface charging by change lipid composition and preparing with electrolyte for all studied systems. First, we changed the percentage of negatively charged lipids (Fig.4-4A). Second, we screened head group charge of charged lipid by hydration with NaCl (Fig.4-4B). We observed morphology of lipid membrane for each condition. By comparison between these conditions, we can discuss more deeply about the contribution of electric charge on membrane morphology.

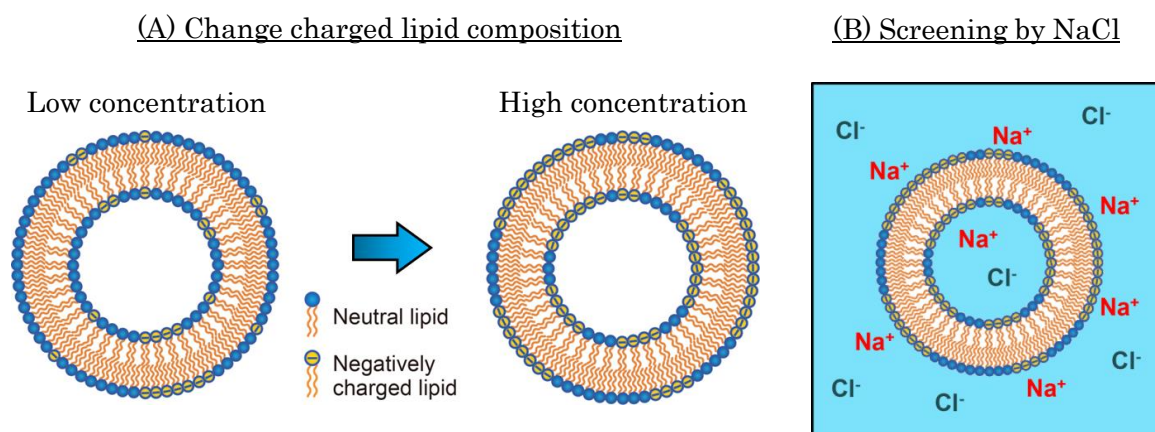


Fig.4-4 Schematic of experimental condition

4-3 Experimental results

4-3-1 Binary lipid mixtures (Unsaturated lipid/ Saturated lipid)

First, we investigated the effect of charge on membrane morphology in binary unsaturated/saturated lipid mixtures. We used neutral unsaturated lipid DOPC, neutral saturated lipid DPPC, negatively unsaturated lipid DOPG⁽⁻⁾, and negatively saturated lipid DPPG⁽⁻⁾ in this section. The fluorescent dye Rho-DHPE was used for label liquid disorder (L_d) phase that is unsaturated lipid-rich phase. We changed the fraction of unsaturated/saturated lipid mixture, and observed membrane shapes for each composition.

Fig.4-5 shows the microscope images of membrane morphology and phase diagrams in binary mixtures. We observed membrane morphology using both of phase-contrast and fluorescent microscopy, and took microscopic images for each mixture. For neutral lipid mixtures with DOPC/DPPC, vesicles formed spherical shape in all compositions, as shown in Fig.4-5A and C. Next, we replaced saturated lipid DPPC with DPPG⁽⁻⁾, and observed vesicular shape in DOPC/DPPG⁽⁻⁾ mixtures. In this case, vesicles also formed spherical shape in all compositions as shown in Fig.4-5C (microscopic image is not shown). Furthermore, we observed membrane morphology in DOPG⁽⁻⁾/DPPC mixtures. We observed the spherical shape vesicles below 50% of DPPC. However, above 60% of DPPC, some vesicles formed open pore as shown in Fig.4-5B. This pore formation rate was increased with DPPC concentration (Fig.4-5C). At higher concentrations of saturated lipids (DPPC or DPPG⁽⁻⁾), membrane morphology could not be observed because stable vesicle formation by gentle hydration method was prevented by the larger amount of saturated lipid. According to our previous study in chapter 2, phase

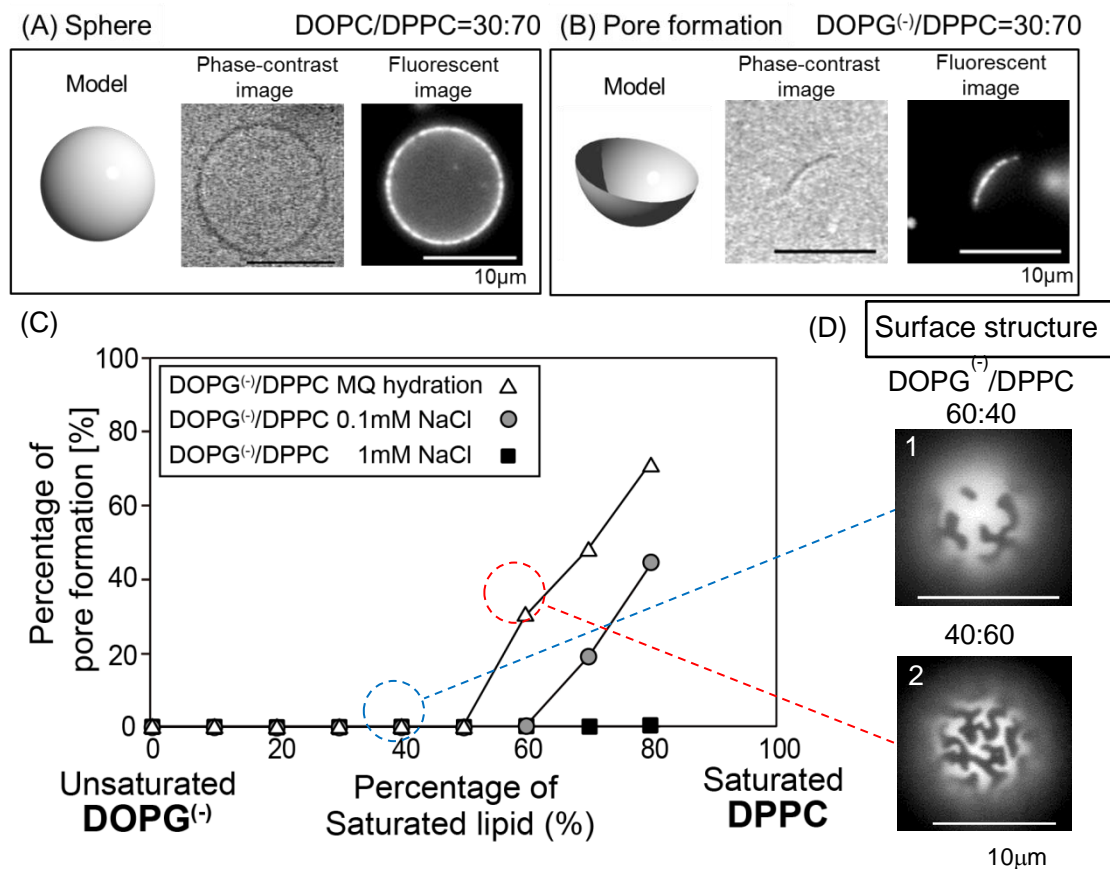


Fig.4-5 Microscopic images of membrane morphology and phase diagrams in binary mixture of unsaturated lipid/saturated lipid. Each microscopic image of GUV is taken at 22°C. (A) Spherical structure at composition of DOPC/DPPC=30:70. (B) Pore formation structure of GUV at composition of DOPG⁽⁻⁾/DPPC=30:70. (left: schematic model, center: phase-contrast image, right: fluorescent image).(C) Percentage of pore formation vesicles in binary mixture of DOPG⁽⁻⁾/DPPC. at 22°C (open triangle: MQ hydration, gray circle: 0.1mM NaCl, filled square: 1mM NaCl). (D) Surface structure of GUV at composition of DOPG⁽⁻⁾/DPPC= 60:40 (image 1), and 40:60 (image 2) in MQ hydration at 22°C.

separation structures were also observed in binary mixture of DOPG⁽⁻⁾:DPPC. It is suggested that phase separation structure may contribute to pore formation. We will discuss the difference of behavior between DOPG⁽⁻⁾/DPPC and DOPC/DPPG⁽⁻⁾ mixtures, and elaborate the relationship between 2D phase behavior and 3D membrane morphology in discussion section.

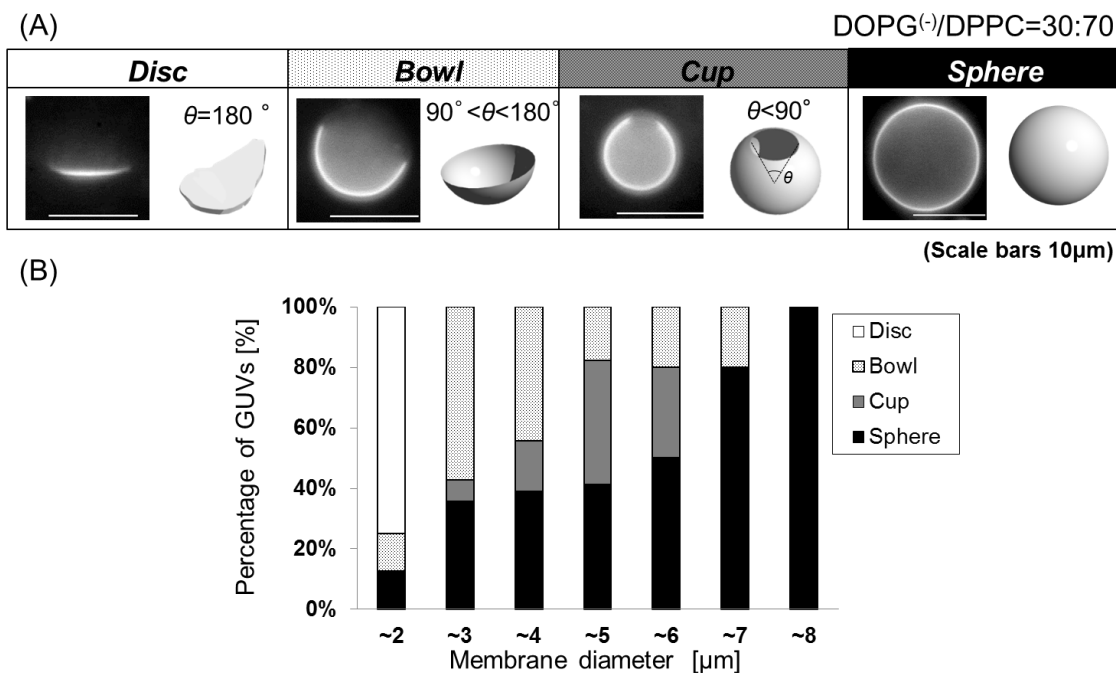
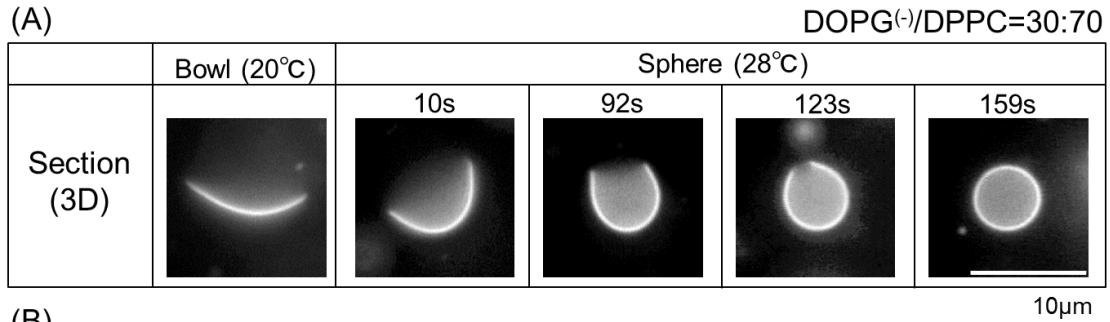


Fig.4-6 (A) Microscopic image and schematic model of GUVs in binary mixture of DOPG⁽⁻⁾/DPPC. The individual shapes are defined as to aperture angle. (B) Size distribution of each of membrane morphologies in binary mixture of DOPG⁽⁻⁾/DPPC=30:70 (white: Disc, light gray: Bowl, gray: Cup, black: Sphere)

In addition, we also investigated the behavior of vesicular morphology in presence of salt (with 1mM and 10mM NaCl). Fig.4-5C shows the percentage of pore formation in binary mixtures of DOPG⁽⁻⁾/DPPC by hydration with Milli Q water, 0.1mM NaCl, and 1mM NaCl, respectively. The percentage of pore formation tends to decrease with salt concentration. When DOPG⁽⁻⁾/DPPC vesicles were prepared with 0.1mM NaCl, the pore formation rate was decreased as compared to preparation with Milli Q water. In the case of 1mM NaCl hydration, pore formation vesicles were not observed. These results suggest that electric charge of lipid molecule has an important role of pore formation.

Next, we focused on the relationship between membrane morphology and vesicular size. We measured membrane diameter of spherical and pore formation vesicles. In the case of pore formation vesicles, we used following methods. First, we measured



10μm

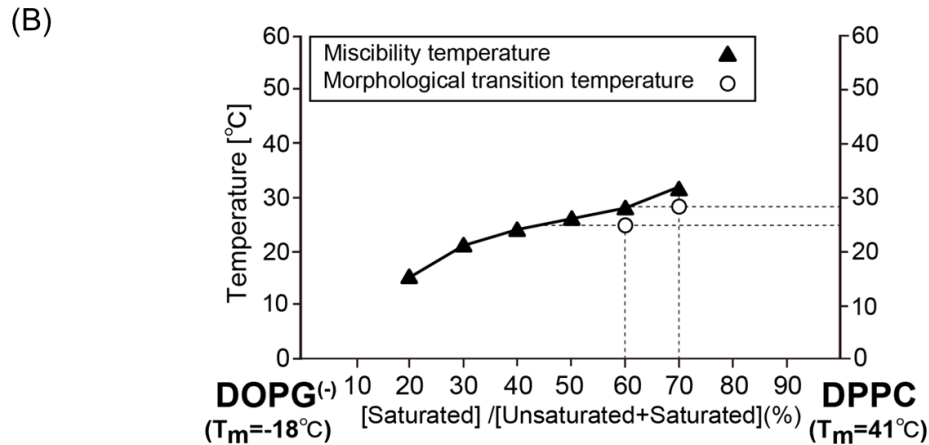


Fig.4-7 (A) Morphological change from Bowl to Sphere in binary mixture of DOPG⁽⁻⁾/DPPC=30:70 by changing the temperature. (B) Phase diagram of miscibility temperature and morphological transition temperature in DOPG⁽⁻⁾/DPPC (filled triangle: miscibility temperature, open circle: morphological transition temperature).

membrane surface are of pore formation vesicles. Second, we calculated the diameter of sphere having a measured surface area. We defined this spherical diameter as pore formation diameter. Fig.4-6 shows the percentage of membrane morphology for each vesicular diameter. We classified pore formation structures by aperture angle θ . We defined pore formation structures as Disc: $\theta = 180^\circ$, Bowl: $90^\circ < \theta < 180^\circ$, and Cup: $\theta < 90^\circ$, respectively. We measured diameter of vesicles and summarized percentage of membrane morphology for each size as shown in Fig.4-6B. In under $2\mu\text{m}$, most of the vesicles formed disc shape. In increasing with diameter, bowl and cup shapes were appeared. These pore formation structures tend to decrease with diameter. Finally, over $8\mu\text{m}$, all vesicles formed sphere. This result implies that pore formation structure of

charged membrane strongly depend on vesicular size.

Furthermore, we observed the temperature dependence of pore formation. Fig.4-7A shows structural change of pore formation vesicle by increasing in temperature at DOPG⁽⁻⁾/DPPC=30:70. We focused on the vesicle which was forming pore at 20°C, and increased the temperature to 28°C by 10°C/min. At 28°C, membrane pore was beginning to close, and finally formed spherical shape after 159 seconds. When we cooled sample solution to room temperature at 20°C by 20°C/min, this vesicles re-formed pore (data is not shown). We also measured this morphological transition temperature in DOPG⁽⁻⁾/DPPC=40:60. The morphological transition temperature showed 25°C lower than 28°C of DOPG⁽⁻⁾/DPPC=30:70. In chapter 2, we investigated the miscibility temperature in binary mixture of DOPG⁽⁻⁾/DPPC. Fig.4-7B shows the comparison between miscibility temperature and morphological transition temperature. Morphological transition temperatures of DOPG⁽⁻⁾/DPPC=40:60 and 30:70 are lower than miscibility temperature.

4-3-2 Ternary lipid mixtures (neutral and charged saturated lipids /cholesterol)

In this section, we prepared the ternary mixture of GUVs using neutral saturated DPPC, negatively saturated lipid DPPG⁽⁻⁾, and cholesterol. The fluorescent dye Rho-DHPE and BODIPY-Chol was used for fluorescent microscopy. We investigated the membrane morphology in DPPC/DPPG⁽⁻⁾/Chol. The effect of salt screening was also performed using NaCl.

Fig.4-8 shows the microscope images of membrane morphology and phase diagrams in ternary mixture. We observed membrane morphology using differential interference contrast (DIC) and confocal laser scanning microscopy. For neutral lipid mixtures of DPPC/Chol=80:20, all of vesicles formed spherical shape as shown in Fig.4-8A. On the other hand, when some fraction of DPPC were replaced with DPPG⁽⁻⁾, some vesicles formed pore (Fig.4-8B). Fig.4-8C shows the percentage of pore formation vesicles in DPPC/DPPG⁽⁻⁾/Chol for fixed Chol=20%. Pore formation rate was increased with the concentration of DPPG⁽⁻⁾. At DPPG⁽⁻⁾/Chol=80:20, most of the vesicles had pore. We also investigated the effect of charge on membrane morphology in presence of salt (10mM NaCl) for DPPC/DPPG⁽⁻⁾/Chol mixture. Percentage of pore formation with 10mM NaCl is indicated by open circle in Fig.4-8C. The pore formation rate was significantly decreased by adding salt as compared with Milli Q water (MQ) hydration. This implies that negatively charge of DPPG⁽⁻⁾ has a critical role to form membrane pore. According to our study in chapter 2, DPPC/DPPG⁽⁻⁾/Chol mixture is observed phase separation structure as shown in Fig.4-8D. The area percentage of domain is increased with DPPG⁽⁻⁾ concentration,. Thus, phase separation structure may also have a role of pore

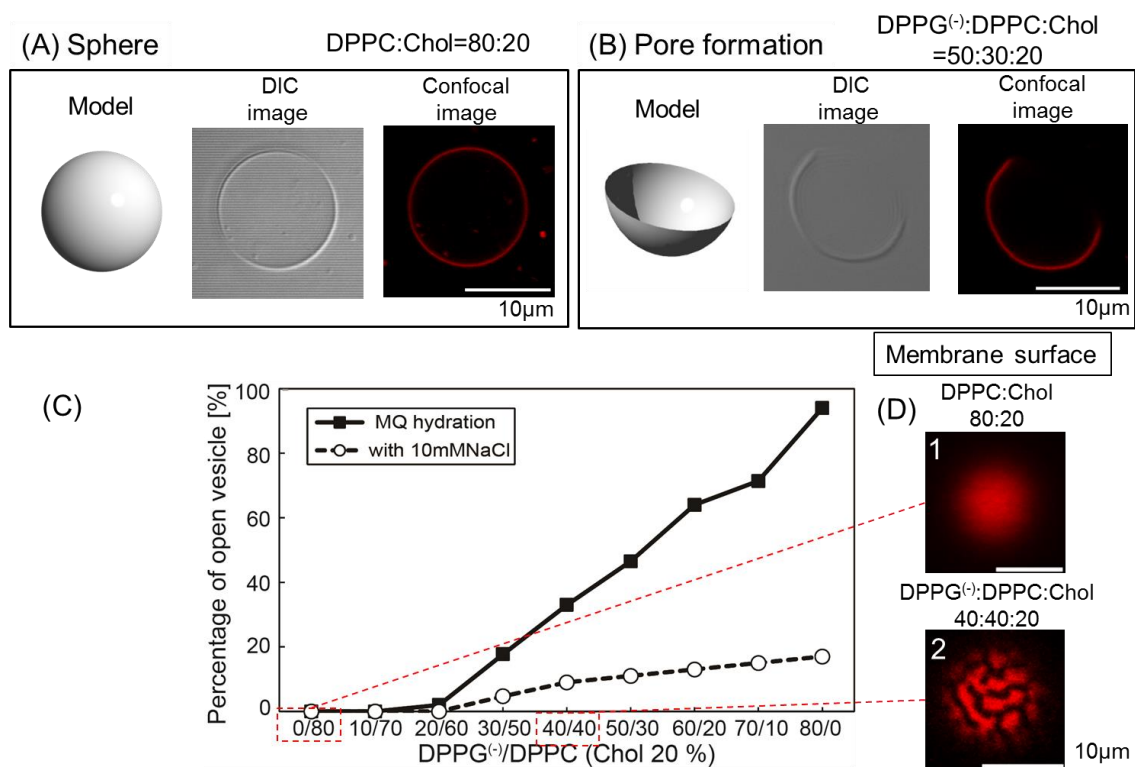


Fig.4-8 Microscopic images of membrane morphology and phase diagram in ternary mixture of saturated lipids (neutral and charged)/ cholesterol. Each microscopic images of GUVs are taken at 22 °C . (A) Spherical structure of GUV at composition of DPPC/Cholesterol=80:20 (left: schematic models, center: phase-contrast image, right: fluorescent image). (B) Pore formation structure of GUV at composition of DPPC/DPPG⁻/Chol=50:30:20. (C) Percentage of pore formation vesicles in DPPC/DPPG⁻/Chol at 22°C (filled square: hydration by Milli Q water, open circle: hydration by 10mM NaCl).(D) Surface structure of GUV at composition of DPPC/Chol= 80:20 (image 1), and DPPC/DPPG⁻/Chol= 40:40:20 (image 2) in MQ hydration at 22°C.

formation.

Next, we changed the ratio between DPPC and cholesterol for fixed DPPG⁻=50%, and measured percentage of pore formation for each composition as shown in Fig.4-9. In MQ hydration, pore formation rate was increased with DPPC concentration. In particular, pore formation rate was dramatically increased between DPPC/DPPG⁻/Chol=30:50:20 and 40:50:10. When cholesterol concentration is 15~45%, saturated lipid and cholesterol forms liquid order phase (L_o). On the other hand, at low concentration of cholesterol

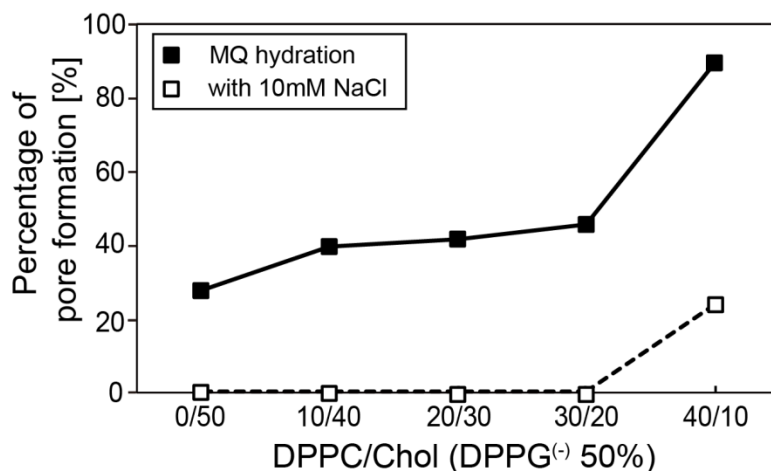


Fig.4-9 Percentage of pore formation vesicles in DPPG⁽⁻⁾/DPPC/Chol for fixed DPPG⁽⁻⁾=50% at 22°C (filled square: hydration by Milli Q water, open square: hydration by 10mM NaCl).

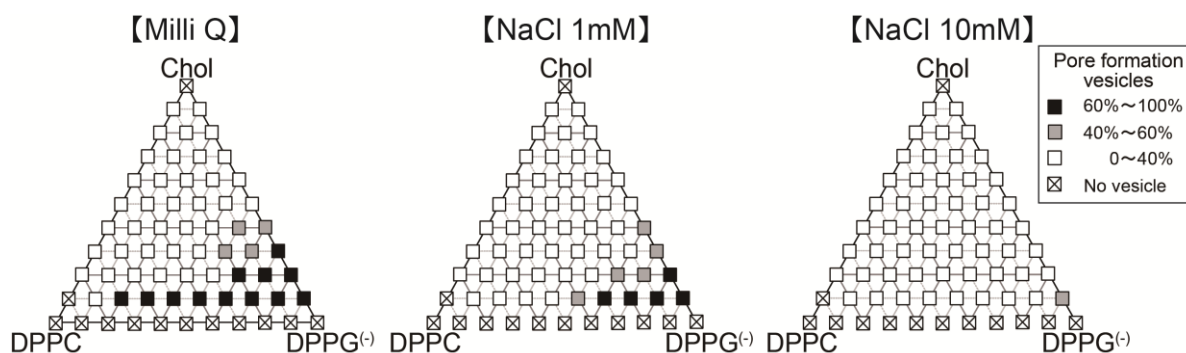


Fig.4-10 Phase diagrams of DPPC/DPPG⁽⁻⁾/Chol mixtures in Milli Q and NaCl solutions (left: Milli Q, centre: NaCl 1 mM, right: NaCl 10 mM) at room temperature (~22 °C). Filled, grey, and open squares correspond to systems where 60–100%, 40–60%, and 0–40% of the pore formation vesicles, respectively.

(~15%), saturated lipid-rich region forms Solid order phase (S_0). Previous research suggested that the bending rigidity of S_0 phase is higher than L_0 phase²⁹. This result implies that bending rigidity also affects membrane morphology.

Pore formation of DPPC/DPPG⁽⁻⁾/Chol mixtures for Milli Q water and NaCl aqueous solutions is summarized in Fig. 4-10. The left diagram shows pore formation rate of DPPC/DPPG⁽⁻⁾/Chol mixtures in Milli Q water. For higher concentrations of DPPC or cholesterol, pore formation vesicles were not observed or rarely observed (open squares).

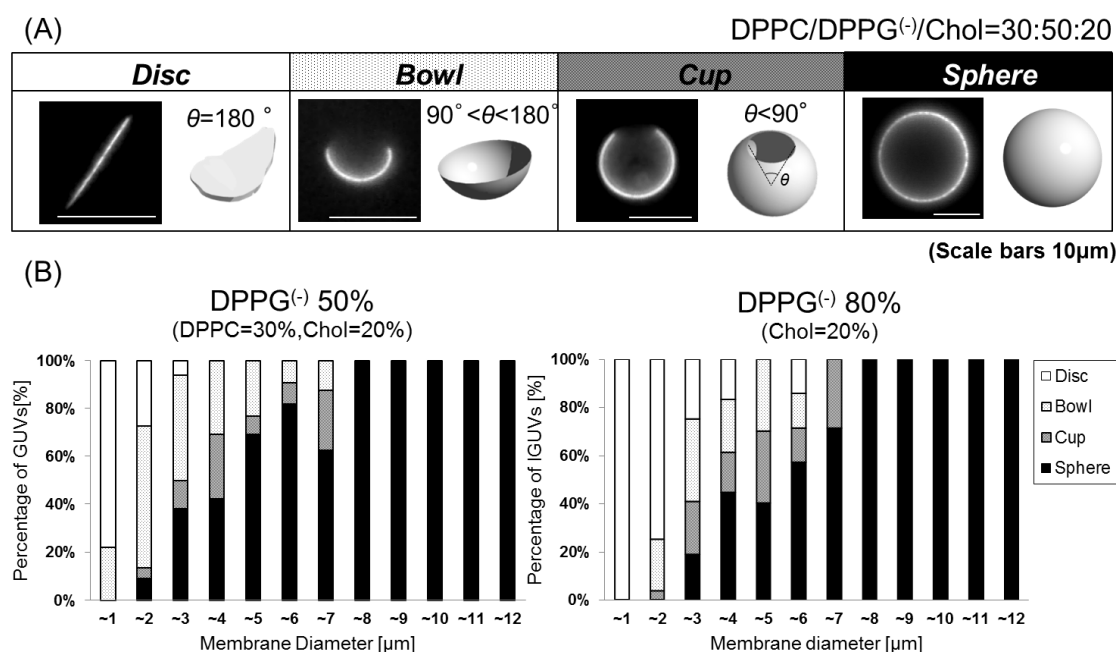


Fig.4-11 (A) Microscopic image and schematic model of GUVs in ternary mixture of DPPC/DPPG⁽⁻⁾/Chol. The individual shapes are defined as to aperture angle. (B) Size distribution of each of membrane morphologies in DPPC/DPPG⁽⁻⁾/Chol=30:50:20, 0:80:20, respectively. (white: Disc, light gray: Bowl, gray: Cup, black: Sphere)

On the other hand, their percentage clearly increases with the DPPG⁽⁻⁾ concentration (filled squares). In addition, the pore-formation regions with 1 mM and 10 mM of NaCl are indicated the center and right of diagram in Fig.4-10. As the salt concentration is increased, the pore formation rate tends to decrease significantly. In particular, most of the vesicles formed spherical shape in hydration with 10mM NaCl. This is because DPPG⁽⁻⁾ is screened in the presence of salt and approaches the behaviour of the neutral DPPC.

Next, we examined the size dependency of membrane morphology in the same way as binary mixture of DOPG⁽⁻⁾/DPPC. Fig.4-11 shows the percentage of membrane morphology for each vesicular diameter. Pore formation structures were also classified by aperture angle θ (Fig.4-11A). We measured membrane diameter and summarized percentage of membrane morphology in DPPC/DPPG⁽⁻⁾/Chol=30:50:20 and 0:80:20. As

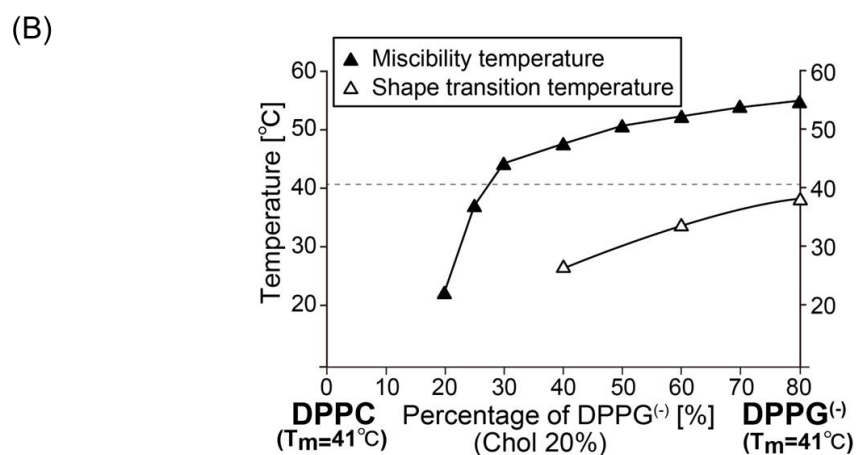
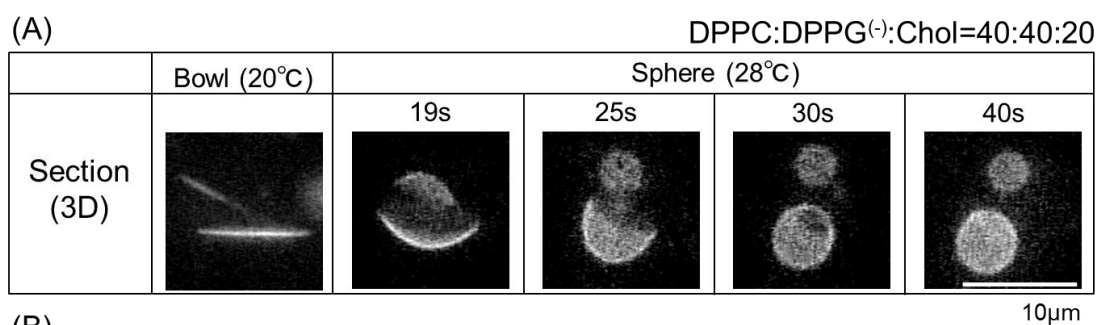


Fig.4-12 (A) Morphological change from bowl to sphere in ternary mixture of DPPC/DPPG⁽⁻⁾/Chol=40:40:20 by changing the temperature. (B) Phase diagram of miscibility temperature and morphological transition temperature in DPPC/DPPG⁽⁻⁾/Chol (filled triangle: miscibility temperature, open triangle: morphological transition temperature).

shown in Fig.4-11B, the percentage of pore formation vesicles such as disc, bowl, and cup were decreased with membrane diameter in both compositions. Over 8 µm, all vesicles formed sphere. These results were same tendency as binary mixture of DOPG⁽⁻⁾/DPPC. In addition, high concentration of DPPG⁽⁻⁾=80% tends to form disc and bowl in large diameter compared with middle concentration of DPPG⁽⁻⁾=50%. It is suggested that charged lipid of DPPG⁽⁻⁾ stabilizes the edge of membrane pore.

Furthermore, we observed temperature dependence of pore formation vesicles by. Fig.4-12A shows structural change of pore formation vesicle in DPPC/DPPG⁽⁻⁾/Chol=40:40:20. At 28°C, membrane morphology was changed from pore formation structure to spherical shape. When we cooled this vesicular solution to room

temperature at 20°C, vesicles formed pore again (data is not shown). We changed DPPG⁽⁻⁾ concentration and measured morphology transition temperatures. In DPPC/DPPG⁽⁻⁾/Chol=20:60:20 and 0:80:20, morphology transition temperatures were 34°C and 38°C, respectively. In chapter 2, we investigated the miscibility temperature in ternary mixture of DPPC/DPPG⁽⁻⁾/Chol. Fig.4-12B shows the comparison between miscibility temperature and morphology transition temperature. All morphology transition temperatures were lower than miscibility temperature. Difference of these temperatures were larger than binary mixture of DOPG⁽⁻⁾/DPPC in Fig.4-7B. In addition, shape transition temperatures were lower than phase transition temperature of DPPC and DPPG⁽⁻⁾ $T_m=41^\circ\text{C}$.

4-4 Discussion

According to our result, pore formation can be observed at some lipid compositions, while screening of head group charge of charged lipid by adding salt (NaCl) suppress pore formation. This suggests that electrostatic interaction plays a key role of membrane morphology stability. We discuss the mechanism of pore formation in charged lipid mixtures based on Fromherz's theory³⁰. The membrane elastic free energy of a membrane can be written as

$$E_{(total)} = E_{\kappa} + E_{\gamma} \quad (1)$$

where E_{κ} is bending energy of membrane and E_{γ} is line energy at the membrane edge. E_{κ} can be obtained from Helfrich bending energy³¹ as

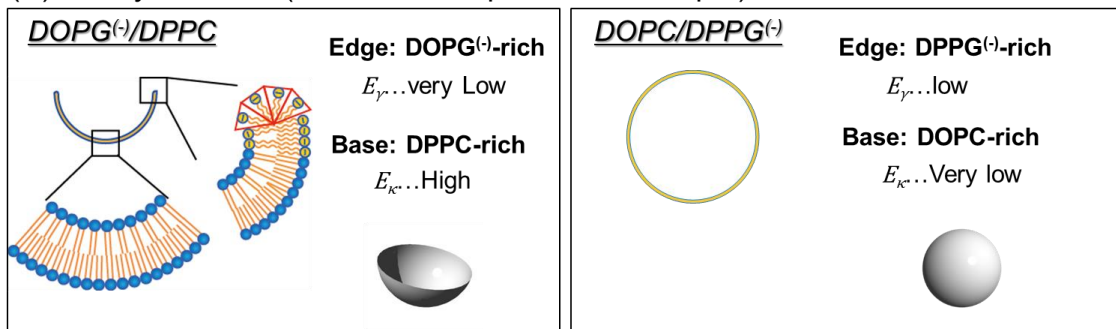
$$E_{\kappa} = \int \left[\frac{\kappa}{2} (c_1 + c_2 - c_0)^2 + \kappa' c_1 c_2 \right] dA \quad (2)$$

where dA is the are element of membrane surface, c_1 and c_2 are the two principal curvatures, c_0 is the spontaneous curvature, κ is bending rigidity, and κ' is Gaussian bending modulus. In addition, E_{γ} can be expressed as

$$E_{\gamma} = \gamma \int dl = 2\pi\gamma R \quad (3)$$

where dl is the line element along the membrane edge, γ is line tension, and R is membrane radius. Membrane shapes are determined by competition between bending and line energies. If line energy E_{γ} is more dominant than bending energy E_{κ} , membrane shape is sphere to reduce the line energy. Conversely, if bending energy E_{κ} becomes dominant than line energy E_{γ} , lipid membrane forms pore and becomes flat to decrease the bending energy. Previous study suggested that charged lipid molecules decrease line tension γ and stabilize edge of membrane pore^{32,33}. Charged lipid has

(A) Binary mixtures (Unsaturated lipid/Saturated lipid)



(B) Ternary mixtures (Saturated (neutral and charged) lipids/ cholesterol)

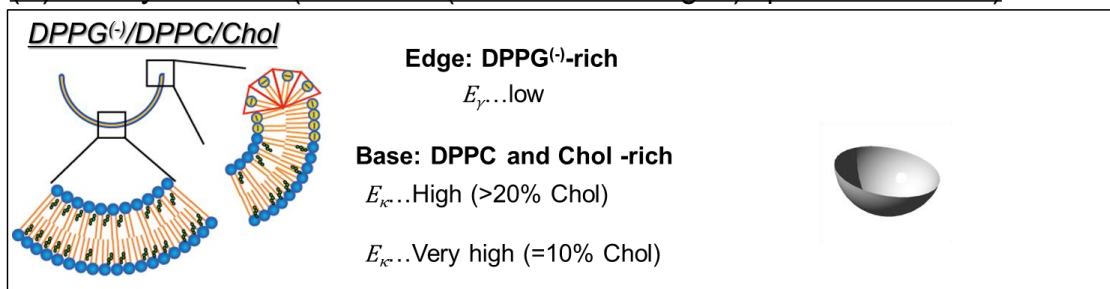


Fig.4-13 Relationship between membrane elastic energy and membrane morphology. (A) Schematic model of binary mixtures of DOPG⁽⁻⁾/DPPC and DOPC/DPPG⁽⁻⁾. (B) Schematic model of ternary mixtures of DPPC/DPPG⁽⁻⁾/Chol.

positively spontaneous curvature due to head group repulsion and can stabilize edge of pore. In addition, charged lipid can obtain entropy gain by counterion in bending part as compared to flat part. Thus, charged lipids favor to form edge of pore like a lipid which has positively spontaneous curvature³⁴.

Bending energy E_{κ} is affected by bending rigidity κ . Some studies investigated about κ in various kinds of lipid molecules. Commonly, at room temperature, κ of unsaturated lipid tends to have smaller than saturated lipid one. For example, the κ of unsaturated lipid DOPC is $1.5 \times 10^{-20} [J]$ at $21^{\circ}C$ ³⁵, while saturated lipid DPPC is $1.0 \times 10^{-18} [J]$ at $23^{\circ}C$ ³⁶. In charged unsaturated lipid DOPG⁽⁻⁾ and saturated lipid DPPG⁽⁻⁾, the value of κ could be not so different from neutral unsaturated or saturated lipids because acyl chain structures are same.

Fig.4-13 shows the relationship between membrane elastic free energy and membrane morphology. In binary mixtures of unsaturated lipid/saturated lipid, neutral mixtures of DOPC/DPPC form spherical shape in all compositions. Therefore, the contribution of E_{κ} is larger than that of E_{γ} in neutral mixture in μm scale. When we replaced neutral unsaturated lipid DOPC with charged unsaturated lipid DOPG⁽⁻⁾, pore formation vesicles were observed in DOPG⁽⁻⁾/DPPC=40:60, 30:70, 20:80. In these compositions, charged lipid DOPG⁽⁻⁾ may be localized at membrane edge and decrease line tension γ . However, we could not observe the localization of DOPG⁽⁻⁾ by optical microscopy. In addition, base part of membrane is composed of mainly saturated lipid DPPC which has high bending rigidity κ . As a result, bending energy E_{κ} becomes more significant than E_{γ} , and pore formation structures were observed (Fig.4-13A left). In high concentration of DOPG⁽⁻⁾, E_{γ} becomes lower by reduction of line tension γ . However, bending energy E_{κ} is also low because bending rigidity κ of unsaturated charged lipids DOPG⁽⁻⁾ is small, and some fraction of DOPG⁽⁻⁾ is localized in base part of membrane. Thus, bending energy E_{κ} is low enough, and lipid membrane forms spherical shape in high concentration of DOPG⁽⁻⁾.

On the other hand, when we replace saturated lipid DPPC with negatively saturated lipid DPPG⁽⁻⁾, pore formation structure were not observed in all composition of DOPC/DPPG⁽⁻⁾. In this case, charged lipid DPPG⁽⁻⁾ can decrease line tension, but base part of membrane is composed of unsaturated lipid DOPC. Bending rigidity κ of unsaturated lipid is one hundredth compared with saturated lipid one. As a result, because bending energy E_{κ} is low enough, membrane forms spherical shape in all compositions (Fig.4-13A right).

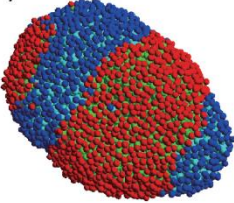
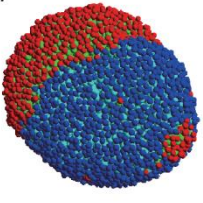
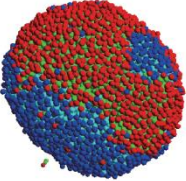
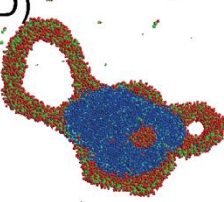
	DOPC/DPPG ⁽⁻⁾	DOPG ⁽⁻⁾ /DPPC
Salt concentration 1M	(A) 	(B) 
Salt concentration 100mM	(C) 	(D) 

Fig.4-14 Coarse-grained molecular dynamics simulations of binary mixtures of unsaturated lipid and saturated lipid. (A) DOPG⁽⁻⁾/DPPC in 100mM salt (B) DOPG⁽⁻⁾/DPPC in 1M salt (C) DOPC/DPPG⁽⁻⁾ in 100mM salt (D) DOPC/DPPG⁽⁻⁾ in 1M salt

Furthermore, we also observed pore formation structure in saturated lipid (neutral and charged) /cholesterol mixtures of DPPC/DPPG⁽⁻⁾/Chol. We observed pore formation in wide range of compositions (Fig.4-10). In this mixture, both lipid molecules are saturated lipid. Thus, bending energy E_K is high in all compositions. In addition, line energy E_γ is decreased by charged lipid DPPG⁽⁻⁾. As a result, the percentage of pore formation structure increase with DPPG⁽⁻⁾ concentration(Fig.4-13). At low cholesterol concentration, it is known that saturated lipid-rich region forms solid phase^{16,37}. In 10% cholesterol, pore formation rate was significantly increased (Fig4-9). It indicates that E_K increases significantly due to phase transition to solid phase by decreasing cholesterol concentration. In schematic model of Fig.4-13, charged lipid molecules localize the edge of membrane pore, while the large amount of neutral lipid molecule is

include in base part of membrane. This structure can regard as phase separation. Chapter 2 shows the phase separation is occurred between neutral lipid and charged lipid. Thus, it is possible that phase separation structure triggers pore formation. At low temperature, unsaturated lipid is enriched in liquid phase, while saturated lipid is enriched in rich in solid phase. However, when temperature increase, each of lipids begins mixing in both phases, and finally forms homogeneous structure. According to Fig.4-7 and Fig.4-12, pore formation structure was changed to spherical structure before miscibility transition temperature. It implied that membrane edge enriched in charged lipids was destabilized by mixing of neutral lipids.

Finally, we reproduced experimental system using coarse-grained molecular dynamics simulations. For simplicity, we calculated binary charged lipid membranes. A lipid molecule is represented by one hydrophilic bead and two hydrophobic beads, and these beads are connected by two bonds. The excluded-volume interaction between these beads is

$$V_{\text{rep}}(r;b) = \begin{cases} 4\nu \left[\left(\frac{b}{r}\right)^{12} - \left(\frac{b}{r}\right)^6 + \frac{1}{4} \right], & r \leq r_c \\ 0 & r > r_c \end{cases} \quad (4)$$

where $r_c = 2^{1/6}b$. ν and σ are the units of energy and length, respectively. We choose $b_{\text{head,head}} = b_{\text{head,tail}} = 0.95\sigma$ and $b_{\text{tail,tail}} = \sigma$ to form bilayer stably. The potentials for stretching and bending of bond between beads are described as

$$V_{\text{bond}}(r) = -\frac{1}{2}k_{\text{bond}}r_{\infty}^2 \log[1 - (r/r_{\infty})^2], \quad (5)$$

and

$$V_{\text{bend}}(r) = \frac{1}{2}k_{\text{bend}}(r - 4\sigma)^2, \quad (6)$$

where $k_{\text{bond}} = 30v/\sigma^2$ is the bond stiffness, $r_\infty = 1.5\sigma$ is the divergence length, and $k_{\text{bend}} = 10v/\sigma^2$ is the bending stiffness. The attractive potential between hydrophobic beads is expressed as

$$V_{\text{attr}}(r) = \begin{cases} -v & r < r_c \\ -v \cos^2 \frac{\pi(r-r_c)}{2w_c}, & r_c \leq r \leq r_c + w_c \\ 0 & r > r_c + w_c \end{cases} \quad (7)$$

The cutoff length for this attractive potential is w_c . When w_c is large, the lipid takes solid phase. Whereas the lipid becomes liquid phase in small w_c . Finally, the electrostatic repulsion between charged head group is expressed as Debye-Hückel potential

$$V_{\text{elec}}(r) = \ell_B z_1 z_2 \frac{\exp(-r/\ell_D)}{r}, \quad (8)$$

where $\ell_B = \sigma$ is the Bjerrum length, z_1 and z_2 are valency of charged head-group, and $\ell_D = \sqrt{(\epsilon k_B T)/(n_0 e^2)}$ is the Debye-Hückel screening length which is related with bulk salt concentration n_0 (ϵ , k_B , T , and e are dielectric constant of solution, Boltzmann constant, temperature, and elementary charge, respectively). Since the negatively charged head group PG⁽⁻⁾ has monovalent ion, we set $z_1 = z_2 = -1$.

For comparison, two systems are calculated to correspond to DOPC/DPPG⁽⁻⁾ and DOPG⁽⁻⁾/DPPC. We choose $w_{c(\text{DOPC-DOPC})} = 1.6$, $w_{c(\text{DPPG-DPPG})} = 1.8$, and $w_{c(\text{DOPC-DPPG})} = 1.5$ for DOPC/DPPG⁽⁻⁾ and $w_{c(\text{DOPG-DOPG})} = 1.6$, $w_{c(\text{DPPC-DPPC})} = 1.8$, and $w_{c(\text{DOPG-DPPC})} = 1.5$ for DOPG⁽⁻⁾/DPPC. In neutral system, a lipid takes liquid phase for

$w_c = 1.6$ and solid phase for $w_c = 1.8$ ³⁹. The number of lipid molecules is 5000, and the mixing ratio is unsaturated lipid: saturated lipid=50:50. The snapshots of course-grained MD simulation are shown in Fig.4-14. When the salt concentration in solution is high (1M), the vesicle shape is spherical in both DOPC/DPPG⁽⁻⁾ and DOPG⁽⁻⁾/DPPC systems Fig.4-14 (A) and (B). In addition, we can see the phase separated structures. The vesicle shape of DOPC/DPPG⁽⁻⁾ in low salt concentration (100mM) is also spherical shape (Fig.4-14 (C)), but the disc shape is found in DOPG⁽⁻⁾/DPPC as shown in Fig.4-14 (D). In experiment, Since we could find the pore formation in DOPG⁽⁻⁾/DPPC, and could not observe any morphological changes in DOPC/DPPG⁽⁻⁾, these results are consistent with the experimental results. Also, we can see the same salt concentration dependence of morphological change as experiment.

Interestingly, the charged lipids which are denoted by red color are localized at the edge of disc. Since the electrostatic repulsion between charged head groups becomes dominate than the attraction between hydrophobic beads, the spontaneous curvature of charged lipid becomes larger and the charged lipids are localized at the edge of disc to reduce the line energy. This result supports our experimental findings and theoretical predictions.

4-5 Conclusion

In this chapter, we investigated the effect of charge on membrane 3D structure and discussed relationship between membrane 2D and 3D structures by comparison to chapter 2. We observed membrane morphology in various mixtures containing charged lipids. In binary mixtures of unsaturated lipid/saturated lipid, neutral composition of DOPC/DPPC formed spherical shape, whereas pore formation structures were observed in DOPG⁽⁻⁾/DPPC mixtures. Pore formation was suppressed due to screening of electric charge of DOPG⁽⁻⁾ by adding salt. In ternary mixtures of DPPC/DPPG⁽⁻⁾/Chol, pore formation structures were also observed. Percentage of pore formation is increased with DPPG⁽⁻⁾ concentration. In presence of salt, pore formation was suppressed same as binary mixture. These results revealed that electric charge of lipid affects membrane morphology. Moreover, the results from experiment and theoretical model corresponded to the result of Coarse-grained molecular dynamics simulations. Our findings will be advanced understanding of the mechanism of dynamic process in biomembrane that are endocytosis, autophagy, and vesicular transport.

4-6 References

1. Simons K, Ikonen E. Functional rafts in cell membranes. *Nature* 1997;387(6633):569-572.
2. Simons K, Sampaio JL. Membrane Organization and Lipid Rafts. *Cold Spring Harbor Perspectives in Biology* 2011;3(10).
3. Parton RG, Simons K. The multiple faces of caveolae. *Nature Reviews Molecular Cell Biology* 2007;8(3):185-194.
4. Simons K, Toomre D. Lipid rafts and signal transduction (vol 1, pg 31, 2000). *Nature Reviews Molecular Cell Biology* 2001;2(3):216-216.
5. Barlowe C, Orci L, Yeung T, Hosobuchi M, Hamamoto S, Salama N, Rexach MF, Ravazzola M, Amherdt M, Schekman R. COPII - A MEMBRANE COAT FORMED BY SEC PROTEINS THAT DRIVE VESICLE BUDDING FROM THE ENDOPLASMIC-RETICULUM. *Cell* 1994;77(6):895-907.
6. McMahon HT, Gallop JL. Membrane curvature and mechanisms of dynamic cell membrane remodelling. *Nature* 2005;438(7068):590-596.
7. Ishimoto H, Yanagihara K, Araki N, Mukae H, Sakamoto N, Izumikawa K, Seki M, Miyazaki Y, Hirakata Y, Mizuta Y and others. Single-cell observation of phagocytosis by human blood dendritic cells. *Japanese Journal of Infectious Diseases* 2008;61(4):294-297.
8. Rothman JE. Transport of the vesicular stomatitis glycoprotein to trans Golgi membranes in a cell-free system. *The Journal of biological chemistry* 1987;262(26):12502-10.
9. Beckers CJ, Block MR, Glick BS, Rothman JE, Balch WE. Vesicular transport between the endoplasmic reticulum and the Golgi stack requires the NEM-sensitive fusion protein. *Nature* 1989;339(6223):397-8.
10. Kovacs AL, Rez G, Palfia Z, Kovacs J. Autophagy in the epithelial cells of murine seminal vesicle in vitro - Formation of large sheets of nascent isolation membranes, sequestration of the nucleus and inhibition by wortmannin and 3-methyladenine. *Cell and Tissue Research* 2000;302(2):253-261.
11. Juhasz G, Neufeld TP. Autophagy: A forty-year search for a missing membrane source. *Plos Biology* 2006;4(2):161-164.
12. Dall'Armi C, Devereaux KA, Di Paolo G. The Role of Lipids in the Control of Autophagy. *Current Biology* 2013;23(1):R33-R45.
13. Haucke V, Di Paolo G. Lipids and lipid modifications in the regulation of membrane.

- Current Opinion in Cell Biology 2007;19(4):426-435.
14. Cohen BE, Bangham AD. Diffusion of small non-electrolytes across liposome membranes. *Nature* 1972;236(5343):173-4.
 15. Hamada T, Miura Y, Komatsu Y, Kishimoto Y, Vestergaard M, Takagi M. Construction of Asymmetric Cell-Sized Lipid Vesicles from Lipid-Coated Water-in-Oil Microdroplets. *Journal of Physical Chemistry B* 2008;112(47):14678-14681.
 16. Veatch SL, Keller SL. Separation of liquid phases in giant vesicles of ternary mixtures of phospholipids and cholesterol. *Biophysical Journal* 2003;85(5):3074-3083.
 17. Hamada T, Miura Y, Ishii K-i, Araki S, Yoshikawa K, Vestergaard Md, Takagi M. Dynamic processes in endocytic transformation of a raft-exhibiting giant liposome. *Journal of Physical Chemistry B* 2007;111(37):10853-10857.
 18. Hamada T, Sugimoto R, Vestergaard MdC, Nagasaki T, Takagi M. Membrane Disk and Sphere: Controllable Mesoscopic Structures for the Capture and Release of a Targeted Object. *Journal of the American Chemical Society* 2010;132(30):10528-10532.
 19. Veatch SL, Keller SL. Organization in lipid membranes containing cholesterol. *Physical Review Letters* 2002;89(26):4.
 20. Baumgart T, Hess ST, Webb WW. Imaging coexisting fluid domains in biomembrane models coupling curvature and line tension. *Nature* 2003;425(6960):821-824.
 21. Dowhan W. Molecular basis for membrane phospholipid diversity: Why are there so many lipids? *Annual Review of Biochemistry* 1997;66:199-232.
 22. Schlame M. Thematic review series: Glycerolipids - Cardiolipin synthesis for the assembly of bacterial and mitochondrial membranes. *Journal of Lipid Research* 2008;49(8):1607-1620.
 23. William D, Mikhail B, Mileykovskaya. Functional roles of lipids in membranes. In: Vance DE, Vance JE, editors. *Biochemistry of Lipids, Lipoproteins and Membranes*. 5 ed. Elsevier Press 2008. p 1-37.
 24. Shimokawa N, Hishida M, Seto H, Yoshikawa K. Phase separation of a mixture of charged and neutral lipids on a giant vesicle induced by small cations. *Chemical Physics Letters* 2010;496(1-3):59-63.
 25. Shimokawa N, Komura S, Andelman D. Charged bilayer membranes in asymmetric ionic solutions: Phase diagrams and critical behavior. *Physical Review E* 2011;84(3):10.
 26. Vequi-Suplicy CC, Riske KA, Knorr RL, Dimova R. Vesicles with charged domains.

- Biochimica Et Biophysica Acta-Biomembranes 2010;1798(7):1338-1347.
27. Blosser MC, Starr JB, Turtle CW, Ashcraft J, Keller SL. Minimal Effect of Lipid Charge on Membrane Miscibility Phase Behavior in Three Ternary Systems. *Biophysical Journal* 2013;104(12):2629-38.
 28. Patarraia S, Liu Y, Lipowsky R, Dimova R. Effect of cytochrome c on the phase behavior of charged multicomponent lipid membranes. *Biochimica Et Biophysica Acta-Biomembranes* 2014;1838(8):2036-2045.
 29. Gracia RS, Bezlyepkina N, Knorr RL, Lipowsky R, Dimova R. Effect of cholesterol on the rigidity of saturated and unsaturated membranes: fluctuation and electrodeformation analysis of giant vesicles. *Soft Matter* 2010;6(7):1472-1482.
 30. Fromherz P. Lipid-vesicle structure: size control by edge-active agents. *Chemical Physics Letters* 1983;94(3):259-266.
 31. Helfrich W. Elastic properties of lipid bilayers: theory and possible experiments. *Zeitschrift fur Naturforschung. Teil C: Biochemie, Biophysik, Biologie, Virologie* 1973;28(11):693-703.
 32. Betterton MD, Brenner MP. Electrostatic edge instability of lipid membranes. *Physical Review Letters* 1999;82(7):1598-1601.
 33. May S. A molecular model for the line tension of lipid membranes. *European Physical Journal E* 2000;3(1):37-44.
 34. Sakuma Y, Taniguchi T, Imai M. Pore Formation in a Binary Giant Vesicle Induced by Cone-Shaped Lipids. *Biophysical Journal* 2010;99(2):472-479.
 35. Niggemann G, Kummrow M, Helfrich W. THE BENDING RIGIDITY OF PHOSPHATIDYLCHOLINE BILAYERS - DEPENDENCES ON EXPERIMENTAL-METHOD, SAMPLE CELL SEALING AND TEMPERATURE. *Journal De Physique Ii* 1995;5(3):413-425.
 36. Chau-Hwang L, Wan-Chen L, Jyhpyng W. Measuring the bending rigidity of giant unilamellar liposomes with differential confocal microscopy. *Conference on Lasers and Electro-Optics (CLEO 2000). Technical Digest. Postconference Edition. TOPS Vol.39 (IEEE Cat. No.00CH37088) 2000:592-3.*
 37. Hamada T, Kishimoto Y, Nagasaki T, Takagi M. Lateral phase separation in tense membranes. *Soft Matter* 2011;7(19):9061-9068.

Chapter 5

General conclusion

5-1 General conclusion

In the present study, we clarify the electric charge effects on the 2D dynamics (phase behaviour) and 3D dynamics (membrane morphology). We also explored the salt screening effect on charged membranes. We discussed the effects of charge on membrane 2D and 3D dynamics based on free energy model.

In chapter 2, we investigated the phase separation induced by negatively charged lipids. As compared to the phase-coexistence region (in the phase diagram) of neutral unsaturated lipid (DOPC)/ saturated lipid (DPPC) mixtures, the phase separation in the charged unsaturated lipid (DOPG⁽⁻⁾)/DPPC case is suppressed, whereas it is enhanced for DOPC/ charge saturated lipid (DPPG⁽⁻⁾) system. The phase behaviours of both charged mixtures approach that of the neutral mixture when salt is added due to screening of electrostatic interactions. In DPPC/DPPG⁽⁻⁾/Chol ternary mixtures, the phase separation occurs when the fraction of charged DPPG⁽⁻⁾ is increased. This result implies that cholesterol localization is influenced by the head group structure as well as the hydrocarbon tail structure. Furthermore, we observed three-phase coexistence in four-component DOPC/DPPC/DPPG⁽⁻⁾/Chol mixtures, and that the phase-separation strongly depends on the amount of charged DPPG⁽⁻⁾.

In chapter 3, we investigated the localization of cholesterol and phase behavior in various mixtures of charged lipid membranes. Cholesterol prefers to be localized in DOPG⁽⁻⁾-rich phase, while does not to be localized in DPPG⁽⁻⁾-rich phase. Our results showed that cholesterol tends to be localized in the order of DOPG⁽⁻⁾>DPPC>DOPC>DPPG⁽⁻⁾. In presence of salt, localization of cholesterol was changed significantly. In addition, the screening effects in phase behavior by presence of

monovalent cation Na^+ and divalent cation Mg^{2+} are also difference. These results suggest that the interaction between charged lipid and cholesterol plays an important role in structural regulation of phase separation in lipid membrane.

In chapter 4, we investigated the effect of charge on membrane 3D structure and discussed relationship between membrane 2D and 3D structures by comparison to chapter 2. We observed membrane morphology in various mixtures containing charged lipids. In binary mixtures of unsaturated lipid/saturated lipid, neutral composition of DOPC/DPPC formed spherical shape, whereas pore formation structures were observed in DOPG⁽⁻⁾/DPPC mixtures. Pore formation was suppressed due to screening of electric charge of DOPG⁽⁻⁾ by adding salt. In ternary mixtures of DPPC/DPPG⁽⁻⁾/Chol, pore formation structures were also observed. Percentage of pore formation is increased with DPPG⁽⁻⁾ concentration. In presence of salt, pore formation was suppressed same as binary mixture. These results revealed that electric charge of lipid affects membrane morphology. Moreover, the results from experiment and theoretical model corresponded to the result of Coarse-grained molecular dynamics simulations

Our findings will be advanced understanding of the mechanism of dynamic process in biomembrane such as 2D dynamics of lipid rafts structure, and 3D dynamics of membrane morphology including endocytosis, autophagy, and vesicular transport during the signal transduction. Moreover, our finding may help to understand the mechanisms that play an essential role in the interactions of proteins with lipid mixtures.

Acknowledgement

The studies in this thesis were performed in School of Materials Science, Japan Advanced Institute of Science and Technology (JAIST).

I would like to thank Prof. Masahiro Takagi (JAIST) who gave me invaluable comments and warm encouragements. I have learned from him about the attitude for research. I would like to express my gratitude to Dr. Naofumi Shimokawa (JAIST) for fruitful discussion and constructive advice, and technical support of numerical simulation. I also thank to Prof. Tsutomu Hamada (JAIST) for helpful support and technical advice of GUVs experiments. I would like to express my gratitude to Prof. David Andelman (Tel Aviv Univ.) and Shigeyuki Komura (Tokyo metropolitan Univ.) for fruitful discussion and comments about theoretical idea of free energy modeling. I am indebted to Dr. Yuji Higuchi (Tohoku Univ.) and Mr. Hiroaki Ito (Kyoto Univ.) for helpful support of numerical simulation. I would like to thank to Prof. Joerg Lahann (UMich) and Prof. Henry Wang (UMich.) for kindness support of my sub-theme research during the stay of Michigan.

I also thank to members of Masahiro Takagi lab. I want to thank Mr. Ko Sugahara, Ms. Phan Huong Thi Thanh, for their kindness support to creating a good environment for studying in Lab. Experimental support and technical assistance from Mr. Takumi Saida is greatly appreciated.

This research was financially supported by the Sasagawa Scientific Research Grant from The Japan Science Society.

Finally, I would like to express deepest appreciation to my friend in Japan and USA, and my dear family.

Publication

Articles

1) "Charge-induced phase separation in lipid membranes"

Hiroki Himeno, Naofumi Shimokawa, Shigeyuki Komura, David Andelman, Tsutomu Hamada, Masahiro Takagi

Soft matter, 2014, 10(40), 7959 - 7967

2) "The effect of charge on membrane morphology: coupling between phase separation and vesicular shape"

Hiroki Himeno, Hiroaki Ito, Yuji Higuchi, Tsutomu Hamada, Naofumi Shimokawa, Masahiro Takagi

submitting to Biophysical journal

Conferences

Poster presentations at international conference

1. ○Hiroki Himeno, Tsutomu Hamada, Masahiro Takagi

"Charge-induced transition in membrane mesoscopic structure"

Phase Transition Dynamics in Soft Matter, Kyoto University (Japan), 2012.02.20

2. ○Hiroki Himeno, Tsutomu Hamada, Masahiro Takagi

"Mesoscopic structures of charged lipid membrane Lateral domains and vesicle formation"

14th International Association of Colloid and Interface Scientists Conference, Sendai International Center (Japan), 2012.05.17

3. ○Hiroki Himeno, Tsutomu Hamada, Masahiro Takagi

"Charge-induced transition in membrane mesoscopic structures: lateral domains and vesicular shapes"

The First International Symposium on Biofunctional Chemistry 2012(Japan), 2012, 11, 30

4. ○ Hiroki Himeno, Naofumi Shimokawa, Shigeyuki Komura, David Andelman, Tsutomu Hamada, and Masahiro Takagi

“Charge-induced phase separation in lipid membranes”

Biomembrane Days 2014, Max Planck Institute (Germany), 2014, 09, 1

Poster presentation at domestic conference

1. ○ 姫野泰輝, 濱田勉, 高木昌宏

「荷電脂質膜における相分離形成と曲率変化」

平成 23 年度日本化学会北陸地区講演会 金沢大学 2011 年 11 月 18 日

2. ○ 姫野泰輝, 濱田勉, 高木昌宏

「脂質分子の電荷が引き起こす膜構造変化：2次元相分離と3次元曲率」

平成 24 年度未踏科学サマー道場 湘南国際村センター 2012 年 8 月 16 日

3. ○ 姫野泰輝, 濱田勉, 高木昌宏

「荷電脂質ベシクルにおける相分離構造と膜曲率のカップリング」

日本化学会支部合同福井大会（平成 24 年度北陸地区講演会と研究発表会）

福井大学文京キャンパス 2012 年 11 月 17 日

4. ○ 姫野泰輝, 下川直史, 濱田勉, 高木昌宏

「ベシクル系における荷電脂質が引き起こす相分離構造」

日本物理学会第 69 回年次大会 東海大学湘南キャンパス 2014 年 3 月 30 日

Oral presentations at domestic conference

1. ○ 姫野泰輝, 網野雅人, 杉本涼子, 濱田勉, 高木昌宏 「荷電脂質膜の構造安定性」

日本物理学会第 66 回年次大会 新潟大学五十嵐キャンパス 2011 年 3 月 25 日

2. ○ 姫野泰輝, 濱田勉, 高木昌宏 「荷電ベシクル系におけるドメインと曲率のカップリング」

日本物理学会 2011 年秋季大会 富山大学五福キャンパス 2011 年 9 月 22 日

3. ○ 姫野泰輝, 濱田勉, 高木昌宏 「荷電脂質ベシクルの相分離形成と曲率変化」

日本化学会 第 92 回春季大会 慶応義塾大学日吉キャンパス 2012 年 3 月 27 日

4. ○ 姫野泰輝, 濱田勉, 高木昌宏

「脂質ベシクル系における電荷が引き起こす膜構造変化：2次元相分離と3次元曲率」

第 6 回バイオ関連化学シンポジウム 北海道大学高等教育推進機構 2012 年 9 月 8 日

5. ○姫野泰輝,濱田勉,高木昌宏
「脂質ベシクル系における電荷が引き起こす相分離形成と曲率変化」
日本物理学会 2012 年秋季大会 横浜国立大学 2012 年 9 月 21 日
6. ○姫野泰輝,濱田勉,高木昌宏
「脂質分子の電荷が引き起こす膜構造変化 : 2 次元相分離と 3 次元曲率」
第 50 回日本生物物理学会年会 名古屋大学東山キャンパス 2012 年 9 月 24 日
7. ○姫野泰輝,濱田勉,高木昌宏
「ベシクル系における脂質分子の電荷が引き起こす相分離形成と曲率変化」
膜シンポジウム 2012 神戸大学 2012 年 11 月 8 日
8. ○姫野泰輝,濱田勉,高木昌宏
「荷電ベシクル系における相分離形成と曲率変化のカップリング」
日本物理学会第 68 回年次大会 広島大学東広島キャンパス 2013 年 3 月 28 日
9. ○姫野泰輝,下川直史,濱田勉,高木昌宏
「荷電脂質を含むベシクルにおける膜孔形成と相分離構造とのカップリング」
中部大学春日井キャンパス 2014 年 9 月 7 日
10. ○齊田拓巳, 姫野泰輝, 下川直史, 高木昌宏
「塩の添加が支配する荷電脂質膜の相分離」
中部大学春日井キャンパス 2014 年 9 月 7 日

Short time stays for cooperation research

Prof. Joerg Lahann lab at University of Michigan (Ann Arbor, USA) 2013.9~2013.12

Research fellowship

- 1.平成 24 年度 日本化学協会 笹川研究助成 採択 研究番号 24-230
「静電作用による脂質膜の秩序構造形成」